MAPPING SOIL ORGANIC CARBON STOCKS BY COMBINING NIR SPECTROSCOPY AND STOCHASTIC VERTICAL DISTRIBUTION MODELS:
a Case Study in the Mvoti River Catchment, KZN, South Africa

by
Liesl Wiese

Thesis presented in fulfilment of the requirements for the degree of
Doctor of Philosophy (Ph.D.)
in the Faculty of AgriSciences at Stellenbosch University

Supervisor: Dr. Andrei B. Rozanov, Department of Soil Science
Co – Supervisors: Dr. Willem P. De Clercq, Water Institute, SU
Prof. Thomas Seifert, Department of Forestry and Wood Science

April 2019

Declaration

By submitting this thesis/dissertation electronically, I declare that the entirety of the work contained therein is my own, original work, that I am the sole author thereof (save to the extent explicitly otherwise stated), that reproduction and publication thereof by Stellenbosch University will not infringe any third-party rights and that I have not previously, in its entirety or in part, submitted it for obtaining any qualification.

19 February 2019

Liesl Wiese

Summary

The agricultural and environmental importance of maintaining and increasing soil organic carbon (SOC) has been increasingly recognized globally. To a large extent, this recognition can be attributed to soil being the largest terrestrial carbon pool, as well as to soil's responsiveness to land use and management. Land use and land use change are major factors affecting SOC levels with changes from natural vegetation (forests, grasslands and wetlands) to croplands, for example, causing significant SOC losses. The topsoil (0-30 cm depth) is especially sensitive to changes in land use and management and the highest variation in SOC levels is observed in this zone.

In this study SOC stocks in the first meter of soil were quantified and mapped under different land uses and management systems using a vertical SOC distribution model, applying near-infrared (NIR) spectroscopy for SOC analysis and estimating the uncertainty of the maps created using different approaches. The study area was chosen as a quaternary catchment of 317 km^{-2} south and southeast of Greytown in the Midlands area of KwaZulu-Natal, South Africa. The catchment exhibits complex topography and predominantly shale and dolerite parent material. Soils in the area have high organic carbon content ranging from 0.08 to 22.85 % (mean = 3.48 %), with clay content ranging from 3 to 49 % (mean = 14.7 % clay) and pH(H_20) between 3.3 and 6.7 (mean pH(H_20) = 4.5).

Vertical SOC distribution functions were developed for 69 soil profiles sampled from different land uses (mainly forestry plantations, grasslands and croplands) in and around the study catchment. Bulk density samples were taken at 2.5, 7.5, 12.5, 17.5, 30, 40, 50, 75 and 100 cm depths. The aim was to reduce the number of soil observations required for SOC accounting to one point close to the soil surface by applying negative exponential vertical depth functions of SOC distribution. To achieve this, the exponential functions were normalized using the volumetric SOC content observed close to the surface and grouped as a function of land use and soil types. Normalization reduced the number of model parameters and enabled the multiplication of the exponential decline curve characteristics with the SOC content value observed at the surface to present an adequately represented value of soil carbon distribution to 1 m at that observation point. The integral of the exponential function was used to calculate the soil carbon storage to 1 m.

The vertical SOC distribution functions were refined for soils under maize production systems using reduced tillage and conventional tillage. In these soils, the vertical SOC

distributions are described by piecewise, but still continuous functions where the distribution within the cultivated layer (0-30 cm) is a linear decline under reduced tillage or a constant value under conventional tillage, followed by an exponential decline to 1 m (30-100 cm).

The value of predicting SOC concentrations in soil samples using wet oxidation (Walkley-Black method) and dry near-infrared (NIR) spectrometry was assessed by comparing them to the dry combustion method. NIR spectrometry is considered to be an especially promising method, since it may be used in both proximal and remote sensing applications. In addition, the effect of using paired samples with single SOC determination versus paired samples with replicated (three times) analysis by all (reference and test) methods was tested. It was shown that the use of paired tests without replication dramatically decreases the precision of SOC predictions of all methods, possibly due to high variability of SOC content in reference values analysed by dry combustion. While reasonable figures of merit were obtained for all the methods, the analysis of non-replicated paired samples has shown that the relative RMSE for the SOC NIR method only falls below 10 % for values above ~8 % SOC. For the corrected SOC Walkley Black method the relative RMSE practically never falls below 10 %, rendering this method as semi-quantitative across the range. It was concluded that for method comparison of soil analysis, it is essential that reference sample analysis be replicated for all methods (reference and test methods) to determine the "true" value of analyte as the mean value analysed using the reference method.

Finally, the above elements of vertical SOC distribution models as a function of land use and soil type, predicting SOC stocks to 1 m using only a surface (0-5 cm) sample, and the use of NIR spectroscopy as SOC analysis method were combined to assess the changes in SOC stock prediction errors through mapping. Results indicated a dramatic improvement in precision of SOC stock predictions with increasing detail in the input parameters using vertical SOC distribution functions differentiated by land use and soil grouping. Still, the relative error mostly exceeded 20 % which may be seen as unacceptably high for carbon accounting, trade and tax purposes, and the SOC stock accuracy decreased in terms of map R^2 and RMSE. The results were generally positive in terms of the progressive increase in complexity associated with SOC stock predictions and showed the need for a substantial increase in sampling density to maintain or increase map accuracy while increasing precision. This would include an increase both in surface samples for the prediction of SOC stocks using the vertical SOC distribution models, as well as an increase in the sampling of profiles to include more soil types and increase the profile density per land use to improve the vertical SOC prediction models.

Opsomming

Die landbou- en omgewingsbelang van die handhawing en toename van grondorganiese koolstof (GOK) word wêreldwyd toenemend erken. Tot ‘n groot mate kan hierdie erkenning toegeskryf word aan grond wat uit die grootste aardse koolstofpoel bestaan, sowel as die grond se responsiwiteit op grondgebruik en bestuur. Grondgebruik en grondgebruikverandering is belangrike faktore wat GOK-vlakke beïnvloed, met byvoorbeeld veranderinge van natuurlike plantegroei (woude, grasveld en vleilande) na gewaslande wat beduidende GOK-verliese tot gevolg het. Die bogrond (0-30 cm diepte) is veral sensitief vir veranderinge in grondgebruik en bestuur en die hoogste variasie in GOK-vlakke word in hierdie sone waargeneem.

In hierdie studie is GOK-inhoud in die eerste meter grond gekwantifiseer en gekarteer onder verskillende grondgebruike en bestuurstelsels deur gebruik te maak van 'n vertikale GOK-verspreidingsmodel, die toepassing van naby-infrarooi (NIR) spektroskopie vir GOK-analise en die bepaling van die onsekerheid van die kaarte wat geskep is deur verskillende benaderings. Die studiegebied is gekies as 'n kwaternêre opvanggebied van 317 km^{-2} suid en suidoos van Greytown in die KwaZulu-Natalse Middellande, Suid-Afrika. Die opvanggebied vertoon komplekse topografie en oorheersende skalie- en dolerietmateriaal. Grond in die gebied het 'n hoë organiese koolstofinhoud van 0,08 tot 22,85 % (gemiddeld = 3,48 %), met kleiinhoud wat wissel van 3 tot 49 % (gemiddeld = 14.7 % klei) en pH (H_20) tussen 3,3 en 6,7 (gemiddelde pH(H_20) = 4.5).

Vertikale GOK-verspreidingsfunksies is ontwikkel vir 69 grondprofiele wat in verskillende grondgebruike (hoofsaaklik bosbouplantasies, grasveld en gewaslande) in en om die opvanggebied gemonster is. Bulk digtheid monsters is geneem op 2,5, 7,5, 12,5, 17,5, 30, 40, 50, 75 en 100 cm dieptes. Die doel was om die aantal grondwaarnemings wat nodig is vir GOK-rekeningkunde tot een punt naby die grondoppervlak te verminder deur negatiewe eksponensiële vertikale diepte funksies van GOK verspreiding toe te pas. Om dit te bereik is die eksponensiële funksies genormaliseer met die volumetriese GOK-inhoud wat naby aan die oppervlak waargeneem word en gegroepeer as 'n funksie van grondgebruik en grondtipes. Normalisering het die aantal modelparameters verminder en moontlik gemaak om die die eksponensiële afname kurwe eienskappe met die GOK inhoud op die oppervlak te vermenidgvuldig ten einde 'n voldoende verteenwoordigende waarde van grondkoolverspreiding tot 1 m by daardie waarnemingspunt te bepaal. Die integraal van die eksponensiële funksie is gebruik om die grondkoolstofopberging tot 1 m te bereken.

Die vertikale GOK-verspreidingsfunksies is verfyn vir grond onder mielieproduksiestelsels wat verminderde bewerking en konvensionele bewerking toepas. In hierdie gronde word die vertikale GOK-verdelings deur stuksgewyse, maar steeds deurlopende funksies beskryf. Die GOK-verspreiding binne die bewerkingslaag (0-30 cm) toon 'n lineêre afname onder verminderde bewerking en konstante waarde onder konvensionele bewerking, gevolg deur 'n eksponensiële afname tot 1 m (30-100 cm).

Die waarde van die voorspelling van GOK konsentrasies in grondmonsters deur gebruik te maak van nat oksidasie (Walkley-Black metode) en droë naby-infrarooi (NIR) spektrometrie, is beoordeel deur dit met die droëverbrandingsmetode te vergelyk. NIR-spektrometrie word beskou as 'n besonder belowende metode, aangesien dit in beide proksimale en afstandswaarneming toepassings gebruik kan word. Daarbenewens is die effek van die gebruik van gepaarde monsters met enkele GOK-bepaling versus gepaarde monsters met herhaalde (drie keer) analise met alle (verwysings- en toets) metodes getoets. Daar is getoon dat die gebruik van gepaarde toetse sonder replikasie die presisie van GOK-voorspellings van alle metodes dramaties verminder, moontlik as gevolg van die hoë veranderlikheid van GOK -inhoud in verwysingswaardes wat deur droë verbranding ontleed word. Terwyl redelike merietesyfers vir al die metodes behaal is, het die ontleding van nie-gerepliseerde gepaarde monsters getoon dat die relatiewe RMSE vir die GOK NIR-metode slegs onder 10 % val vir waardes bo ~8 % GOK. Vir die gekorrigeerde SOC Walkley Black-metode val die relatiewe RMSE feitlik nooit onder 10% nie, wat hierdie metode as semi-kwantitatief oor die reeks lewer. Daar is tot die gevolgtrekking gekom dat, vir die vergelyking van grondanalisemetodes, dit noodsaaklik is dat die verwysingsmonster analise vir alle metodes (verwysings- en toetsmetodes) herhaal word (ten minste drie keer) om die "ware" waarde van analiet te bepaal as die gemiddelde waarde wat met behulp van die verwysingsmetode geanaliseer is.

Ten slotte is die bogenoemde elemente van vertikale GOK verspreidingsmodelle, te wete as 'n funksie van grondgebruik en grondtipe, wat SOC-voorrade vir 1 m voorspel met slegs 'n oppervlakmonster (0-5 cm) en die gebruik van NIR-spektroskopie as GOK-analise metode, gekombineer ten einde die veranderinge in GOK-voorspellingsfoute deur kartering te evalueer. Resultate dui op 'n dramatiese verbetering in die akkuraatheid van GOK-voorspellings met toenemende detail in die insetparameters deur vertikale GOK-verspreidingsfunksies te gebruik wat gedifferensieer word as ‘n funksie van grondgebruik en grondgroepering. Tog het die relatiewe fout meestal 20% oorskry, wat as onaanvaarbaar hoog vir koolstofrekeningkunde, handels- en belastingdoeleindes beskou kan word, en die GOK-

voorraad akkuraatheid het verminder in terme van kaart R^2 en RMSE. Die resultate was oor die algemeen positief in terme van die progressiewe toename in kompleksiteit wat in verband met GOK-voorspellings en toon die behoefte aan 'n aansienlike toename in monsternemingsdigtheid om die akkuraatheid van kaarte te behou of te verhoog. Dit sal 'n toename in oppervlakmonsters insluit vir die voorspelling van GOK-voorrade deur die vertikale GOK-verspreidingsmodelle te gebruik, asook 'n toename in die monsterneming van profiele om meer grondsoorte in te sluit en die profieldigtheid per landgebruik te verhoog ten einde die vertikale GOK voorspellingsmodelle te verbeter.

Acknowledgements

- This research was funded by: (1) the South African National Research Foundation (NRF) through the Department of Science and Technology/NRF Green Landscapes project, the Applied Centre for Climate & Earth Systems Science (ACCESS) programme, as well as the NRF Thuthuka programme; and (2) The Maize Trust.

- I would like to sincerely thank Mondi Forests for sharing the soil survey data in the study area and for their assistance during field work.

- To Steve Stamp, Kevin Cockburn, Rene Stubbs, and Garth Ellis: this study would not have been possible without your support and access to your farms. It was a sincere pleasure to meet you and thank you for the long discussions about soil, management, carbon, and life. I wish you all the best in your future farming activities.

- Special gratitude also goes to SAPPI, Steve Stamp and Kevin Cockburn (Pidelta) (Pty) Ltd for logistical support in the field.

- My sincere gratitude to every at the Department of Soil Science, Stellenbosch University, who helped with analyses and administrative support.

- To Attie Boshoff and Trevan Flynn, your help with the digital soil mapping aspect of this study was crucial. Thank you!

- Special thank you to Helene Nieuwoudt for showing me the ropes with the NIR spectrometer and for the open access to the lab. The NIR analysis was a big part of this study.

- To my co-supervisors, Thomas Seifert and Willem de Clercq, it was a pleasure to work with you. I'm especially grateful to you Thomas, for welcoming me into the Green Landscapes project team and Willem, for your help in organizing GIS training, helping with a bursary, and to both of you for your overall support and discussions on modelling the vertical distribution of SOC and mapping.

- I thoroughly enjoyed working on this project and the field work and fun moments in between was a key part of that. Ignacio Ros Mesa and Michael Esmeraldo, you were the best colleagues to work and spend long days in the field with. Thanks for all the

good times, but also for your hard work in helping with sample preparation and analysis!

- My biggest support in this journey came from my supervisor, Andrei Rozanov. Andrei, thank you for the endless discussions, brainstorming, support and also fun times during this long journey. I learned a tremendous amount from you and truly admire your grasp of soils and soil science.

- Finally, to my family and friends who always supported me in this long journey and encouraged me when it got tough. I love you all and am grateful to have you in my life.

Thank you.

Table of Content

List of Figures

List of Tables

List of symbols and abbreviations commonly used in the text

Soil characteristics

C_s – carbon stock [kg·m^{-2}]

C_v – volumetric carbon content [kg·m^{-3}]

SOC – soil organic carbon

ρ_b – soil bulk density [Mg·m^{-3}]

ρ_s – soil particle density [Mg·m^{-3}]

Analytical methods

NIR(S) – near-infrared (spectroscopy)

(SOC) DC – (soil organic carbon determined using) dry combustion [%]

(SOC) NIR – (soil organic carbon determined using) NIR spectroscopy [%]

(SOC) WB - (soil organic carbon determined) using Walkley and Black (1934) method [%]

Statistical parameters

AE – absolute error

MAE – mean absolute error

LOD – limit of detection

LOQ – limit of quantification

PLS(R) – partial least squares (regression)

R^2 – correlation coefficient

RAE – relative MAE

RMSE – root mean square error

RRMSE – relative RMSE

α – significance level

δ – standard deviation

μ – mean value

1 Introduction

1.1 Background

The agricultural and environmental importance of maintaining and increasing soil organic carbon (SOC) has been progressively recognized globally. This includes the role of SOC in contributing to food production, as well as its role in efforts of adapting to and mitigating the effects of a changing climate (England et al., 2018; Lal and Stewart, 2011; Minasny et al., 2017; Soussana et al., 2017; Vitharana et al., 2019). To a large extent, this recognition can be ascribed to soil being the largest terrestrial carbon pool (Batjes, 1996; Jackson et al., 2017), as well as to soil's responsiveness to land use and management (Nave et al., 2018).

In recent years, numerous global initiatives focused their attention on SOC (England et al., 2018), for example: (1) the United Nations Sustainable Development Goal (SDG) Indicator 15.3.1 on "the Proportion of land that is degraded over total land area" includes SOC stock as one of the first metrics used; (2) in the same vein, the United Nations Convention to Combat Desertification (UNCCD) will use SDG Indicator 15.3.1, including SOC stocks, as one of the indicators to monitor progress towards its land degradation neutrality targets (Orr et al., 2017); and (3) the "4 per 1000" initiative was launched at the 21st session of the United Nations Framework Convention on Climate Change (UNFCCC) in Paris, setting an ambitious target to increase global SOC stocks at a rate of 0.4 % (i.e. 4 per 1000) per year with a focus on agricultural land (Soussana et al., 2017).

As a result of these developments, measuring, mapping and monitoring of SOC have become well-studied topics over the last two decades to quantify and understand the status, trends, variability, and sequestration potential of SOC and more (Adhikari et al., 2014; Baldock, 2008; Beltrame et al., 2016; Chatterjee et al., 2009; Corbeels et al., 2018, 2016; Deng et al., 2013; England et al., 2018; Guevara et al., 2018; Haddaway et al., 2017; Henry et al., 2009; Hobley and Wilson, 2016; Jackson et al., 2017; Jobbagy et al., 2000; Kempen et al., 2019, 2010; Le Quéré et al., 2016; Mäkipää et al., 2008; Malone et al., 2017; Meersmans et al., 2009; Minasny et al., 2017, 2006; Minasny and McBratney, 2016; Mishra et al., 2009; Olson et al., 2013; Olson and Al-Kaisi, 2015; Paustian et al., 2016, 1997, Sleutel et al., 2007, 2003; Stolbovoy et al., 2007; Suddick et al., 2013; Tan et al., 2007; VandenBygaart and Kay, 2004; Vitharana et al., 2019; Waltman et al., 2010; Z. Wang et al., 2012b; Wiese et al., 2016; Yang et al., 2016, 2012, 2008). In addition, several past and present studies and initiatives focus on SOC accounting and the inclusion of SOC in carbon (C) trading schemes (Australia Department of

Climate Change and Energy Efficiency, 2012; Baldock, 2008; Bispo et al., 2017; Brenna et al., 2014; England et al., 2018; Gershenson et al., 2011; Goglio et al., 2015; Heath and Smith, 2000; Malone et al., 2017; Sanderman and Baldock, 2010; Schaltegger and Csutora, 2012; Stechemesser and Guenther, 2012; Suddick et al., 2013; Viscarra Rossel and Brus, 2018; Viscarra Rossel et al., 2014; White and Davidson, 2015; Wiese et al., 2016). England et al. (2018) highlighted that the development of new SOC accounting technologies is important for: (1) national greenhouse gas (GHG) emissions reporting to fulfil obligations under the UNFCCC, and (2) domestic schemes that aim to reduce or offset GHG emissions by implementing different activities such as improved land management practices and managing or preventing land use change.

Land use and land use change is a major factor affecting SOC change (Poeplau and Don, 2013; Smith, 2008), with changes from natural vegetation (forests, grasslands and wetlands) to croplands, for example, causing significant SOC losses (Paustian et al., 2016; Smith, 2008; Swanepoel et al., 2016). On the other hand, SOC stocks can be increased by increasing organic matter inputs (for example, by restoring degraded lands to perennial forest or grassland) or by decreasing soil organic matter decomposition rates (i.e. through reduced soil disturbance) (Paustian et al., 2016; Poeplau and Don, 2013). The topsoil (0-30 cm depth) is especially sensitive to changes in land use and management (Poeplau and Don, 2013) and is the zone of higher SOC variability (Beaudette et al., 2013).

Assessing the effect of land use, land use change and management practices on SOC requires the measurement of baseline SOC stock values, as well as the quantification of changes and variability in SOC stock in both space and time (England et al., 2018; Suddick et al., 2013). This, in turn, requires accurate and cost-efficient methods to measure and monitor SOC stocks (Bellon-Maurel and McBratney, 2011; Bispo et al., 2017; Cremers et al., 2001; Davis et al., 2018; De Gruijter et al., 2016; England et al., 2018). The determination of SOC stock requires measurements of SOC concentration, bulk density and gravel content (Batjes and Wesemael, 2015; England et al., 2018) and it is essential that relevant measurements are based on agreed upon standards to ensure comparable estimations of SOC stocks (Bispo et al., 2017). Furthermore, it is essential that analytical methods have sufficient accuracy, precision and the ability to detect and measure small quantities of the analyte. These requirements of analytical methods can be evaluated by calculating the relevant figures of merit which have been developed to assess and compare the performance of analytical methods (Bouabidi et al., 2010; Currie, 1999; De Vos et al., 2007; Eksperiandova et al., 2010;

Harris, 2007; Sangmanee et al., 2017; Shrivastava and Gupta, 2011; Valderrama et al., 2007; Wenzl et al., 2016), as well as the mean method prediction error (Olivieri, 2015).

When it comes to SOC mapping, the use of pedometrics, geostatistics and digital soil mapping has become especially popular and is used in an abundance of SOC studies (Adhikari et al., 2014; Aldana Jague et al., 2016; Brodský et al., 2013; De Brogniez et al., 2015; Dorji et al., 2014b; Guevara et al., 2018; Kempen et al., 2019; Lacoste et al., 2014; Malone et al., 2017; Minasny et al., 2006, 2013; Roudier et al., 2012; Sindayihebura et al., 2017; Somarathna et al., 2016; Thompson et al., 2010; Tsui et al., 2013; Vågen and Winowiecki, 2013; Veronesi et al., 2014; Vitharana et al., 2019; Zhao et al., 2005). In digital soil mapping, field and laboratory observation methods are coupled with quantitative spatial prediction techniques to create a spatial soil information system (Minasny et al., 2013). Therefore, it is equally important to quantify the errors and uncertainties associated with the resultant maps to determine whether a particular map is usable for a specific intended purpose (De Gruijter et al., 2016; Heuvelink, 2018; Minasny and McBratney, 2016; Stumpf et al., 2017). Furthermore, uncertainty propagation analysis is used to determine how uncertainty in input parameters is propagated in the modelling and mapping process and can identify the main sources of uncertainty. There are many sources of uncertainty accumulating in the modelling and mapping process, including field and laboratory measurement error, positional error, classification error, model parameter and structural errors, errors arising from spatial interpolation, errors from fitting and applying regression models and more (Heuvelink, 2018). However, reporting of errors and uncertainty in digital SOC mapping in literature generally excludes laboratory measurement errors. According to Heuvelink (2018) the main challenge in including all the various errors and uncertainties is to characterise the error sources with realistic probability distribution.

1.2 Problem Statement

Measuring and mapping SOC stocks is increasingly in demand to monitor progress in the achievement of goals such as reduced GHG emissions, land degradation neutrality and increasing SOC stocks by 0.4 % per year (4 per 1000 initiative) (England et al., 2018; Orr et al., 2017; Soussana et al., 2017). However, the measurement of SOC stocks at different soil depths and spatial scales is often expensive and time consuming due to field soil sampling, sample preparation and laboratory analysis (Akumu and McLaughlin, 2013; Chatterjee et al., 2009; Mäkipää et al., 2008; Sleutel et al., 2007). Furthermore, based on the assessed literature, error and uncertainty propagation arising from laboratory measurements are usually not included

in the estimation of overall SOC map accuracy, which may have a direct impact on the usability of such maps for potential users and the financial well-being of carbon market players.

1.3 Aims and Objectives

The overall aim of this study was to quantify and map SOC stocks in the first meter of soil under different land uses and crop management systems in a quaternary catchment using a vertical SOC distribution model, applying near-infrared spectroscopy for SOC analysis and estimating the uncertainty of the maps created using different approaches.

The specific objectives of this research were to:

1. Fit and group exponential vertical distribution functions for SOC stocks upon normalizing values observed throughout the soil profile by the SOC content close to soil surface (0-5 cm layer).

2. Develop a novel approach for soil carbon accounting using field soil sampling and stochastic modelling of vertical SOC distribution for a quaternary catchment area covered to a large extent by a detailed soil survey.

3. Compile a local NIR spectral library for the study area and use it to develop a PLS regression model for predicting the SOC content. Evaluate the loss in accuracy and precision of replacing the dry combustion analysis of SOC measurement by the cheaper Walkley and Black (1934) or NIR spectroscopy methods.

4. Find the best possible continuous functions describing the vertical distribution of SOC under different intensities of cultivation, so that a single surface sample would be sufficient to estimate the stocks down to various depths (20, 30, 100 cm). Analyse the changes in the stochastic models imposed by land use.

5. Determine the values of SOC content, bulk density and stone content at the soil surface (0-5 cm) from random sampling points throughout the study area to assess the volumetric SOC content at the soil surface. Use the existing soil map, land use classification and DEM derivatives, together with the vertical distribution functions developed previously to map SOC stocks in the study catchment, and assess the uncertainty of the maps produced.

1.4 Structure of the thesis

The technical part of the thesis is structured to address the above objectives in the presented order in Chapters 3 to 6. These Chapters have been, or will be submitted for publication in peer-reviewed journals. For this reason, Chapter 1 provides a summarised introduction of pertinent literature relevant to this study. More detailed references to existing literature are provided in Chapters 3 to 6.

Chapter 2 provides an overview of the study area in terms of location, geology, climate, and soils and describes the soil sampling strategy. The materials and methods are described in the respective technical chapters.

Chapter 3 describes the application, normalization and grouping of exponential vertical distribution functions to model SOC stocks under forests, grasslands and croplands. Upon normalization and grouping of exponential functions, a novel approach to soil carbon accounting is tested in a subsection of the study catchment where detailed soil information is available.

Chapter 4 compares the accuracy and precision of SOC analysis using NIR spectroscopy and the Walkley Black method by comparing these methods to dry combustion analysis.

Chapter 5 focuses on the effect of different tillage practices for maize production on the vertical distribution of SOC to find the best possible continuous distribution functions using grasslands as reference.

Following on the developments in Chapters 4 and 5, Chapter 6 assesses the changes in SOC stock prediction errors in the study catchment as a function of increased complexity and detail of model input parameters by mapping the SOC stocks and associated propagated error (measurement and prediction errors) of SOC stock determinations.

Chapter 7 summarizes the main conclusions arising from this research and Chapter 8 provides the full list of references.

2 Study area and sampling strategy

2.1 Site description.

A quaternary catchment (U40A), shown in Figure 2-1, was selected in the Midlands area of KwaZulu-Natal (KZN), South Africa, measuring 317 km^2 (Department of Water and Sanitation, 2018) with altitudes ranging from 950 to 1540 m. The catchment is located south and southeast of Greytown which is located on the banks of the Mvoti River. The Mvoti River includes the Mvoti Vlei wetland within the Mvoti Vlei Nature Reserve (2.67 km^2) in the study catchment. This wetland and nature reserve were excluded from the study due to the potentially deep layers of SOC stocks with layers of peat and mineral sediment, as well as the common presence of fresh sediment on the surface of wetland soils which would not suit the purposes of this study.

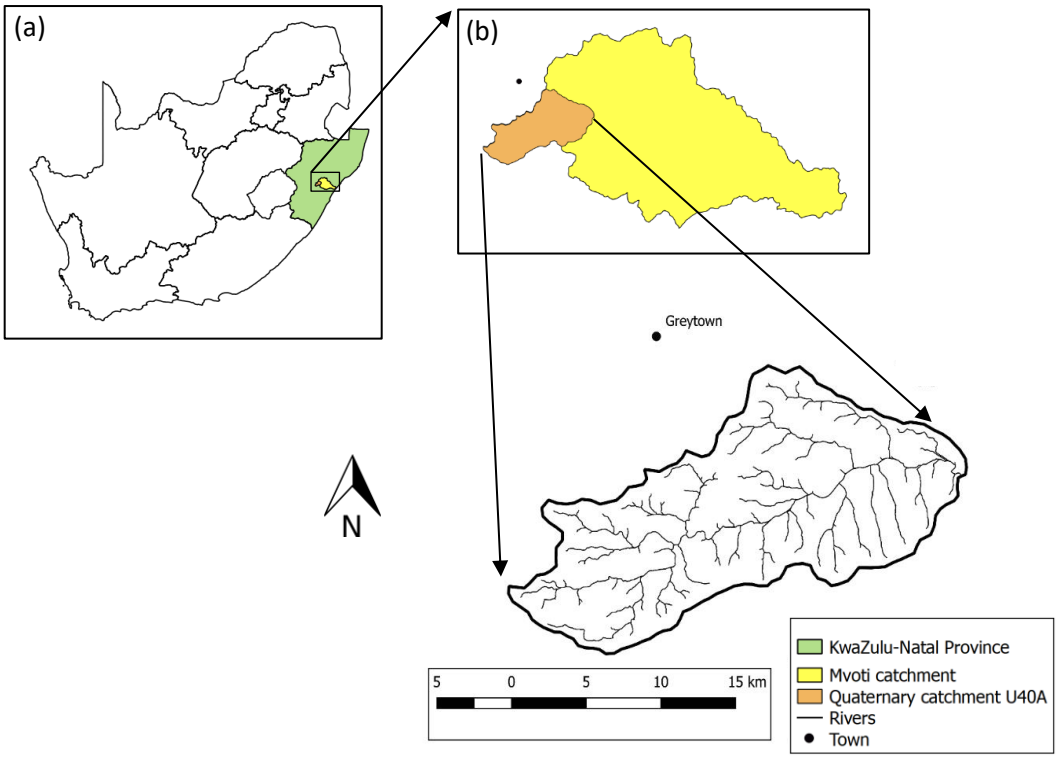

Figure 2-1. Location of the study area – quaternary catchment U40A – within the upper reaches of the Mvoti River in KwaZulu-Natal. The inset maps show the location of the study area (a) within South Africa and (b) within the Mvoti catchment.

Geologically, the study area falls in the Ecca Group of the Karoo Subgroup - from west to east, the area spans across the Volksrust, Vryheid, and Pietermaritzburg Formations. The primary parent materials for the three Formations are: Volksrust - mudstone and shale; Vryheid – sandstone and shale; and Pietermaritzburg: shale. According to Camp (1999) the

shales of the Ecca group tend to be dark and exposed in the midlands area and are often used to make good-quality bricks that burn red due to their high iron (Fe) content. Dolerite (diabase) dykes often pierce the Karoo system shale, frequently forming isolated hills within the general incline of the Drakensberg escarpment. Sandstones of the Ecca group crown the escarpment that extends in part to the west of Greytown. These sandstones have a coarser grain size and crumble more easily than those of the Natal Group Sandstone (Camp, 1999). Although a narrow band of sandstone occurs in the centre of the study area, sampling focused on the shale and dolerite parent materials (soils on sandstone parent material were not sampled).

Due to the complex topography, the climate varies along the altitudinal gradient, but is generally warm temperate in Greytown with mean winter (June) temperatures of 12 °C and summer (January) temperatures of 28 °C. Minimum winter temperatures can fall below 0 °C and frost is common in valley bottoms. Winters are relatively dry, with summer rainfall (mainly November to March) averaging from 900 mm.yr^{-1} (Ros Mesa, 2015). The mean monthly rainfall and temperatures (day and night) are presented in Figure 2-2.

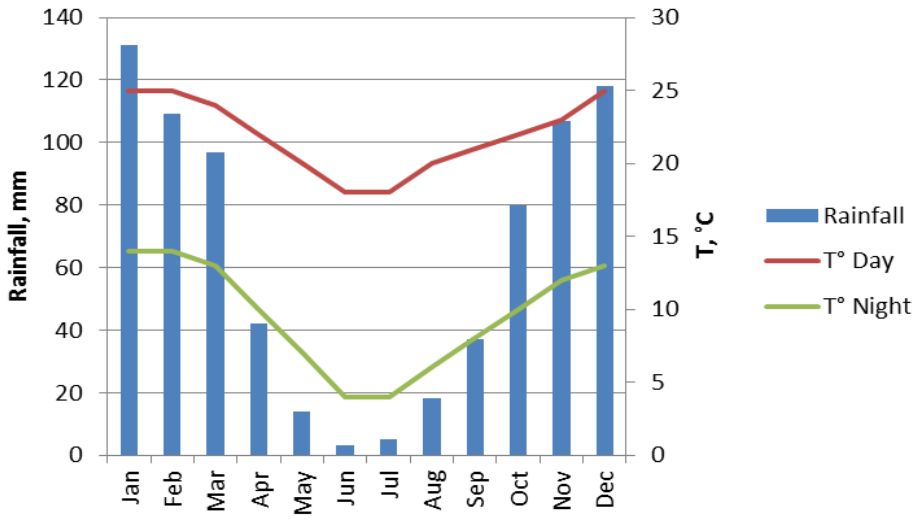

Figure 2-2. Mean monthly rainfall, day and night temperatures: Greytown (South African Weather Bureau data) (Ros Mesa, 2015).

The study area falls within the Mistbelt vegetation type which is characterized by a mosaic of grasslands and indigenous Afromontane forest. However, these grasslands and forests have been largely replaced by agriculture and commercial timber plantations (Camp, 1999) which is particularly well suited due to the high rainfall and mild temperatures in the area (Winter and Morris, 2001). Isolated patches of natural forest remain (Camp, 1999), along with small, fragmented patches of Mistbelt grassland (Winter and Morris, 2001). Agricultural land uses

are mostly limited to maize for grain and seed production, limited sugarcane production (in frost-free areas), pastures, and plantations (forestry) of eucalypts and pines (with residual wattle stands in the process of conversion to eucalypts).

2.2 Sampling strategy and soils

Soil sampling was conducted during two sampling campaigns in June 2013 and June 2014. Soil profiles were sampled to enable the modelling of vertical SOC distribution under different land uses, while a set of surface (0-5 cm) samples were taken for the final prediction and mapping of SOC stocks in the quaternary catchment.

For profile sampling, a random stratified sampling approach was selected with the random sampling locations represented by two to four profiles in a catenary sequence. This was done to capture the changes in soil type and carbon stocks along the hill slope and down to the valley bottom. Soil profiles were excavated in positions in and around the catchment based on ease of access and land use. During the 2013 sampling campaign, 50 profiles were sampled mainly from plantation forests, grasslands and maize fields, with isolated profiles sampled from natural forest, wetland and sugarcane. In 2014 an additional 19 profiles were sampled to focus on different maize production systems using conventional tillage, reduced tillage and no-till. The closest available no-till farm was situated in the Karkloof area of KZN to the southwest of the main study catchment. The locations of the 69 sampling profiles are shown in Figure 2-3.

Soil profiles were dug to 1 m unless restricted by rock or a water table occurring at shallower depth. All the soils were classified using the Taxonomic Soil Classification system of South Africa (Soil Classification Working Group, 1991). Core samples were taken in triplicate per sampling depth (Figure 2-4a) using steel cores of 48 mm length and a volume of 98 cm^3 to account for variability in bulk density. The vertical centres of the cores were placed at 2.5, 7.5, 12.5, 17.5, 30, 40, 50, 75 and 100 cm depths as illustrated in Figure 2-4b. As reported by Ros Mesa (2015) and Esmeraldo (2016), all the samples were analysed for particle size distribution and pH. A summary of the number of profiles with the same South African classification is given in Table 2-1. For purposes of this study the litter layer in plantations was not considered part of the mineral soil. The litter layer in these soils was therefore removed prior to sampling as illustrated in Figure 2-4c.

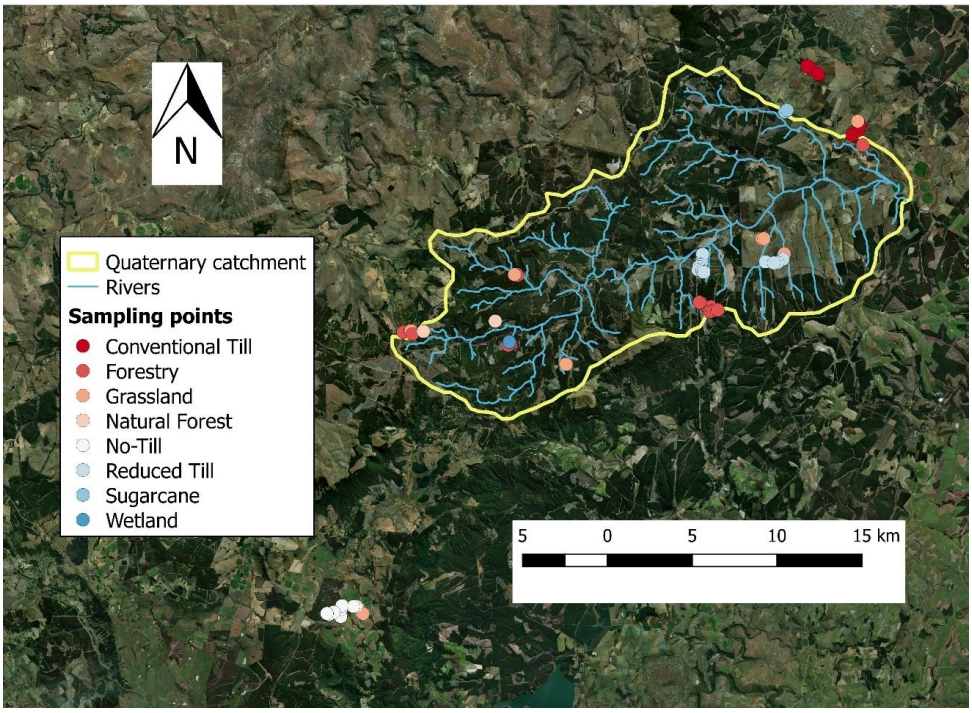

Figure 2-3. Location of the 69 profiles sampled in and around the quaternary catchment. Sampling points are stratified by land use and maize production tillage system. Satellite imagery was obtained from the Bing Aerial open layer in QGIS 2.18.

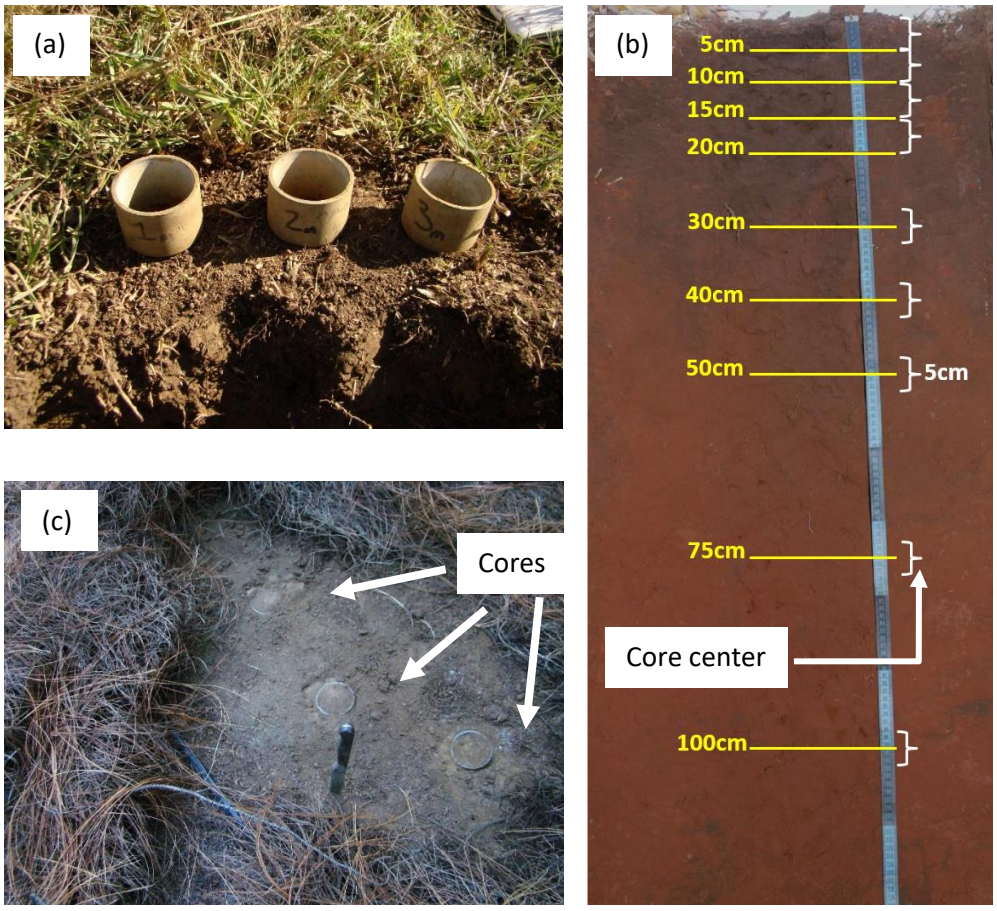

Figure 2-4. For each profile, core samples were taken in triplicate as shown in Figure (a) with Figure (b) indicating the sampling depth increments. Figure (c) shows the triplicate core sampling of surface soils for the final mapping exercise.

Table 2-1. Summary of the number of profiles per soil type according to the South African Classification under forestry, grassland, and the three maize cultivation systems (conventional tillage, reduced tillage and no-till) (61 profiles).

Soil type	Count				
	Forestry	Grassland	Conventional Tillage	Reduced Tillage	No-Till
Avalon (Av)				3	
Dundee (Du)			1		
Glencoe (Gc)			1		
Glenrosa (Gs)		1			
Griffin (Gf)			1	1	
Inanda (Ia)	3	1		3	1
Katspruit (Ka)		1			
Kranskop (Kp)	2	3	1	4	2
Magwa (Ma)	10	1	2		4
Nomanci (No)	6	3	2	1	1
Pinedene (Pn)		1			
Willowbrook (Wo)					1

During the 2014 sampling campaign, surface (0-5 cm) core samples were taken across the catchment to be used as prediction set for the final mapping of SOC stocks. For this purpose, a random set of 150 sampling points was generated in the catchment using QGIS 2.16 software. During sampling, every effort was made to reach these exact locations, but access was often restricted on private land, or due to terrain and vegetation. In such cases, alternative points were sampled as close as possible to the specified locations. From each predefined sampling location, a transect of 3 points was sampled along the catena at a total of 322 locations shown in Figure 2-5. At each of these locations, core samples were taken in triplicate as illustrated in Figure 2-4c.

The soils of the area have been studied intensively. This includes a study by Turner (2000), documenting the soil forms regularly found in association with the major geology formations in KZN (and Mpumalanga), as well as the range of variation sampled across the two provinces. Soils in the area have high organic carbon content ranging from 0.08 to 22.85 % (μ = 3.48 %), with clay content ranging from 3 to 34 % (μ =14.7 % clay) and pH(H_20) between 3.3 and 6.7 (μ = pH(H_20) = 4.5). Summary statistics of the SOC content, soil particle size distribution and pH

are provided in Table 2-2. The sand grade was not determined. However, based on the nature of the parent material, the sand fraction is expected to be dominated by fine sands in soil from the Volksrust and Pietermaritzburg Formation shales, and fine to medium sand in the Vryheid Formation with isolated occurrences of coarse sand (Camp, 1999; Turner, 2000). Since isolated areas with sandstone parent material were not sampled, it is assumed that sand grades for this study remain in the fine and medium sand classes.

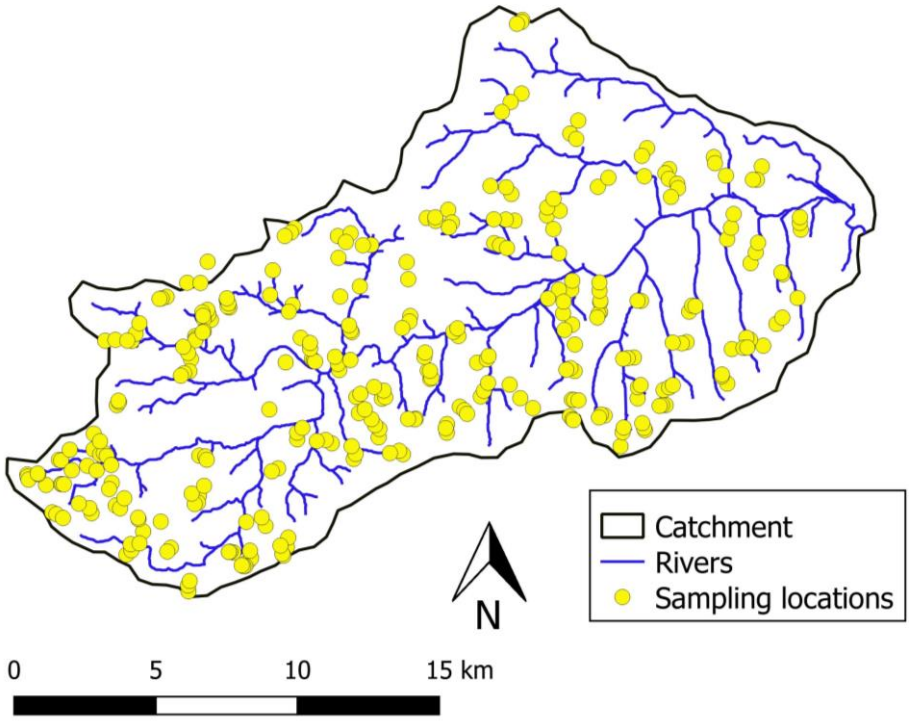

Figure 2-5. Location of the 322 sites in the quaternary catchment sampled in triplicate with 98 cm³ steel cores at 0-5 cm.

Table 2-2: Summary statistics of percentage sand, silt and clay, as well as pH for all soil samples in the study area.

	Minimum	Maximum	μ	Median	δ[a]
SOC %	0.08	22.85	3.5	2.98	2.74
% Sand	16.1	82.2	56.3	56.8	12.2
% Silt	6.1	62.1	29.0	28.7	10.4
% Clay	3.3	49.0	14.7	14.2	4.3
pH (H_20)	3.3	6.7	4.5	4.5	0.7
pH (KCl)	2.8	6.2	4.1	4.0	0.6

[a]δ = Standard deviation

3 An approach to soil carbon accounting and mapping using vertical distribution functions for known soil types[1]

3.1 Introduction

Soil organic carbon (SOC) estimates in two dimensions for large areas are increasingly in demand for climate change reporting (Mäkipää et al., 2008), but such estimates at large spatial scales and different soil depths are generally time consuming and expensive (Akumu et al., 2003; Mäkipää et al., 2008; Sleutel et al., 2003). Numerous studies in recent years have modelled the vertical distribution of SOC based on various distribution patterns, most notably exponential functions (Hilinski, 2001; Kempen et al., 2011; Minasny and McBratney, 2006; Sleutel et al., 2003). The integral of the exponential function is then used to represent the carbon storage at selected soil depths. The exponential function is generally chosen for its mathematical simplicity in conjunction with its apparent similarity to SOC decline with soil depth (Minasny and McBratney, 2006). Such modelling of SOC distribution in the soil profile enables the prediction of SOC stocks at unsampled soil depths and, if adequately developed, could reduce the need for soil sampling. The exponential decline function is generally expressed as:

$$C = C_0 \cdot e^{-kz} \qquad (3\text{-}1)$$

where the SOC content, C, is related to the SOC concentration at the soil surface (C_0) and decreases at a rate of k to depth z (Russell and Moore, 1968).

The aim of this Chapter was to fit and group exponential vertical distribution functions for SOC stocks upon normalizing values observed throughout the soil profile by the SOC content close to soil surface (0-5cm layer). This approach assumes that the SOC content at any depth, under relatively stable vegetation conditions, can be functionally related to the concentration at the soil surface in the absence of major recent disturbances (e.g. landslides, soil stock piling, etc.). This would reduce the number of required observations for carbon accounting to one point close to the soil surface. The integral of the exponential SOC distribution function would then be applied in a spatial environment to map the two-dimensional distribution of SOC

[1] The material presented in this chapter is reproduced with minor changes from a prior publication: Wiese, Liesl; Ros, Ignacio; Rozanov, Andrei; Boshoff, Adriaan; Clercq, Willem de; Seifert, Thomas (2016): An approach to soil carbon accounting and mapping using vertical distribution functions for known soil types. In *Geoderma* 263, pp. 264–273. DOI: 10.1016/j.geoderma.2015.07.012.

stocks.

3.2 Materials and Methods

3.2.1 Test area for SOC mapping

A test area for SOC stock mapping was selected as a collection of sub-catchments in the southwestern part of the quaternary catchment as shown in Figure 3-1. This area was selected based on the availability of proprietary digital, geo-referenced soil point data (1:10 000 scale) provided by Mondi Forests (Pty) Ltd for its properties located in the study catchment. For each soil point, data were available for effective rooting depth (ERD) and soil type according to the Taxonomic Soil Classification system of South Africa (Soil Classification working group, 1991). This data was necessary for the development of interpolated ERD and soil type maps for SOC stock mapping as discussed in Section 3.2.3.

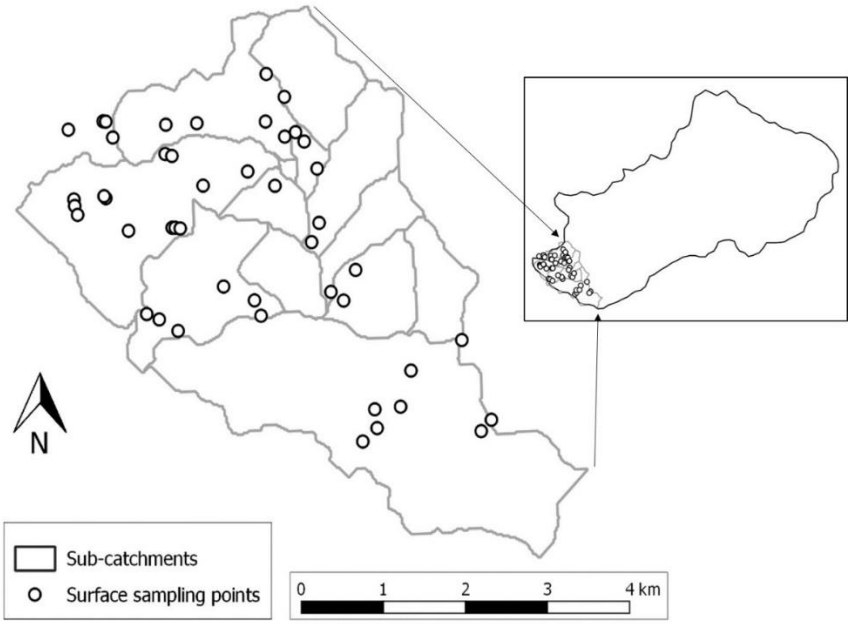

Figure 3-1. The test area for SOC stock mapping showing the locations of 40 random sampling points for surface (0-5 cm) core samples. The inset map indicates the location of test site and sampling points in the quaternary catchment.

3.2.2 Soil samples and analyses

Soil samples from 38 of the 69 sampled profiles as described in Chapter 2 were used. This included 6 profiles in grasslands, 12 in cultivated land and 20 in forest plantations, yielding a total of 948 samples from 316 sampling positions. A summary of the number of profiles with the same South African classification is given in Table 3-1, along with the corresponding

grouping according to Soil Taxonomy (Soil Survey Staff, 2014) and World Reference Base (WRB) Classification (IUSS Working group WRB, 2014).

Table 3-1. Summary of number of profiles per soil type used in this Chapter according to the South African Classification, as well as the corresponding Soil Taxonomy and WRB Classification.

SA soil type (Mapping code)		Count	Soil Taxonomy	WRB
Avalon	(Av)	3	Plinthic Haplustox	Plinthic Ferralsol
Glencoe	(Gc)	1	Petroferric Haplustox	Petroplinthic Ferralsol
Griffin	(Gf)	1	Typic Haplustox	Haplic Ferralsol
Inanda	(Ia)	6	Humic Rhodic Haplustox	Umbric Rhodic Ferralsol
Katspruit	(Ka)	1	Typic Endoaquent	Umbric Gleysol
Kranskop	(Kp)	7	Humic Haplustox	Umbric Ferralsol
Magwa	(Ma)	10	Humic Xanthic Haplustox	Umbric Xanthic Ferralsol
Nomanci	(No)	8	Lithic Humlustept	Skeletic Umbrisol
Pinedene	(Pn)	1	Oxyaquic Haplustox	Oxyaquic Xanthic Ferralsol

Triplicate core samples were oven-dried at 90 °C, weighed and bulk density (ρ_b) determined as the mass of oven-dried soil per unit bulk volume ($Mg.m^{-3}$) (Robertson and Paul, 2000). Mean ρ_b values were calculated per sampling depth from triplicates for further data analysis.

Following ρ_b analysis, triplicate samples were combined to give one composite sample per soil depth. Fine roots were manually removed, following which samples were pounded and sieved to 2 mm and the coarse (gravel) fraction content gravimetrically determined, when present.

Subsamples of the 2 mm fraction were ball-milled to < 0.5 mm for total SOC [$\%_{wt}$] which was determined by DC gas chromatography elemental analysis as in the method outlined by Nelson and Sommers (1974) using a EuroVector EA 3000 elemental analyser at Stellenbosch University. Since the soils do not contain inorganic carbon, the total carbon results obtained by DC constitutes total SOC.

The < 2 mm samples were scanned once to acquire the near-infrared (NIR) reflectance spectral characteristics using a Bruker MPA (Multi-Purpose Analyser) with a quartz beam

splitter and RT-PbS detector. The reflectance of the samples was measured from 12500 to 3600 cm^{-1} (800 – 2778 nm) at 1 cm^{-1} using a rotating macro sample sphere at 128 scans per sample. The software OPUS 7.2.139.1294 supplied with the Bruker MPA was used for spectral data collection. The OPUS statistical Quant2 module was used to optimize and calibrate the raw NIR reflectance spectra using the DC SOC values ranging from 0.18 to 22.85 %.

An NIR spectral library was developed from these analyses using a subset of 313 samples as calibration set and the remaining 86 samples as validation test set. Results from the calibration and validation tests were considered sufficient for this exercise, with a validation R^2 value of 0.9237, a root mean square error of prediction (RMSEP) of 0.982 and a ratio of performance deviation (RPD) of 3.62.

The volumetric SOC content (*Cv*) was calculated as

$$Cv\ [kg \cdot m^{-3}] = 10 \cdot SOC\ [\%_{wt}] \cdot \rho_b\ [Mg \cdot m^{-3}] \qquad (3\text{-}2)$$

The *Cv* value was corrected for stone content, where present as:

$$Cv = Cv_{(2mm)} \cdot (1 - S_m \cdot \rho_b / \rho_s) \qquad (3\text{-}3)$$

where $Cv_{(2mm)}$ is the volumetric carbon content in the < 2 mm fraction, S_m is the mass fraction of stones in the bulk sample determined gravimetrically, and ρ_s = 2.65 $Mg \cdot m^{-3}$.

The $\sum Cv \cdot \Delta z$, where Δz is a depth increment, was used to calculate carbon stocks per profile within the sampled depth intervals for model calibration.

Soil surface core samples (0-5 cm) from 40 of the 322 sampling positions described in Chapter 2 were used for the interpolation of a *Cv* raster data layer. These samples were selected from grassland and plantation areas in the mapping test site as shown in Figure 3-1. In these samples the ρ_b and stone content (where present) were again determined gravimetrically, while the SOC content in the < 2mm fraction was determined only by NIR spectroscopy using the methods and NIR calibration set described above.

3.2.3 Interpolation of mapping layers

A 20 m digital elevation model (DEM) derived from contour data obtained from South African Surveys and Mapping was used, as well as a set of sub catchments developed within the study area for a separate hydrological study using QGIS/SAGA tools. The DEM was used to derive slope and curvature layers for use as covariates for kriging interpolation of soil data.

Interpolation of the surface volumetric SOC values from 45 surface sampling points (40 surface samples and 5 surface samples obtained from profiles) was performed in ArcMap 10.1 using ordinary kriging with the DEM, slope and curvature as covariates. The ERD values were interpolated from the proprietary 100 m grid soil survey point dataset mentioned above using the same co-kriging procedure to improve predictions for areas outside the mapped compartments. The same co-kriging procedure was used to interpolate the exponential coefficients (*k*-values) characterizing soil type. Details of *k*-value derivation and association with soil types are described in Section 3.4.1.

Uncertainties of interpolated and subsequent maps were not calculated and are not shown or discussed in this Chapter. Estimates of the propagated error and map accuracy are presented and discussed in Chapter 6 as part of the overall estimation of errors incurred in SOC modelling and mapping across the quaternary catchment.

3.3 Results and Discussion

3.3.1 Vertical SOC distribution

For all 38 profiles, *Cv* vs depth functions were plotted using MS Excel 2013. Each individual profile in this set was characterized by the best-fit exponential decline function, though it was evident that in some instances the fit was poor based on visual observation and R^2 values < 0.5. The general exponential decline of SOC with soil depth has been confirmed in many studies (Hilinski, 2001; Kempen et al., 2011; Kulmatiski et al., 2003; Minasny and McBratney, 2006; Mishra et al., 2009; Sleutel et al., 2003). However, the zone of higher SOC variability in the first 30 cm may lead to a poor exponential fit in individual profiles (Beaudette et al., 2013). The stratified averaging of SOC concentration values for all the studied profiles (mean values calculated for each fixed depth increment) confirmed that the general pattern for the area may be well approximated to such exponential decline of SOC with depth as shown in Figure 3-2 and Table 3-2.

Distribution of bulk density values (ρ_b) followed the opposite trend and was approximated to a logarithmic function with asymptotic line at 1m depth (Figure 3-3).

A combination of the models for SOC and ρ_b may have been used to model and predict the carbon stocks, but that would require the collection of bulk density samples to a depth of 1 m for all future predictions. Such a requirement was used, for example, in the Century model (Porter et al., 2009) which relies on two values of SOC and ρ_b determined at depths of 0 cm

and 1 m to calculate SOC content in the profile. To avoid this, *Cv* values were calculated for each sample and modelled separately. The distribution of *Cv* [kg·m^{-3}] with depth, or 10x multiplication product of SOC(z) and $\rho_b(z)$ functions (using Eq. 3-2) remains strongly exponential (Figure 3-4) due to the large difference in values of the exponential and logarithmic coefficients.

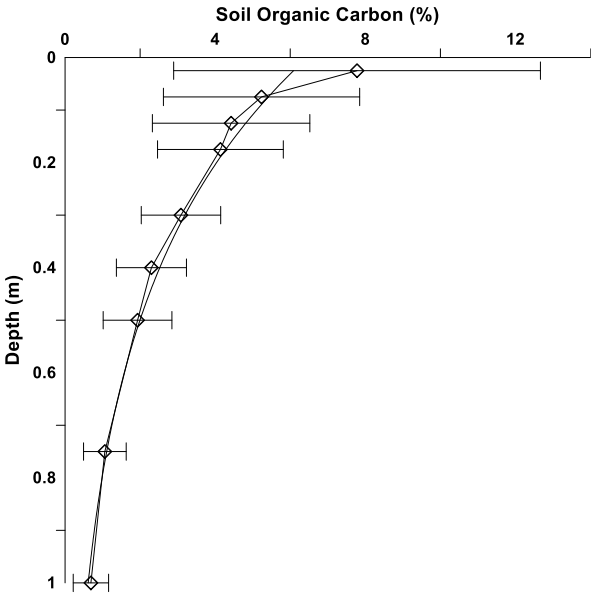

Figure 3-2. Fitting the distribution of SOC vs depth using exponential functions for stratified mean values. The dashed line connects the data points, the solid line represents the fitted exponential trendline, and the error bars indicate the standard deviations. The model parameters are summarized in Table 3-2.

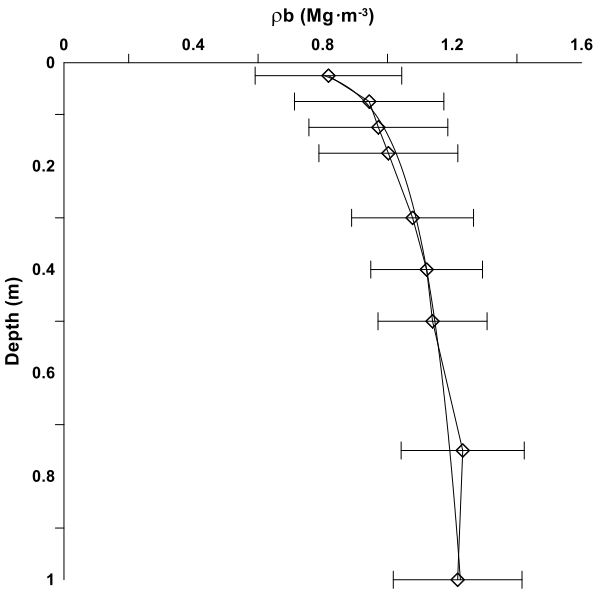

Figure 3-3. Fitting the distribution of bulk density vs depth using a logarithmic function for stratified mean values. The dashed line connects the data points, the solid line represents the fitted exponential trendline, and the error bars indicate the standard deviations. The model parameters are summarized in Table 3-2.

Table 3-2. Model parameters for the averaged distribution of SOC, ρ_b and Cv_s for 38 profiles, stratified by depth (z).

Parameter	μ - δ	μ	μ + δ
SOC [$\%_{wt}$]	$SOC = 3.59e^{-2.665z}$ $R^2 = 0.98$	$SOC = 6.46e^{-2.349z}$ $R^2 = 0.98$	$SOC = 9.32e^{-2.262z}$ $R^2 = 0.95$
ρ_b ($Mg \cdot m^{-3}$)	$\rho_b = 0.1285\ln(z) + 1.05$ $R^2 = 0.98$	$\rho_b = 0.1140\ln(z) + 1.23$ $R^2 = 0.98$	$\rho_b = 0.0995\ln(z) + 1.40$ $R^2 = 0.95$
Cv_s	$Cv_s = 1.2144e^{-1.544z}$ $R^2 = 0.992$	$Cv_s = 1.0175e^{-1.826z}$ $R^2 = 0.9944$	$Cv_s = 0.8293e^{-2.424x}$ $R^2 = 0.9933$

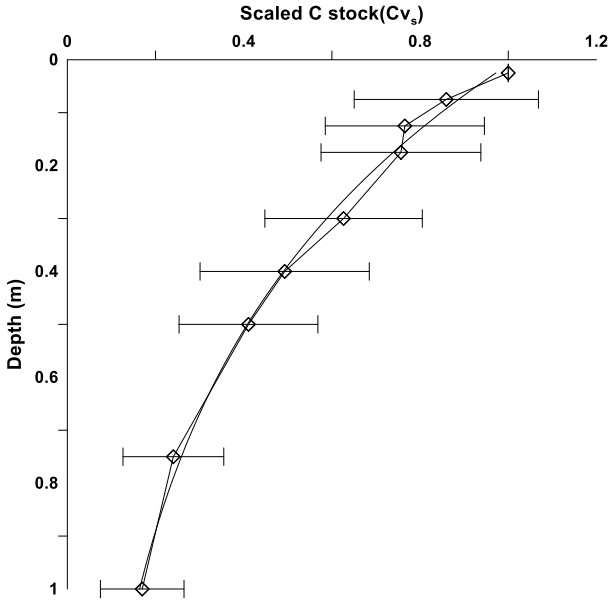

Figure 3-4. Fitting the distribution of Cv_s vs depth using an exponential function for stratified mean value. The dashed line connects the data points, the solid line represents the fitted exponential trendline, and the error bars indicate the standard deviations. The model parameters are summarized in Table 3-2.

Cv values for each profile were normalized by the value of C_v^0 - the value of the volumetric SOC content in the surface (0-5 cm) sample of the specific profile. The common normalization (scaling) procedure which produces values in the range of 0 - 1, is

$$Cv_{si} = \frac{Cv_i - Cv_{min}}{Cv_{max} - Cv_{min}} \qquad (3\text{-}4)$$

where Cv_{si} is the scaled volumetric carbon (no unit) at depth *i*, Cv_i is the volumetric carbon at depth *i*, and Cv_{min} and Cv_{max} are the minimum and maximum values of volumetric carbon

respectively for the specific profile. Based on the assumption of exponential decline in SOC with depth, the value for Cv_{max} in Eq. 3-2 was substituted for C_v^0 which is the volumetric carbon content at a depth of 2.5 cm (0-5 cm sample). In addition, the value for Cv_{min} at infinite soil depth was assumed to be zero (0), hence Eq. 3-4 was simplified and applied as

$$Cv_{si} = \frac{Cv_i}{C_v^0} \qquad (3\text{-}5)$$

Vertical Cv_s distribution functions were fitted to individual profiles by plotting Cv_s against sampling depth (z), fitting an exponential trendline (Figure 3-4) and setting the y-intercept to 1. This gives an exponential decline function of

$$Cv_s = e^{-kz} \qquad (3\text{-}6)$$

where e is the exponential function, k is the exponential coefficient describing the rate of change and z is the soil depth. From Eq. 3-6, a k-value was obtained for each soil profile.

Since actual (measured) values for Cv were available for the sampled depth increments per profile, the cumulative SOC stocks for those increments were calculated as the sum of the definite integrals per depth increment:

$$\int_{z_1}^{z_2} C_v^0 \cdot e^{-kz}\, dz = \frac{C_v^0}{k} \cdot \left(e^{-kz_1} - e^{-kz_2}\right) \qquad (3\text{-}7)$$

where z_1 and z_2 are the respective depths at the bottom and top boundaries of the soil core during sampling. A further k'-value was determined per profile which is the exponent coefficient perfectly describing the hypothetical curve with area equalling the measured SOC stock, using the above integral and the known volumetric SOC content from core samples per profile. However, since this integral could not be solved for k' algebraically, values for k' were determined by manual iterative substitution until the value of measured SOC was obtained.

For the 38 profiles combined, the mean Cv_s plotted against soil depth (Figure 3-4) gives an exponential coefficient k of 1.798 (R^2 = 0.9941) when the y-intercept of the exponential function is set to 1. This suggests that a single k-value may be used to predict SOC stocks in soils regardless of soil type or land use. Variation in exponential functions fitted to individual profiles, with y-intercepts set to 1, showed R^2 values ranging from 0.6034 to 0.9547. The respective k-values ranged from 0.820 to 3.891 with a mean of 2.049 and standard deviation of 0.6927. There was a clear difference in k-values obtained from averaging the Cv_s values per

soil depth and plotting these means against depth (Figure 3-4) to obtain a single *k*-value (1.798), compared to averaging individual *k*-values from the different profiles (*k* = 2.049). Individual *k*-values were therefore submitted to statistical analysis.

To capture the natural variation in SOC distribution in different profiles, *k* and *k'* values needed to be grouped according to either land use or soil type to enable joining of resulting correlation coefficients to Mondi soil data for mapping purposes. Since the correlation coefficient *k* showed a normal distribution (using Shapiro-Wilk, Anderson-Darling, Lilliefors and Jarque-Bera tests), an analysis of covariance (ANCOVA) of *k* and *k'* was done as a function of land use and soil type respectively. As summarised in Table 3-3, the regression of *k* based on soil type covariance provided higher accuracy compared to land use. As a result, soil type was used as clustering criteria for *k* and *k'* grouping as summarized in Table 3-4.

In a similar instance Khalil et al. (2013) developed land cover specific and soil type specific exponential models to predict vertical SOC content. The land cover specific models showed very high prediction power with depth and very little variation in SOC within land cover when compared to the soil type specific models. However, due to over- and under-estimations of SOC in greater soil groups within a specific land cover class, they elected to use soil type specific models to estimate SOC concentration (%) to 1 m.

Table 3-3. Goodness of fit statistics for the regression of k using analysis of covariance of k' and k with land use and soil type.

Statistic	Land Use	Soil type
R^2	0.64	0.81
RMSE	0.44	0.35

Soil profiles were grouped according to the nine represented soil types (Av, Gc, Gf, Ia, Ka, Kp, Ma, No and Pn) and *k* and *k'* values averaged per soil type. Four of the nine soil types (Gc, Gf, Ka and Pn) occurred only once and no mean *k* or *k'* was calculated. K-means clustering was run on the mean *k* and *k'* values using Trace (W) as clustering criterion to minimize the within-group sum-of-squares across all variables and identify the best groupings according to soil type. Clustering into five classes (as shown in Table 3-4) was used to determine how the single soil types grouped with multi-replicated soil types (Gc/Av, Gf/Kp, and Pn/Ma). An exception was accepted for the Ka soil type which only had one replicate and fell into a separate class due to its G-horizon and association with wetness. The Ia/No class was split into two by moving

the Nomanci form to a sixth class due to its generally shallow characteristics resulting from minimal development of the B horizon in weathering rock.

Table 3-4. Results of k-means clustering into 5 classes using k with k' per soil type using Trace (W) as clustering criterion.

				5 Classes	[a]6 Classes
Soil type	Topsoil	Subsoil		Class	Class
Av	Orthic	Yellow-brown apedal B	Soft plinthic	1	1
Gc	Orthic	Yellow-brown apedal B	Hard plinthic	1	1
Gf	Orthic	Yellow-brown apedal B	Red apedal B	2	2
Kp	Humic	Yellow-brown apedal B	Red apedal B	2	2
Ia	Humic	Red apedal B	unspecified	3	3
No	Humic	Lithocutanic B		3	6
Ka	Orthic	G horizon		4	4
Ma	Humic	Yellow-brown apedal B	unspecified	5	5
Pn	Orthic	Yellow-brown apedal B	Unspecified with signs of wetness	5	5

[a]The Nomanci soil type was separated from the Inanda to form a sixth class.

The digital soil dataset contained an additional two soil types, Glenrosa (Gs) and Westleigh (We) which were both grouped with Av/Gc. In the case of Gs, this was due to the orthic A horizon and expected gradual decrease in SOC from the A to B horizon, as well as the depth limiting factors of weathering parent material (Gs) and soft plinthite (Av) B horizons. Westleigh, on the other hand, has a soft plinthic B horizon as does Av and hence groups well with this class.

Variations in k and k' for the final soil type classes is shown in Figure 3-5. With k' representing the actual exponential coefficient to obtain measured vertical SOC stocks, $k > k'$ would result in an underestimation of carbon stocks, with $k < k'$ resulting in an overestimation. From Figure 3-5, underestimation of C stocks using k is expected in soil type groups of Av/Gc, Gf/Kp and No ($k > k'$), with slight overestimation in the Ia and Ma/Pn groups ($k < k'$).

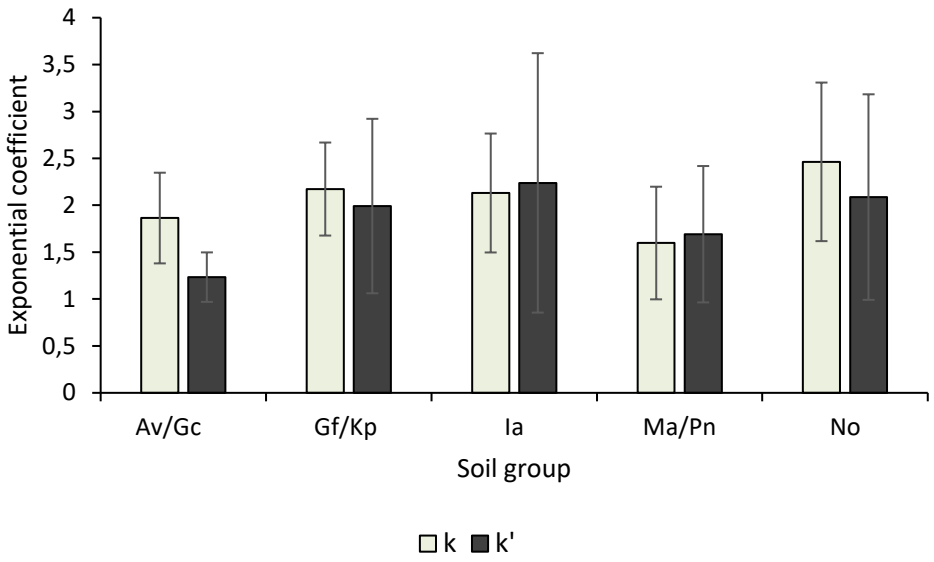

Figure 3-5. Mean exponential coefficients k and k' for soil groups, with bars indicating their standard deviations.

Using Eq. 3-7, the model was validated for accurately predicting the mean SOC stocks [kg·m^{-2}] per soil type or group of soil types, as well as the full data set (Table 3-5). Although the model predicts the means fairly accurately, it does so at the expense of increased standard deviation (reduced precision). The comparison was conducted as follows: The sum of all measured core-sampled Cv values per profile was compared to the sum of integrals of the exponential functions with coefficients listed in Table 3-5 for the same depth increments (0-20, 27.5 - 32.5, 37.5 - 42.5, 47.5 - 52.5, 73.5 - 77.5, 97.5 - 102.5 cm) or to soil depth restricting layer.

In this case the calculation of regression coefficients to predict stocks in individual profiles is meaningless with R^2 close to 0, since regression is tested against the mean hypothesis. However, the relative error estimate per group resulting from regression analysis may be of interest. The predictive capabilities of the *k* and *k'* classes were compared by linear regression of measured incremental SOC content per profile with predicted values using the two mean *k*-values (1.798 and 2.049), as well as the different classes for *k* and *k'*. Results show a reduction in prediction error when *k* and *k'* values are grouped according to soil types compared to using a single *k*-value for all profiles. As expected, predictions using *k'* values have a slightly lower root mean square error (RMSE = 4.068) compared to *k*-value predictions (RMSE = 4.199) (Table 3-6).

Table 3-5. Regression results for the prediction of SOC stock [kg·m^{-2}] using different* k *and* k' *groupings (μ = mean; δ = standard deviation).

	Measured SOC stock	**Stock Predicted with k=2.049**	**Stock Predicted with k=1.798**	**Stock Predicted with class k**	**Stock Predicted with class k'**
μ [kg·m^{-2}]	13.45	14.295	13.94	13.30	13.61
δ	2.66	5.009	4.51	4.40	4.27

Table 3-6. Step-wise reduction in prediction error by using soil classification and depth-distribution parameter optimization (k') of cumulative carbon stocks for the sampled depth increments using three different exponential coefficients.

	Value			
Statistic	[a]*k* = 2.049	[b]*k* = 1.798	[c]Class *k*	[d]Class *k'*
RMSE	5.227	4.412	4.199	4.068

[a]An exponential coefficient of 2.049 was used to predict the cumulative C stock for all 38 profiles by averaging best-fit exponential curve coefficients for individual profiles.

[b]An exponential coefficient of 1.798 was used to predict the cumulative C stock for all 38 profiles by stratified averaging of SOC stocks per depth increment.

[c]The exponential coefficient *k* was applied according to the six soil type classes.

[d]The exponential coefficient *k'* was applied according to the six soil type classes.

3.3.2 Modelling and mapping SOC

Cumulative SOC stocks from the soil surface (z = 0) to selected depths (z) were calculated using the definite integral

$$\int_0^z C_v^0 \cdot e^{-kz}\, dz = \frac{C_v^0}{k} \cdot \left(1 - e^{-kz}\right) \qquad (3\text{-}8)$$

Spatial raster layers were created through kriging interpolation at 20m resolution for each of the variables in Eq. 3-8 (C_v^0, z and k) to map the spatial distribution of cumulative SOC stocks to selected soil depths.

For soil depth (z), effective rooting depth (ERD) data was used from the Mondi soil dataset, using values of ERD ≤ 1 m. All values of ERD > 1 were assigned a value of 1. The Mondi dataset was clipped to selected sub-catchments in the test area with an approximately 1 km buffer zone defined manually by interactive digitizing to include points lying outside the area of

interest for better interpolation results. ERD values were co-kriged to the extent of the dataset with inputs of DEM, slope and curvature using ordinary kriging with default settings in ArcMap 10.1.

To develop raster layers for exponential coefficients, the coefficients *k* and *k'* were related to soil types in the clipped soils data. A lookup table was created based on soil type and associated mean *k* and *k'* values (Table 3-7) which was joined to the Mondi soil point data, yielding *k* and *k'* values for each sampling point. Raster layers for *k* and *k'* were subsequently developed by ordinary kriging of the Mondi point data to the extent of the data itself using the same inputs and parameters as for the ERD layer.

Table 3-7. Lookup table indicating* k *and* k' *values associated with soil types in the Mondi soil data.

Soil type	*k*	*k'*
Av/Gs/We	1.8638	1.2336
Ia	2.1308	2.2388
Ka	2.9430	3.1636
Kp	2.1731	1.9916
Ma/Pn	1.5975	1.6911
No	2.4629	2.0872

A collection of sub catchments was used to identify an eastern boundary for mapping purposes which encompass the geographic sampling points from Mondi and the additional surface samples within the quaternary catchment (U40A). The raster layers for C_v^0, ERD, *k* and *k'* were masked to the extent of overlap between the sub catchments, C_v^0, and the clipped Mondi data to define the final test mapping area.

Masked raster layers for C_v^0, ERD and *k'* are presented in Figure 3-6 to Figure 3-8. Although the C_v^0 (Figure 3-6) ranges from 39 to 91 kg·m^{-3}, the sampling density did not allow for a high level of detail in its distribution. In comparison the ERD layer (Figure 3-7), which ranges in value from 0.3 to 1 m, shows a clearer distinction of values as a result of a much higher sampling density.

The somewhat stratified appearance of the C_v^0 layer roughly mimics the elevation trend in the area. The effect of land use is evident in this case, since forest plantations mostly occur

on steeper slopes and higher lying areas. Higher C_v^0 values therefore also correspond to the higher organic matter inputs found in this land use in the form of leaf litter and fine root turnover.

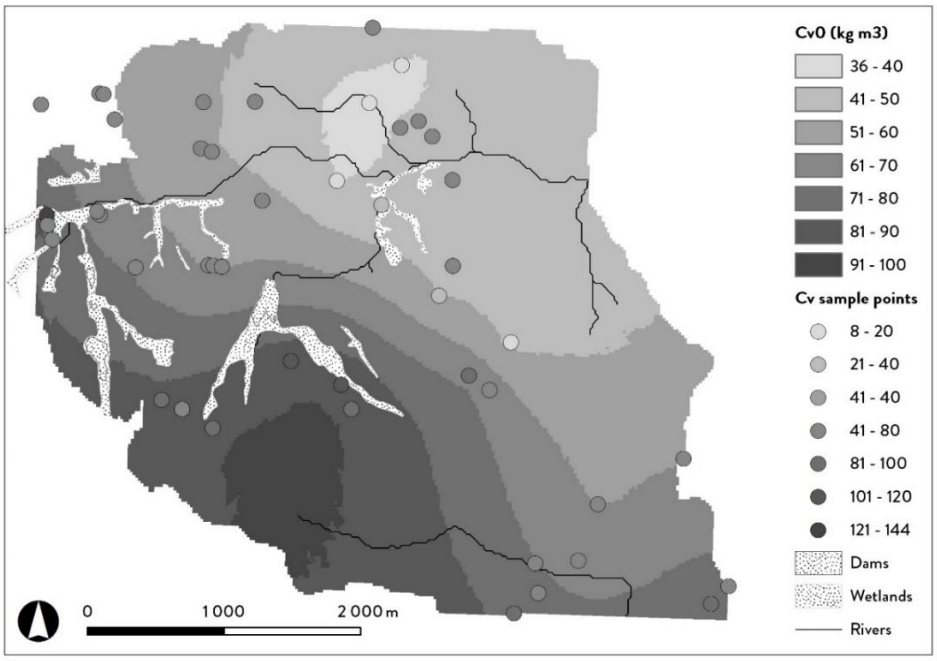

Figure 3-6. The C_v^0 raster layer showing the location of the surface (2.5 cm) sampling points and their relative* Cv *values, as well as the dams and wetlands in the mapping area.

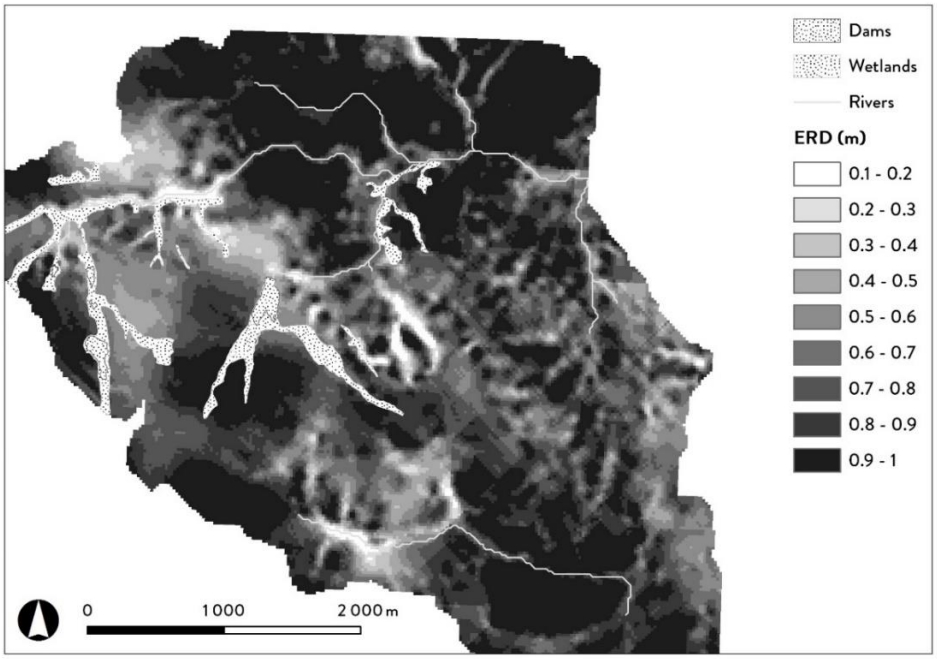

Figure 3-7. The ERD raster layer with depths ranging from 0 to 1 m. Dams, wetlands and rivers in the mapping area are indicated.

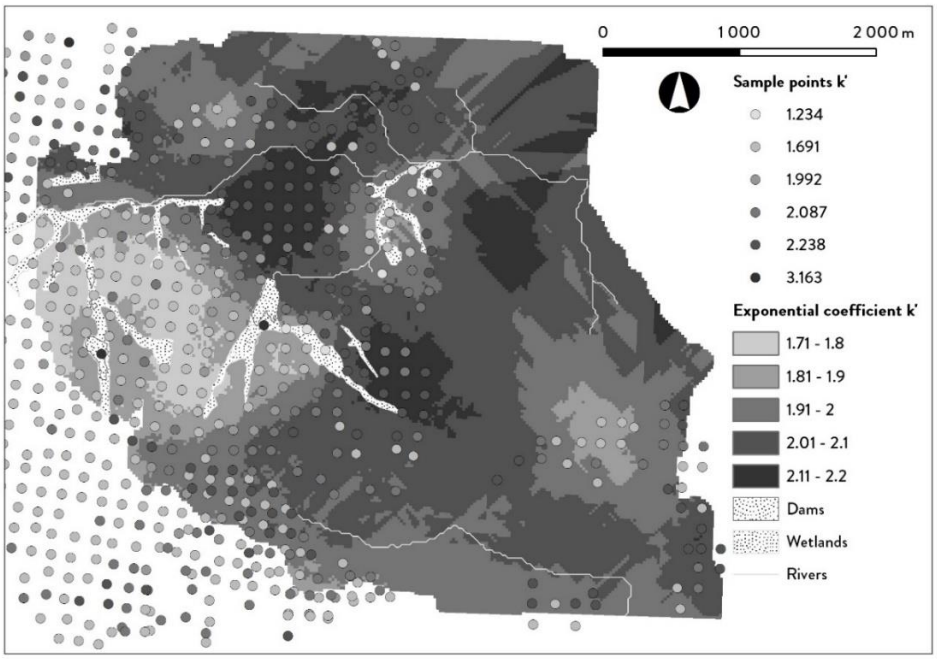

Figure 3-8. The k' raster layer showing the soil grid samples (sample points) from the Mondi dataset to which k' values were linked according to soil type and used for ordinary kriging.

Maps of vertical SOC stock distribution were generated by calculating Eq. 3-8 using the generated raster layers (Figure 3-9 and Figure 3-10). Although, the use of ERD in calculations increases the map variability and introduces more detail (Figure 3-9), one could assume that soil organic matter may be found below such depth, and most likely in concentrations following the exponential distribution pattern. Sampling the fractured and weathered rocks with usual soil surveyor's tools is particularly difficult, and in this case, modelling may be of greater importance. The map in Figure 3-10 ignores the limiting effects of weathered/fractured rock and simulates carbon stocks down to 1 m depth throughout the catchment assuming that the organic material is accumulated in the fractures instead of being dispersed in the soil matrix. Such accumulation, though not proven, may be following the quantitative pattern of distribution with depth observed in unconsolidated materials. A similar assumption was made by Heim et al. (2009) based on the findings of Kulmatiski et al. (2003) who found that the depth distribution of SOC stocks were well described by an exponential model in the presence of stones.

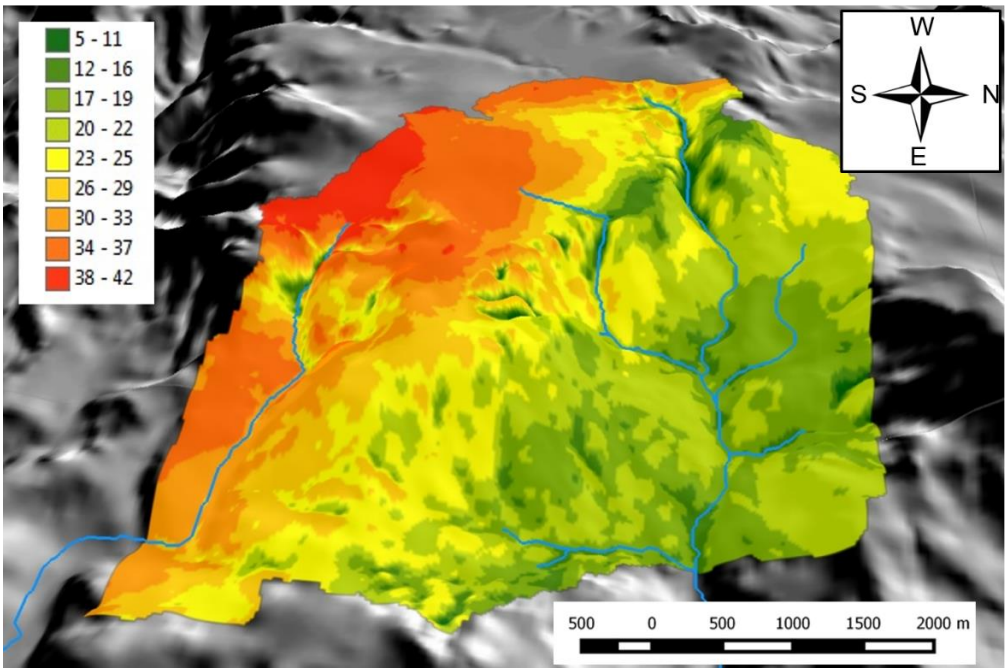

***Figure 3-9. Map of cumulative SOC stocks to ERD depth using* k'.**

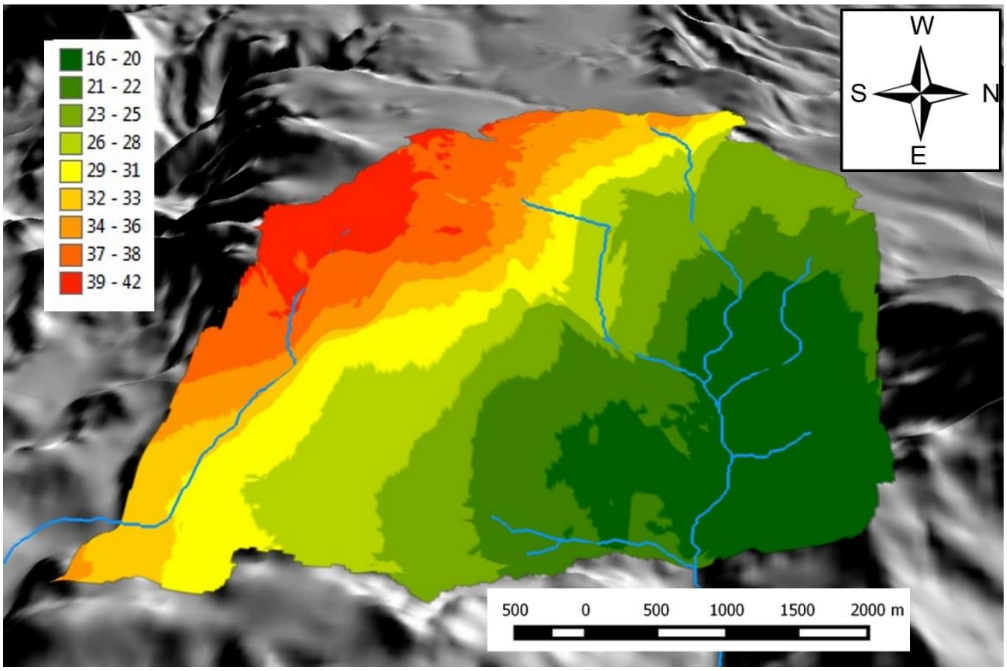

***Figure 3-10. Map of cumulative SOC stocks to 1 m depth using* k'.**

3.4 Conclusions

For soils characterized by exponential decline in SOC content with depth, normalization of the volumetric SOC (Cv) vertical distribution curve by the C_v^0 allowed isolation of the rate of SOC decline for several groups of soils in the study catchment expressed as the *k'* coefficient specific to each group. The confidence level for *k*' coefficients is numerically characterized by

standard deviation, and in combination with measured C_v^0 value may be used for mapping and monitoring carbon stocks over large areas, where soil survey results are available. Since the C_v^0 values are measured, the uncertainty is largely associated with the C_v^0 measurement error, the standard deviation of *k* (or *k'*) values, the density of C_v^0 observations and their interpolation. It was shown that the two independent variables, namely the volumetric carbon content at the soil surface (C_v^0) and the coefficient (*k* or *k'*) are sufficient for mapping and monitoring soil carbon stocks in the areas covered by soil survey.

Due to the natural variation and random mixing processes in soil, particularly pronounced in cultivated fields, no soil exhibits a perfect exponential distribution of SOC content, though stratified averaging has produced very good correlations to characterize the group as a whole by mean values of *k* (k') and their standard deviations.

The overall assessment of uncertainty of the final maps is a complex matter, due to accumulation of errors stemming from analytical errors and method accuracy, the stochastic nature of the depth-distribution model and ending with errors associated with point interpolation. Solutions to these problems are addressed in Chapter 6.

The approach suggested here requires further testing and verification, but may become a useful tool for monitoring SOC dynamics with reduced need for sampling and analysis.

4 Assessing SOC vertical distribution functions for on-farm carbon stock quantification: a case study of maize production systems in the Mvoti River catchment, South Africa

4.1 Introduction

Changes in land cultivation practices, particularly the introduction of no-till systems, are often seen as a way to achieve substantial increases in SOC stocks on cultivated land (Lal, 2018). Initiatives like 4‰ (Minasny et al., 2017) see such changes as a tool to mitigate the increases of CO_2 in the atmosphere. Research on the effect of different land use on soil organic carbon (SOC) stocks is increasing, especially to assess the effect of land use or soil management on SOC losses and/or gains through carbon sequestration. Soil organic carbon forms an integral part of the global carbon cycle (Batjes, 2014; Paustian et al., 1997) and plays an important role in soil fertility, structure, hydrology and microbial health, and hence agricultural productivity and sustainability. In addition, soil provides a potential sink for the sequestration of atmospheric CO_2 to support climate change mitigation efforts (Paustian et al., 1997).

Assessing SOC stock often includes measuring and modelling its vertical distribution in the soil profile to enable carbon accounting and three-dimensional mapping. However, such estimates of vertical SOC distribution are often time consuming and expensive, especially at larger spatial scales, at different soil depths, and when including soil bulk density measurements to enable SOC stock calculations (Akumu and McLaughlin, 2013; Allen et al., 2010; Bai et al., 2016; Mäkipää et al., 2008; Sleutel et al., 2003). Some of the recent attempts to reduce the cost of analysis include various proximal sensing techniques for determining soil bulk density, stone percentage and SOC content in soil cores (Lobsey and Viscarra Rossel, 2016). However, such an approach still requires at least one-meter-deep coring throughout the survey area. Modelling vertical SOC distribution has been done using various distribution patterns such as exponential, power, spline and logarithmic functions (Bai et al., 2016; Bernoux et al., 1998; Chai et al., 2015; Dorji et al., 2014a; Hobley and Wilson, 2016; Kempen et al., 2011; Liu et al., 2016; Minasny et al., 2006; Mishra et al., 2009; Ottoy et al., 2016; Sleutel et al., 2003; Wiese et al., 2016).

In order to reduce the need for soil sampling and analysis in SOC stock assessments, Wiese et al. (2016) suggested modelling vertical SOC distribution using an exponential decline

function and calculating its integral to predict SOC stocks at unsampled soil depths using only samples from the soil surface. To achieve this, SOC stock values observed throughout the profile were normalized by the SOC content close to the soil surface (0-5 cm layer). The resulting vertical distribution functions from 38 profiles were grouped as a function of land use (forest plantation, grassland and cultivated soils) and soil type, assuming that SOC content at any depth can be functionally related to the concentration at the soil surface. This assumption is subject to relatively stable vegetation conditions and no major recent disturbances such as landslides and soil stock piling. The profile groupings revealed that the regression of the exponential coefficient based on soil type provided higher accuracy compared to land use.

In cultivated soils however, especially in cases of conventional or full-tillage, soil in the tillage layer is thoroughly mixed which leads to an almost constant SOC concentration to the depth of tillage (Liu et al., 2016; Meersmans et al., 2009). Even a single ploughing of long term (20 or more years) no-till fields with a mouldboard plough has been shown to homogenize SOC through the ploughed profile and remove SOC stratification (Stockfisch et al., 1999; VandenBygaart and Kay, 2004). No-tillage practices, on the other hand, are often seen to stratify SOC distribution in the upper soil layer (Dolan et al., 2006; Paustian et al., 1997b). Since the upper 30 cm of soil has been found to contain an average of up to 50 % or more of the SOC for different vegetation types (Wang et al., 2004; Brahim et al., 2014), accurate estimation of SOC content in this soil layer is crucial in considering the total amount of SOC in 1 meter of soil.

The objective of this study was to find the best possible continuous functions describing the vertical distribution of SOC under different intensities of cultivation, so that a single surface sample would be sufficient to estimate the stocks down to various depths (20, 30, 100 cm) in order to reduce the cost of carbon accounting in agricultural fields. It was hypothesised that, at farm level, sufficiently robust vertical distribution models may be developed level from a small (<10) number of profile observations with frequent depth sampling increments per established land use system practiced at the specific location for a period longer than ten years (stable in medium-term).

4.2 Materials and Methods

4.2.1 Farming systems and soils

Three farming systems were selected as treatments based on the main tillage methods

applied for maize production as: i) no tillage (NT), ii) reduced tillage (RT) and conventional tillage (CT). The soil carbon was assessed relative to native grasslands (GL) sampled at different locations in and around the catchment as shown in Figure 4-1. The dispersed location of grasslands was used based on the assumption that the vertical distribution of SOC under native grasslands in the study area would exhibit an average exponential decline regardless of their location. The method and depth of soil disturbance was of main interest, therefore each farming system as a whole was considered as a treatment. The implements used and depths of soil disturbance are summarized in Table 4-1 Individual procedures or applications are not considered as separate treatments since all farmers would annually assess the need for tillage and inputs based on climate, costs, soil analyses, availability of seeds, exchange rates, market prices and more.

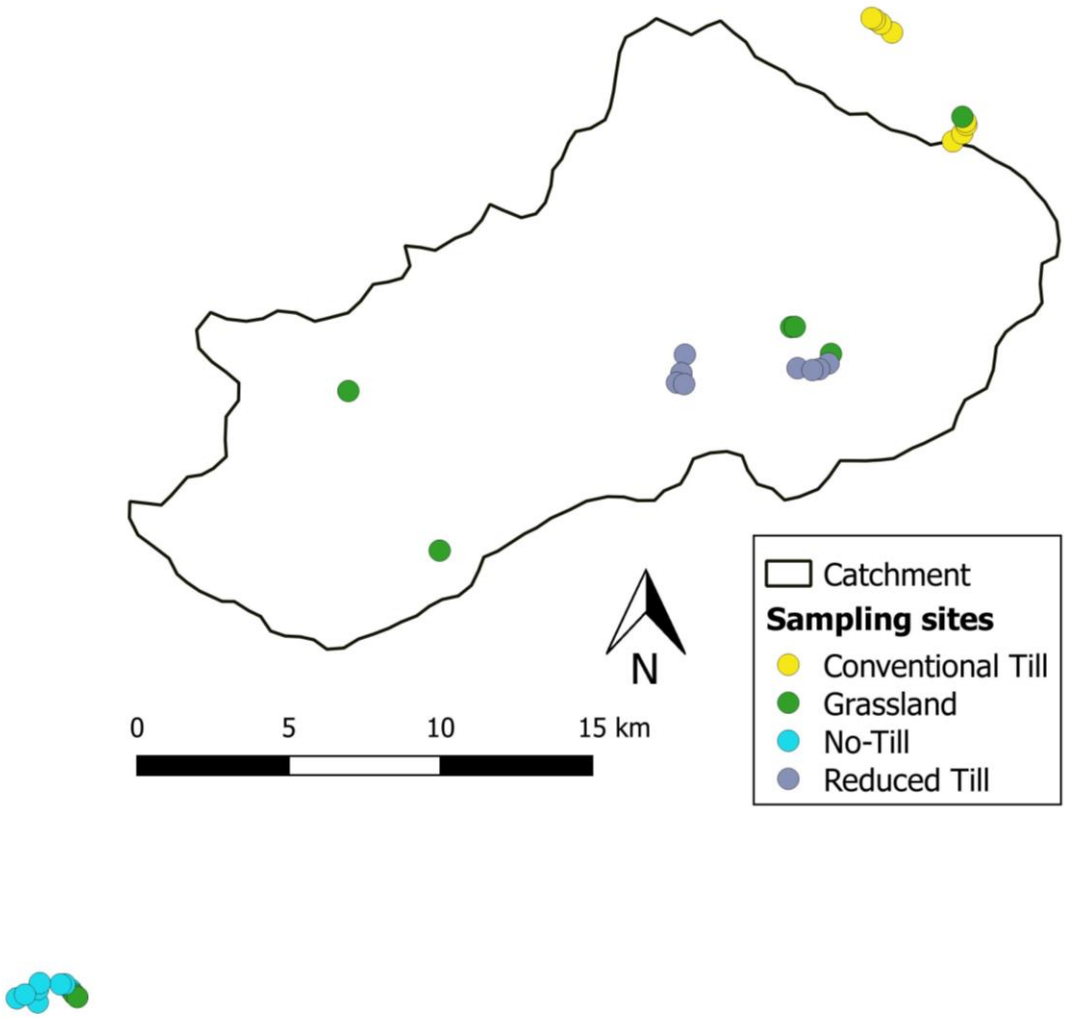

Figure 4-1. Locations of the sampling sites in and around the quaternary catchment. Land uses and management systems are differentiated by colour for the different sampling sites.

Table 4-1. Summary of the implements used and depth of soil disturbance under the different maize farming systems.

	Farming system		
Implement	No tillage	Reduced tillage	Conventional tillage
No till planter	10 cm	25 cm	
Conventional planter			10 cm
Aeration implement	15 cm		
Ripper		[a]45 cm	50 cm
Disc Harrow		10 cm	15 cm
Mouldboard plough			20 cm

[a] Deep ripping was only applied on one of two RT farms following maize harvest.

4.2.1.1 No-till system

A no-till (NT) system was observed on a mixed dairy/maize farm where maize was grown using no-till for 10 to 17 years on different fields. Prior to implementing no-till, the farm was under conventional tillage using deep ripping, ploughing and disking each year prior to planting, as well as incorporation of plant residues with a disc implement after harvesting. The three NT fields sampled in this study were converted from conventional tillage 17, 15 and 12 years prior to sampling.

Maize is planted in early October depending on the soil water status using a no-till planter. After harvesting in May, rye is sown within two weeks as a cover crop and later grazed by cattle. One year prior to sampling, the usually undisturbed soil was aerated for the first time since no-till was adopted. The farmer used an implement designed for this purpose: it loosens the soil to a depth of 15 cm with a steel rod which runs horizontally under the soil surface. This implement is used only when the farmer considers it necessary to address the soil compaction problem. Since the adoption of no-till practices, plant residues from both maize and rye are left on the soil surface and are not incorporated in any way.

Lime is applied on all fields using a tractor-drawn spreader every three years at a rate of 2-3 tons·ha^{-1} depending on the lime requirement of the specific field. Lime is not worked into the soil following application. Nitrogen is always applied as urea at an annual rate of 130-150 kg N·ha^{-1} during the maize growing season. The first nitrogen application is band-placed during planting with a no-till planter at the rate of 40-50 kg N·ha$^{-1.}$ After maize emergence, top dressing is split into two applications of 60-70 kg N·ha^{-1} each.

When no-till was first adopted, maize was rotated with soybeans every other year or once every four years. This rotation was stopped eight years prior to sampling because soybean is not a priority feed for dairy cattle. Maize is primarily used for silage.

4.2.1.2 Reduced tillage

Two farms where varying degrees of soil disturbance occur through reduced tillage (RT) are included in this category and assessed as one treatment. On both farms a disc implement is used prior to planting to prepare the seedbed and incorporate some of the previous season's stubble and plant residue. Oats are planted as cover crop on maize fields within two weeks after maize harvest and grazed by cattle upon maturity. Chemical weed control is applied once per year. Both farmers in this category consider their farming operations to fit the description of reduced tillage based on the systems described below.

On the first RT farm, maize cultivation was initiated just over 10 years prior to sampling, following a complete no-till strategy for the first 5 years. Prior to that, all fields were used for vegetable production using conventional tillage including deep ripping and ploughing each season. Three years into the no-till maize-producing period the build-up of plant residue volume on the soil surface was considered excessive due to slow decomposition. The formation of an O horizon became an obstruction for the direct seeding tine. As a result, the farmer opted to adopt an annual reduced tillage system two years later to incorporate some of the stubble and plant residue into the soil prior to planting. Two months prior to planting a special disc implement penetrating 10 cm into the soil incorporates some of the previous season's plant residue as a part of seedbed preparation. Maize is planted by direct seeding with a no-till planter with a tine in front of the seed dispenser that penetrates the soil to a depth of 25 cm.

Lime on all fields was last applied 7 years prior to sampling at the rate of 2.5 tons·ha^{-1}. Following application with a tractor-drawn spreader, lime was ploughed into the soil to a depth of 25-30 cm. Total annual nitrogen application is 150-160 kg·ha^{-1} split into four applications. At planting the first application is band-placed with the seeds in the form of urea at the rate of 40 kg N·ha^{-1}. Topdressing occurs in three applications using a spreader at a rate of 40 kg N·ha^{-1}. The first top dress is applied two weeks after plant emergence, the second top dress is applied two weeks later and the third application two weeks after the second topdressing.

On the second RT farm a form of reduced tillage has been practiced for the last 10 years

prior to sampling in a maize-soybean rotation system. The farmer would choose the crop to plant each year based on an assessment of the soybean and maize prices. During the last 10 years, however, soybeans were planted at least once every four years. Soil would be disturbed twice a year using two different implements.

The first soil disturbance occurs during maize planting with a no-till planter equipped with tines penetrating the soil to a depth of 25 cm. Cattle would graze the fields as much as possible following each year's harvest to remove most of the plant residues and stubble prior to ripping. In extreme cases, if the stubble and weeds were too much even for the cattle, fields would be burned prior to planting. The second disturbance occurs after maize harvest as part of seedbed preparation for the next season using an implement which is a combination between a ripper and a roller. It has coulters on the front to cut through stubble, followed by ripper blades to break the soil to a depth of 45 cm, and finally a roller at the back, which will break up soil clods and incorporate the stubble into the soil. This implement is not used after soybean harvest due to the reduced volume of stubble on the soil surface compared to maize harvest which rendered it unnecessary. During dry years the ripping action created soil clods on the surface which the roller was not strong enough to break. In such cases a disc implement penetrating 10 cm into the soil would be used to break up the clods prior to planting.

Lime requirement for individual fields is assessed at the beginning of each season. The average amount of lime applied annually was 3 tons·ha^{-1}, but differs from year to year according to the specific requirement. Lime would be applied with a spreader, following which the soil is ripped and disked using the same implements described above. To minimize soil disturbance, lime application would be synchronized as much as possible with annual post-harvest tillage.

Fertilizer applications are split into two, one with planting and a second as topdressing within the first two months after plant emergence. At planting, fertilizer is band placed with seeds, usually as NPK (4:3:4). The second application is applied with a spreader as limestone ammonium nitrate (LAN), a mixture of dolomitic lime and NH_4NO_3. The aim is to apply a total of 180 kg of N·ha^{-1} per season split into two applications of 90 kg nitrogen each as described above.

4.2.1.3 Conventional tillage

A farm specializing in maize seed production has been under conventional tillage for more than 15 years. Soybean rotation is incorporated into the production at least every four years

following maize, but there is no fixed rotation schedule.

After the first rains during late winter or early spring, a mouldboard plough is used to plough to a depth of 20 cm. Fields will be further disc harrowed to 15 cm at least once to incorporate stubble and prepare the seedbed: break up the clods and incorporate the stubble. However, in most cases at least two disc harrow passes are preferred prior to planting in early summer. Soil would not be ploughed following a soybean crop.

After harvest in May to June each year, all fields are ripped, followed by disc harrowing to sufficiently aerate the subsoil and break up clods on the soil surface. In fields where maize has been planted in the previous season, ripping will be done to a depth of 50 cm.

Crop residues (both maize and soybean) are incorporated into the soil each year using the disc harrow. Normally soybeans will yield less residues compared to maize. As a result, the usual ripping will be applied after soybean harvest and only one disc harrowing operation in preparation for maize planting the following year.

Chemical weed control is applied once a year. For both maize and soybeans the planter disturbs the soil to a depth of 10 cm.

A total of 150 kg N·ha^{-1} is applied per growing season split into two applications. The first 20-30 kg N·ha^{-1} is band-placed at planting as a mixture of granular urea and monoammonium phosphate. Top dressing is applied six weeks after planting using a tractor-drawn spreader at a rate of 100-120 kg N·ha^{-1} as granular urea.

Lime is applied as required with the last two applications occurring on selected fields 6 years prior to sampling. When required, lime is applied at a rate of 2 tons·ha^{-1} using a tractor-drawn spreader followed by incorporation with a disc harrow.

4.2.2 Soil sampling and analysis

Thirty-two (32) of the 69 soil profiles sampled as discussed in Chapter 2 were used - eight profiles in each of the following land use systems, NT, RT (4 in each of the two RT farms), CT and GL.

All samples were prepared and analysed as described in Chapter 3 for bulk density (ρ_b) [Mg·m^{-3}] stone content and SOC [$\%_{wt}$] (by dry combustion). As described by Wiese et al. (2016) (Chapter 3), the volumetric SOC content (*Cv*) was calculated for each composite sample as

$$Cv\ [kg \cdot m^{-3}] = 10 \cdot SOC\ [\%_{wt}] \cdot \rho_b\ [Mg \cdot m^{-3}] \quad 4\text{-}1$$

where stone was present, the *Cv* value was corrected as

$$Cv = Cv_{(2mm)} \cdot (1 - S_m \cdot \rho_b / \rho_s) \quad 4\text{-}2$$

where: $Cv_{(2mm)}$ is the volumetric carbon content in the < 2mm fraction, S_m is the gravimetrically determined mass fraction of stone in the bulk sample, and ρ_s = 2.65 $Mg \cdot m^{-3}$. Carbon stocks within the sampled depth intervals were calculated as $\sum Cv \cdot \Delta z$, where Δz is the sampling depth increment.

4.2.3 Modelling vertical SOC distribution

Vertical SOC distribution was modelled and scaled to a value between 0 and 1 as described by Wiese et al. (2016) (Chapter 3), following five steps. In step one, *Cv* values were normalized for each profile by the value of volumetric SOC content in the 0-5 cm sample (C_v^0) to yield Cv_s for each sample. This normalization of the SOC stock distribution curve enables the development of a simple exponential equation to describe the SOC stock distribution. In step two, Cv_s was plotted against sampling depth (*z*) for each profile and the best-fit exponential trendline was fitted using MS Excel 2016, setting the y-intercept to 1. Setting the y-intercept to 1 enabled step 3 in which a value for the exponential coefficient (*k*) was obtained from the trendline equation for each profile. In step 4 cumulative SOC stocks for the sampled depths were calculated as the sum of the definite integrals per depth increment using measured *Cv* values in

$$\int_{z_1}^{z_2} C_v^0 \cdot e^{-kz}\, dz = \frac{C_v^0}{k} \cdot \left(e^{-kz_1} - e^{-kz_2}\right) \quad 4\text{-}3$$

where C_v^0 is the volumetric carbon content at a depth of 2.5 cm (0-5 cm sample), *e* is the exponential function, *k* is the exponential coefficient, and z_1 and z_2 are the respective depths at the bottom and top boundaries of the soil core during sampling. In step 5 a *k'*-value per profile was determined by manual iterative substitution as the exponential coefficient that perfectly describes the hypothetical curve with area equalling the measured SOC stock.

4.2.4 Comparing k and k' values

Prior to statistical analysis, all *k* and *k'* values were transformed using a natural log transformation to ensure a normal distribution of *k* using Shapiro–Wilk, Anderson–Darling, Lilliefors and Jarque–Bera tests. Transformed values were tested for variance using a Fischer's

F-test, and tested for significant differences between treatments using Student's two-sample t-tests. Student's two-sample paired t-tests were applied to evaluate the mean of *k'* against the mean of *k* within the four treatments.

4.2.5 Averaging k and k' values

Profiles were clustered into five groups as follows: i) all cultivated profiles combined (NT+RT+CT); and ii) each of the four land use types as a separate group (GL, NT, RT, and CT). Single *k* values for these five groups were obtained in two ways. In the first instance, a single *k* value per group was obtained from fitted exponential trendlines as in the case of single profiles (referred to as "from graphs"). To obtain this single value, a stratified mean of SOC stocks was obtained by calculating the mean Cv_s for each fixed depth increment within each group of profiles. The mean Cv_s values per group were plotted against sampling depth and an exponential trendline was fitted.

4.3 Results and Discussion

4.3.1 Comparing k and k' values

Testing of variance in *k* and *k'* values using a Fischer's F-test indicated no significant differences in variance for *k* values between the four treatments. Variance in *k'* values were significantly different only between the RT and CT treatments.

Comparison of *k* and *k'* values between the four treatments using Student's two-sample t-test shows that the means for both *k* and *k'* under GL and NT are significantly different from those under RT and CT (Table 4-2). This implies that the average rate of exponential decline in SOC stocks under GL and NT is significantly different from the average exponential decline in RT and CT, both in terms of modelled SOC distribution (*k*) and SOC decline using measured stocks (*k'*). This further indicates that all cultivated fields do not display the same exponential decline in SOC stocks as a function of the farming system applied. In addition, results suggest that no-till farming systems may mimic the SOC stock distribution under natural grasslands.

Results of Student's two-sample paired t-test analysis of *k'* against *k* within the four treatments showed no significant differences between the means of *k* and *k'* for the GL and NT treatments. This indicates that there is no significant difference between the mean modelled (*k*) and mean measured (*k'*) exponential decline in SOC stocks under GL or NT, so the SOC distribution may be well described by *k*. For RT and CT, however, the means of *k* and *k'* were significantly different with p-values of 0.013 and 0.009, respectively. The mean

modelled exponential decline in SOC (*k*) was therefore significantly different from the mean measured SOC stock decline. This implies that the model *k* did not sufficiently describe the measured SOC distribution under RT or CT.

Table 4-2. Summary of p-values for differences between means of k and k' values between the four treatments. Values in bold indicate significant differences for α=0.05.

	k			*k'*		
Treatment	GL	NT	RT	GL	NT	RT
NT	0.331			0.726		
RT	**0.001**	**0.026**		**0.004**	**0.004**	
CT	**0.002**	**0.042**	0.680	**0.002**	**0.003**	0.111

4.3.2 Averaging k and k' values

The variation of Cv_s (volumetric SOC content scaled between 0 and 1) with depth in the 24 cultivated profiles is presented in Figure 4-2 and the fitted exponential functions for the four single treatment groups in Figure 4-2. In order to simplify the exponential equations obtained from the trendlines in Figure 4-2, the y-intercept for each trendline was set to 1. Table 4-3 presents the exponential equations for the five groups, with and without the y-intercept set to 1. From Table 4-3, a single *k*-value was obtained for each group.

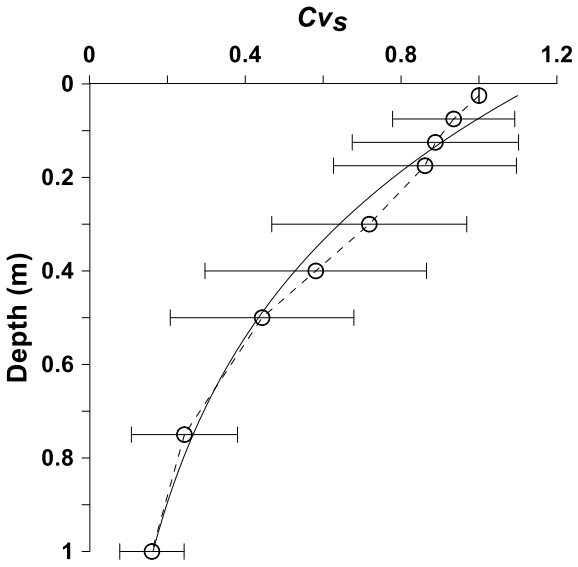

Figure 4-2. Variation in the distribution of Cv_s with depth in all cultivated profiles for stratified mean values with error bars indicating the standard deviation (δ). The dashed line connects the data points and the solid line represents the fitted exponential trendline.

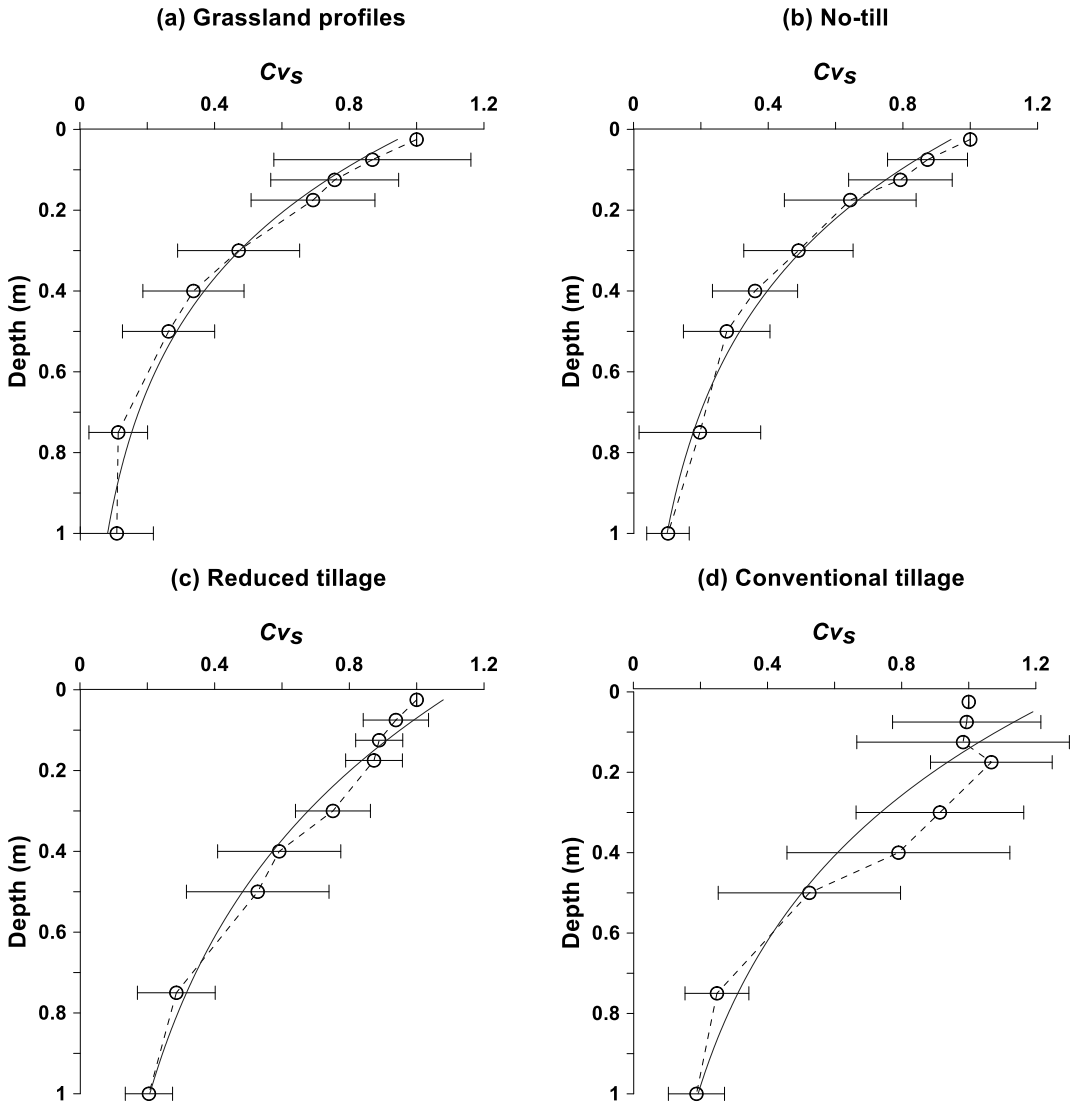

Figure 4-3. Fitted exponential trendlines (solid lines) with error bars indicating the standard deviation for the single treatment groups of eight profiles each. Dashed lines indicate lines connecting the data points.

Table 4-3. Summary of exponential equations obtained from Figure 4-2 and Figure 4-3 (y-intercepts not equal to 1) and simplified equations with y-intercepts set to 1 for the different treatment groups.

Treatment group	[a]n	y-intercept ≠ 1		y-intercept = 1	
		Equation	R^2	Equation	R^2
All cultivated	24	$y = 1.1542e^{-1.957z}$	0.98	$y = e^{-1.73z}$	0.96
Grassland	8	$y = 1.0041e^{-2.502z}$	0.96	$y = e^{-2.495z}$	0.96
No-till	8	$y = 0.9989e^{-2.305z}$	0.99	$y = e^{-2.307z}$	0.99
Reduced tillage	8	$y = 1.1256e^{-1.692z}$	0.98	$y = e^{-1.505z}$	0.96
Conventional tillage	8	$y = 1.3098e^{-1.915z}$	0.93	$y = e^{-1.488z}$	0.85

[a] n = number of profiles

In the second instance, single values of both *k* and *k'* were obtained for each of the five groups by calculating the mean *k* and *k'* values for profiles within each group (referred to as "profile means"). These mean *k* and *k'* values are presented with summary statistics in Table 4-4.

Table 4-4. Summary statistics (n = number of profiles; μ = mean; δ = standard deviation) of k and k' values for 0-100 cm profiles per treatment group obtained from mean values per group.

Treatment		*k*			*k'*		
Group	n	μ	Median	δ	μ	Median	δ
All cultivated	24	1.90	1.76	0.81	1.52	1.38	0.96
Grassland	8	2.97	3.18	0.82	2.68	2.46	1.18
No-till	8	2.57	2.36	1.00	2.43	2.06	0.99
Reduced tillage	8	1.54	1.67	0.47	1.25	1.25	0.41
Conventional tillage	8	1.63	1.51	0.47	0.88	0.75	0.63

From Figure 4-2 it is evident that for GL and NT the exponential distribution closely mimics the actual distribution of the data points and the y-intercepts of these trendlines are close to 1 (Table 4-3). For the combination of all cultivated fields (NT+RT+CT), as well as the RT and CT treatments the y-intercepts for the trendlines deviate further from 1 (Table 4-3) and there is a marked difference between the exponential functions and the data points (Figure 4-3 and Figure 4-2 and d). In these cases, the applied exponential function does therefore not sufficiently describe the decline in SOC stocks from the soil surface. This difference is especially clear for CT. For the combination of all cultivated fields, this implies that using one *k* value to model the decline in SOC stocks in cultivated soils of different management types may not sufficiently capture the variation in these soils. More specifically, it would predict a larger than observed decline in NT and RT soils, while predicting a smaller than observed decline in CT soils. As a result, the profiles for the RT and CT groups were subjected to further analysis by creating separate plots on the same graph of Cv_s against sampling depth (z) for the 0-30 cm and 30-100 cm sections respectively. The best-fit linear trendline was fitted to each 0-30 cm section and the y-intercept was set to 1, yielding the linear decline equation

$$Cv_s = 1 - bz \qquad 4\text{-}4$$

where *b* is the trendline gradient. The best-fit exponential trendlines were fitted to the 30-100 cm sections as presented in Figure 4-4. The resulting piecewise functions are presented in Table 4-5, from which it is observed that for CT the linear distribution of SOC in the upper 30 cm has a near-constant distribution with a *b* value of 0.1165 and R^2 of 0.13.

Figure 4-5 shows that under CT, the values of normalized SOC stocks (Cv_s) for samples at all depth intervals in the 5-30 cm layer (5-10; 10-15; 15-20; 27.5-32.5 cm) (n=32) from eight soil profiles are normally distributed. The mean value converges to 1 (0.99) with a standard deviation of 0.24. From this it can be concluded that within the conventionally cultivated fields the SOC stocks throughout the plough layer are independent of sampling depth and the mean SOC stocks measured at the surface (0-5 cm) on average are equal to carbon stocks measured at any other depth between 0-30 cm within the 5cm intervals. Subsequently the distribution of normalized volumetric SOC stocks under CT at any sampling location in this depth range can be approximated as $Cv_s = 1 \pm 0.24$. For purposes of this study, this equation was simplified to assume constant SOC stock in the 0-30 cm layer under CT with mean $Cv = C_v^0$ at any sampling depth in this layer. The same was found by Meersmans et al. (2009) and Ottoy et al. (2016) when modelling SOC distribution with depth in croplands. In both instances the authors found that SOC remained constant until the tillage depth, from where it declined exponentially with depth. In these instances, the SOC value nearest to the soil surface was used to calculate the constant value for the tillage layer. Also Liu et al. (2016) observed that, for cultivated soils, the soil organic matter concentration in the tillage layer was usually almost constant to the tillage depth resulting from frequent mixing of the topsoil. As a result, they modelled SOM stock in the topsoil using a linear function, defining a slope of 0 for cultivated soils.

The procedure of splitting profile graphs into 0-30 cm and 30-100 cm plots was applied to all individual profiles under RT and CT. The y-intercept for the linear trendlines (0-30 cm) were set to 1, while the y-intercept for the 30-100 cm exponential functions were set to 1.3 for RT profiles and 1.85 for CT profiles to match those from Table 4-5 and ensure uniformity. Unique profile values for *b* and *k* were obtained from the respective trendline equations. As was done for full (0-100 cm) profiles, *k'* values were determined by manual iterative substitution for the 30-100 cm exponential trendline of each profile.

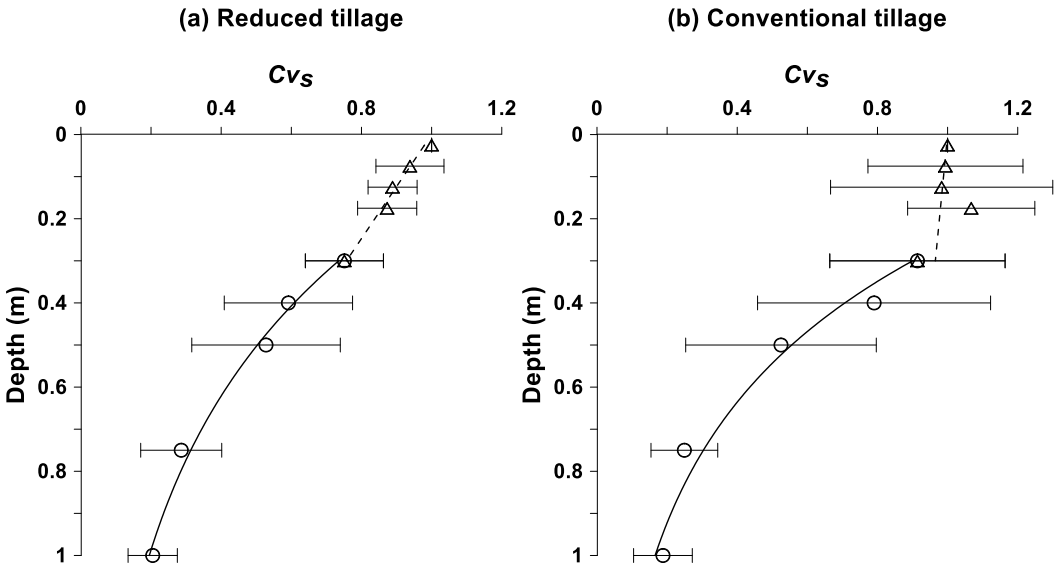

Figure 4-4. Separate modelling of normalized SOC stocks for 0-30 cm (Δ) and 30-100 cm (○) sections for the profiles under reduced and conventional tillage. Dashed lines indicate fitted linear functions (y-intercepts set to 1), solid lines indicate fitted exponential functions, and error bars indicated standards deviations. Trendline equations are presented in Table 4-5.

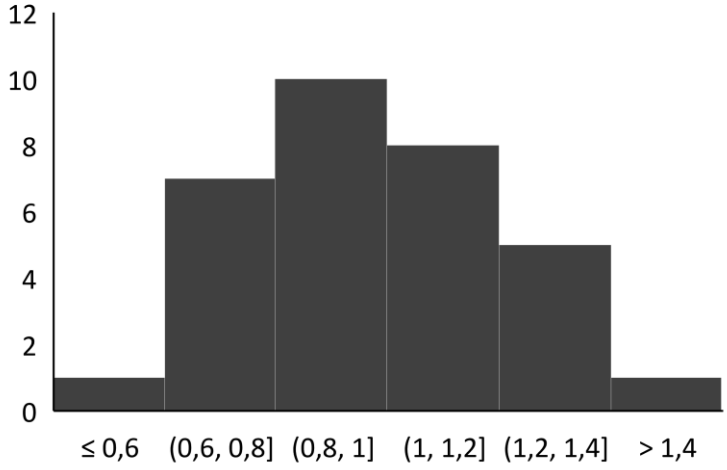

Figure 4-5. Histogram of Cvs distribution for the 32 samples in the first 5-30 cm (0-5, 5-10; 10-15; 15-20; 27.5-32.5 cm) from eight soil profiles in the conventional tillage system.

Table 4-5. Summary of linear (0-30 cm) and exponential (30-100 cm) equations obtained from Figure 4-4. For linear equations the y-intercept was set to 1 for both treatment groups.

Treatment group	Piecewise Functions
Reduced tillage	$y = \begin{cases} 1 - 0.8094z \text{ if } 0 \leq z \leq 30 \text{ cm; } R^2 = 0.98 \\ 1.3e^{-1.897z} \; if \; 30 \leq z \leq 100 \text{ cm; } R^2 = 0.99 \end{cases}$
Conventional tillage	$y = \begin{cases} 1 - 0.1165z \text{ if } 0 \leq z \leq 30 \text{ cm; } R^2 = 0.13 \\ 1.85e^{-2.41z} \; if \; 30 \leq z \leq 100 \text{ cm; } R^2 = 0.96 \end{cases}$

For the 0-30 cm sections, the cumulative SOC stocks for the sampled depths in RT and CT were calculated as the sum of the definite integrals per depth increment using measured *Cv* values as

$$\int_{z_1}^{z_2} C_v^0 \cdot (1 - bz)dz = C_v^0 \cdot \left(\left(z_2 - \frac{b(z_2)^2}{2}\right) - \left(z_1 - \frac{b(z_1)^2}{2}\right)\right) \quad 4\text{-}5$$

Using Eq. 4-3, *b'* values were determined by manual iterative substitution for the 0-30 cm linear trendlines as the line gradient that perfectly describes the hypothetical curve with area equalling the measured SOC stock.

Single *b*, *b'*, *k*, and *k'* values were determined for the RT and CT treatment groups by calculating the mean *b*, *b'*, *k* and *k'* values for profiles within each group as presented in Table 4-6. From Table 4-6 it is evident that for CT profiles the value of *b'* approaches zero at 0.060, which further supports the use of a constant SOC stock for the 0-30 cm section under this tillage system. Based on the earlier assumption that SOC stock under CT is constant as mean *Cv* = C_v^0 at any sampling depth in this layer, values for *b* and *b'* were assumed to be zero (0) under conventional tillage.

Table 4-6. Summary statistics of b and b' values for 0-30 cm sections, as well as k and k' values for 30-100 cm sections under RT and CT obtained from mean values per treatment. (n = number of profiles; μ = mean; δ = standard deviation)

	0-30 cm						
Land use System	*b*				*b'*		
	n	μ	Median	δ	μ	Median	δ
Reduced tillage	8	0.81	0.79	0.31	0.78	0.73	0.37
Conventional tillage	8	0.12	0.03	0.85	0.06	0.08	1.10
	30-100 cm						
	k				*k'*		
	n	μ	Median	δ	μ	Median	δ
Reduced tillage	8	1.96	2.13	0.48	1.34	1.49	0.34
Conventional tillage	8	2.74	2.54	0.67	2.23	2.28	0.39

4.3.3 Calculating SOC stocks

The various model values for *b*, *b'*, *k* and *k'* were used to calculate SOC stocks at each sampling depth in the appropriate land use systems using the same 32 profiles as for model development. The model robustness was tested by the comparison of *k* and *k'* values, as well as *b* and *b'* values.

Since values of *k'* and *b'* were selected such as to predict the sum of the measured stocks per profile correctly for all the sampled increments, the lack of significant difference between *k* and *k'* (or *b* and *b'*) indicates that the model adequately describes the vertical distribution for calculation of SOC stocks with specified accuracy (defined by standard deviation). Applying the model parameters obtained from graphs for each separate treatment group sufficiently predicted the SOC stocks as presented in Figure 4-6.

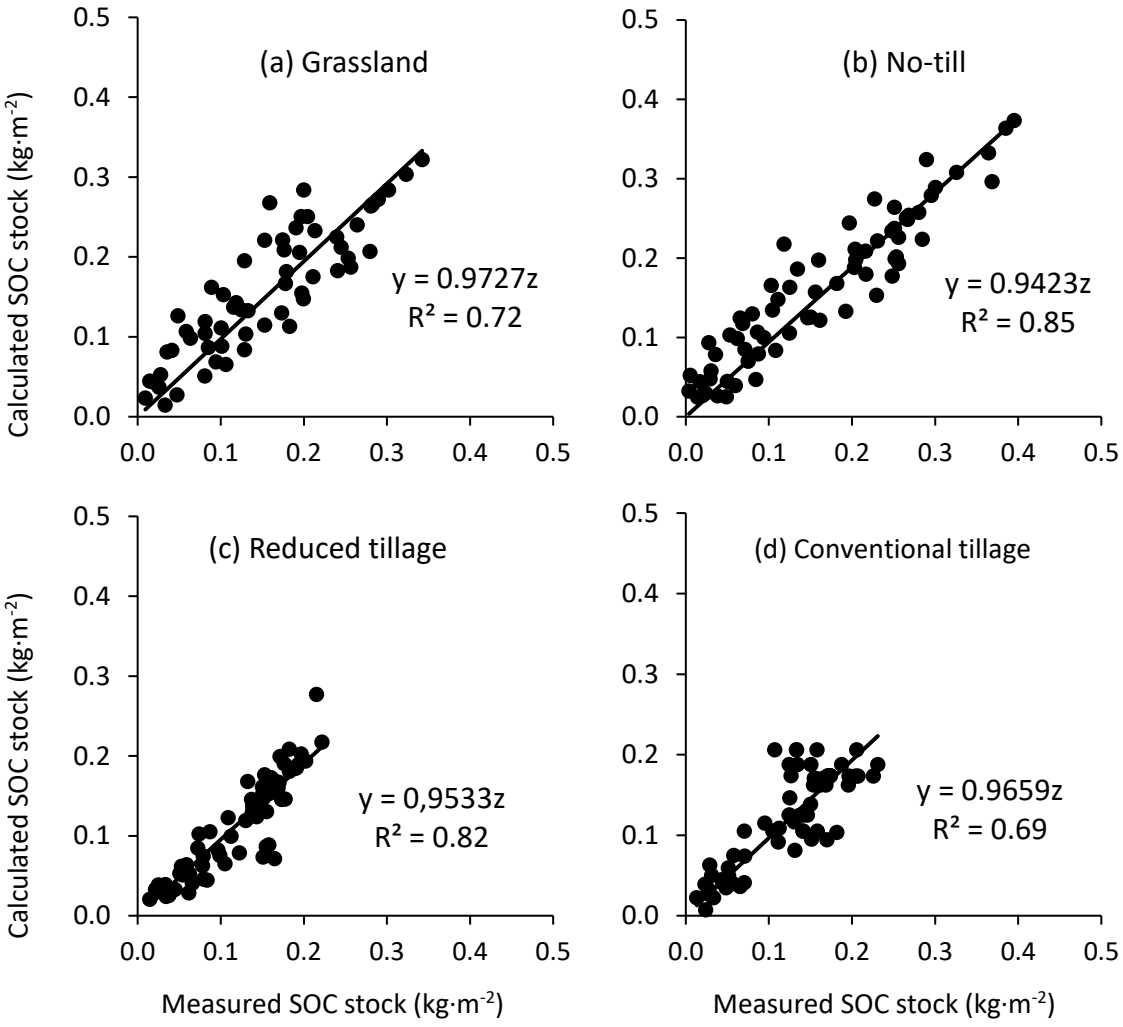

Figure 4-6. Regression plots of predicted vs observed SOC stocks (kg·m^{-2}) under different land use systems. SOC stocks were calculated using relevant b and k values from graphs per land use system.

In Figure 4-6 the linear regression equations were set to a y-intercept of 0 to present a linear model gradient of 1. The model parameters used for each land use system are summarized in Table 4-7.

Table 4-7. Model parameters used to calculate volumetric SOC stocks (kg·m^{-2}) at each sampling depth in the 32 profiles as presented in Figure 4-6.

		0-100 cm	0-30 cm	30-100 cm	
Land use system	[a]n	*k*	*b*	*a*	*k*
Grassland	8	2.495			
No-till	8	2.3070			
Reduced tillage	8		0.8094	1.3	1.897
Conventional tillage	8		0	1.85	2.41

[a] n = number of profiles

For GL and NT, Eq. 4-3 was applied to each sampling depth increment using the *k* values in Table 4-7 to calculate the SOC stocks at all the sampling depths. For RT the SOC stocks in the 0-30 cm samples were calculated using Eq. 4-5, applying the single model parameter *b* (Table 4-7) to all samples in this soil layer. For CT the SOC stocks in the 0-30 cm samples were assumed as constant and equal to the volumetric SOC stock in the uppermost (0-5 cm) sample. The SOC stocks at subsequent sampling depths (40-100 cm) for RT and CT were calculated using a modification of Eq. 4-3 as

$$\int_{z_1}^{z_2} C_v^{30} \cdot ae^{-kz}\, dz = a \cdot \frac{C_v^{30}}{k} \cdot \left(e^{-kz_1} - e^{-kz_2}\right) \qquad 4\text{-}6$$

where *a* is the y-intercept of the respective exponential function and C_v^{30} is the volumetric SOC content in the sample taken at 30 cm (27.5-32.5 cm). Since Eq. 4-6 would require a bulk density sample to be taken at 30 cm depth to calculate *Cv*, the value for C_v^{30} may be substituted by the modelled SOC content at 30 cm using Eq. 4-5 in the case of RT. For CT, since SOC stocks in the 0-30 cm layer are assumed to be constant, C_v^{30} may be substituted by C_v^0 as

$$\int_{z_1}^{z_2} C_v^{0} \cdot ae^{-kz}\, dz = a \cdot \frac{C_v^{0}}{k} \cdot \left(e^{-kz_1} - e^{-kz_2}\right) \qquad 4\text{-}7$$

Equation 4-6 was applied using a single model parameter *k* for all samples under RT and using calculated values for C_v^{30}. Similarly, Eq. 4-7 was applied using a single model parameter *k* for all samples under CT and using measured values for C_v^0.

Since the *b'* and *k'* values were determined manually (through iterative substitution) and were only intended to compare the goodness of fit of the model values *b* and *k*, the values of *b'* and *k'* are not intended to be used for prediction purposes in SOC stock assessments. For comparative purposes however, the goodness of fit regression statistics for the use of *b* and *k* vs *b'* and *k'* in calculating SOC stocks per sampling depth are provided in Table 4-8.

From Table 4-8 it is clear that for all the land use systems there is very little difference between the regression statistics when using either *b* or *b'* and either *k* or *k'* values to predict SOC stocks. This confirms that the SOC decline functions with model parameters *b* (in the case of RT and CT) and *k* can be successfully used to calculate SOC stocks at different sampling depths with reasonable accuracy and that the calculated SOC stocks sufficiently mirror the measured stocks at the different sampling depths. For RT the calculated values for C_v^{30} were used in the calculations using combinations of *b*/*k* as well as *b'*/*k'*. For CT a constant SOC stock was assumed in the 0-30 cm layer in both cases and only the *k* and *k'* values differed in the calculation of the SOC stocks in the 40-100 cm samples.

Table 4-8. Summary regression statistics using XLSTAT, comparing calculated vs measured SOC stocks (kg·m^{-2}) per 5 cm sampled depth increments for the different land use systems using the b and k (from Table 4-7), vs corresponding b' and k' values obtained from graphs. (LU = land use; n = number of samples used in each regression analysis

		Regression statistics			
		Using *b* and *k* values from Table 4-7		Using corresponding b' and k' values from graphs	
LU system	n	R^2	RMSE	R^2	RMSE
Grassland	60	0.77	0.39	0.78	0.39
No-till	70	0.88	0.32	0.88	0.32
Reduced tillage	70	0.82	0.25	0.82	0.22
Conventional tillage	68	0.70	0.32	0.70	0.31

The total SOC stocks in the 0-100 cm, 0-30 cm and 0-20 cm soil layers were calculated for each profile per land use system using the model parameters in Table 4-7 and measured values for C_v^{30} under RT. Figure 4-7 summarizes the mean total SOC stocks (kg·m^{-2}) for these depths under the different land use systems. From Figure 4-7 it is evident that total calculated SOC stocks are slightly higher under NT compared to the other land use systems, including grasslands. The seeming increase in SOC stocks within the NT system compared to grasslands

may be attributed to higher nutrient inputs and, subsequently higher overall system productivity. Such a trend was observed in a study of SOC stocks under different intensities of grassland management in England (Ward et al., 2016).

The difference between the SOC stocks under NT and grasslands is not statistically significant (Table 4-9), though both differ significantly (at α=0.1) from both RT and CT systems. The lack of significant difference between the CT and RT systems indicates that a simple tillage reduction does not lead to considerable recovery in SOC stocks.

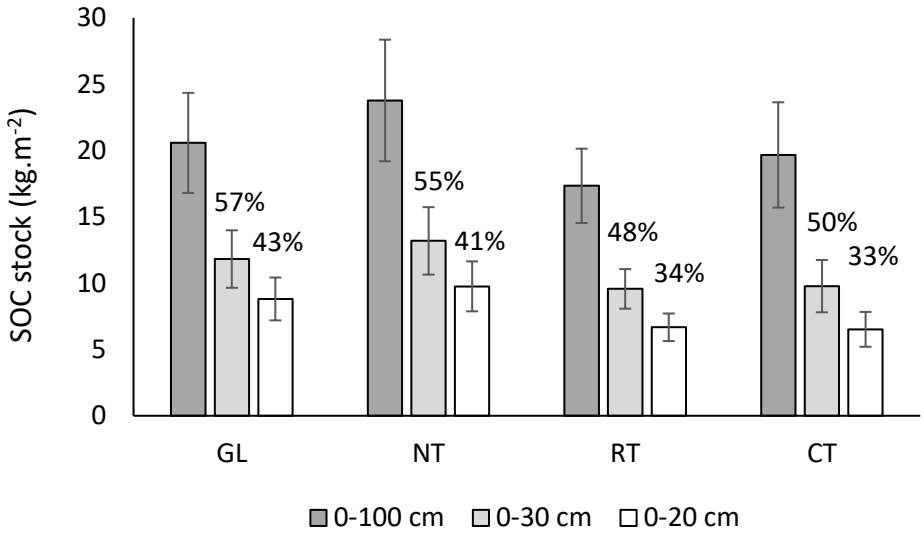

Figure 4-7. Total SOC stocks calculated for the 0-100 cm, 0-30 cm and 0–20 cm depths under the different land use systems. Error bars indicate the standard deviation of the mean SOC stocks for eight profiles within each land use system. Percentage values indicate the percentage of total SOC stocks contained in the 0-30 cm and 0-20 cm soil layers respectively.

Table 4-9. P-values for paired two-tailed T-test for samples with unequal variance showing the difference in carbon stocks calculated by integration of the depth-distribution functions for three depth intervals under different maize production systems in comparison to native grasslands. (GL = grassland; NT = no-till; RT = reduced tillage; CT = conventional tillage).

	0-20 cm			0-30 cm			0-100 cm		
	GL	NT	RT	GL	NT	RT	GL	NT	RT
NT	0.299			0.266			0.151		
RT	0.008[1]	0.002[1]		0.032[1]	0.005[1]		0.074[2]	0.006[1]	
CT	0.008[1]	0.087[2]	0.797	0.069[2]	0.010[1]	0.816	0.646	0.077[2]	0.199

The differences are significant: [1] – at α=0.05; [2] – at α=0.1

Table 4-9 also shows that the significance level describing these differences decreases with the increase in the size of the interval within which the stock assessment is conducted from 0-20 to 0-100 cm. The level of significance (α) may increase to 0.05 (a level commonly used in agricultural research) for all the comparisons of tillage and no-till systems presented here by increasing the number of surface samples, while applying the same vertical distribution models. Highly significant differences between the NT and till systems were reported for Bergville - another area of the KZN midlands in South Africa (Mchunu et al., 2011) for the depth interval of 0-2 cm. The latter finding is in line with our observations and may be attributed not only to soil erosion studied by the authors, but also to the modification of the vertical distribution pattern described here.

The higher SOC stocks under NT are mostly assumed to occur as a result of the continuous input of organic material from crop residues in the upper soil layers, especially compared to grasslands, and the concomitant low level of soil disturbance. Furthermore, measuring the vertical distribution of SOC using profile data from the same study area, Esmeraldo (2016) found that in the 30-100 cm section, grasslands had the lowest cumulative SOC stocks compared to cultivated soils. This was assumed to be due to the roots of the particular grass species not reaching deeper soil layers, hence decreasing the input of organic material and SOC into these layers. The SOC stocks occurring at any location and soil depth is a function of a series of complex interactions between factors such as plant growth, plant type, root growth, climate, soil type, parent material, topography and soil management (Allen et al., 2010; Dietzel et al., 2017). Figure 4-7 further shows that in the studied soils, roughly 48-57 % of SOC occurs in the top 30 cm, and about 33-43 % in the 0-20 cm soil layer. Similar ranges were reported by various authors indicating that 40-54 % of SOC stocks were located in the 0-30 cm soil layer (Brahim et al., 2014; Omonode and Vyn, 2006; Wang et al., 2004), and 33-50 % in the 0-20 cm layer (Dietzel et al., 2017; Jobbagy et al., 2000) relative to the first meter of soil.

4.4 Conclusions

The vertical distributions of SOC stocks under grasslands and croplands with three different types of tillage systems were successfully modelled to a depth of 100 cm. For on-farm accounting, a small number (<10) of individual soil profile observations per land use (in this case 8) to a depth of one meter is sufficient to develop a robust model of mean vertical normalized SOC (Cv_s) distribution for stable land use system practiced for more than 10 years.

The vertical distribution of SOC stocks normalized by C_v^0 may be described with a continuous exponential function in the native grasslands of the study area, as well as in the adjacent fields cultivated using a no-till mixed cattle/maize production system.

In the case of reduced and conventional (full) tillage systems, piecewise functions separately describing the vertical distribution of SOC stocks normalized by the C_v^0 for the plough layer and deeper layers are better suited for predicting SOC stocks compared to a single exponential function. In the case of reduced tillage, a linear decline function may be used for predicting the SOC stocks in the plough layer (0-30 cm), while for conventional tillage the mean vertical distribution throughout the plough layer may be approximated to a constant.

It was shown that, for all the studied land use systems in this study, irrespective of specific soil type, the vertical distribution of soil organic carbon stocks may be successfully predicted with varying degrees of accuracy from only sampling the 0-5 cm increment to determine bulk density, volume of stones (>2 mm fraction) and SOC content in the <2 mm fraction.

5 Method uncertainty: measuring and predicting soil organic carbon (SOC) content

5.1 Introduction

Accurate and cost-effective soil organic carbon (SOC) content determination is a critical step in quantifying carbon stocks for carbon accounting (Bellon-Maurel and McBratney, 2011; Bispo et al., 2017; Cremers et al., 2001; Davis et al., 2018; De Gruijter et al., 2016; England et al., 2018). Therefore, convenience, cost effectiveness and level of accuracy are critical criteria for the selection of appropriate analytical methods (Périé and Ouimet, 2008). However, the performance and range limits of SOC measurement methods are rarely assessed and reported in recent studies (Conyers et al., 2011; De Vos et al., 2007). Furthermore, conventional soil sampling and chemical SOC analysis is often expensive and time consuming, and not always sensitive enough to detect small changes occurring over time as a function of land use or management practices (Chatterjee et al., 2009).

Considering the recent prioritization to increase SOC sequestration in relation to climate change adaptation and mitigation, measuring baselines and changes in SOC becomes even more important (Chatterjee et al., 2009; Cremers et al., 2001; Davis et al., 2018). For example, increased SOC sequestration is central to the “4 per 1000 Initiative: Soils for Food Security and Climate” initiative. The 4 per 1000 initiative has set the goal of increasing global SOC stocks at an annual rate of 0.4 %, focusing mainly on agricultural lands where carbon stewardship of soils would be ensured by farmers (Soussana et al., 2017). To date, the difficulty to detect changes or improvements in SOC has been one of the challenges limiting the attention given to SOC sequestration (Chatterjee et al., 2009), along with issues such as the permanence of sequestered carbon and others (Soussana et al., 2017). According to Bispo et al. (2017) it is essential that SOC measurements be based on agreed upon standards to ensure comparable estimations of stocks and there is an increased call for the harmonization of methods, measurements to support data comparability and exchange, and more .

Dry combustion (DC) analysis allows for the direct measurement of SOC content in soil and is often used as standard or reference method in numerous SOC studies (Abraham, 2013; Chatterjee et al., 2009; Ciric et al., 2014; Cremers et al., 2001; De Vos et al., 2007; Fernandes et al., 2015; Lettens et al., 2007; Mccarty et al., 2010; Mikhailova et al., 2003; Sangmanee et al., 2017; Skjemstad, J.O., Spouncer, L.R. & Beech, 2000; Sleutel et al., 2007). In this method, samples are ignited in a furnace at temperatures between 1000 ℃ and 1600 ℃ which enables

the thermal decomposition of inorganic carbon and oxidation of organic carbon to CO_2. The high temperatures are used to ensure that all the C forms are fully converted to CO_2 (Davis et al., 2018).

Another commonly used method is wet combustion of carbon by dichromate oxidation, commonly known as the Walkley-Black method (WB) (Walkley and Black, 1934) which has undergone numerous modifications over time (Chatterjee et al., 2009). Contrary to DC, wet oxidation of carbon does not allow for the direct measurement of SOC due to incomplete sample oxidation. To account for this incomplete oxidation, (Walkley and Black, 1934) introduced a correction factor of 1.32 (assuming 76 % carbon recovery) to calculate the total SOC content. With time, numerous authors have shown that this correction factor is dependent on factors such as soil type, soil depth and mineralogy (Bisutti et al., 2004; Davis et al., 2018; De Vos et al., 2007; Kamara et al., 2007; Mikhailova et al., 2003; Nelson and Sommers, 1974; Santi et al., 2006; X. Wang et al., 2012a), which may lead to either overestimation or underestimation of SOC. Nonetheless, the WB method has also been regarded as a standard procedure for SOC analysis, especially due to its low cost and minimum requirements in terms of analytical equipment (Abraham, 2013; Bisutti et al., 2004; Chatterjee et al., 2009; X. Wang et al., 2012a).

The use of high-throughput techniques such as near-infrared (NIR) spectroscopy has increasingly been tested and used as rapid technique to measure SOC, both in the laboratory and in the field (Amare et al., 2013; Askari et al., 2018; Awiti et al., 2008; Bushong et al., 2015; Chatterjee et al., 2009; Clairotte et al., 2016; De Souza et al., 2016; Deng et al., 2012; England et al., 2018; Gobrecht et al., 2014; Guerrero et al., 2014; Mccarty et al., 2010; Mouazen et al., 2010; Reeves, 2010; Viscarra Rossel et al., 2017, 2016, Wight et al., 2016, 2005). Due to the complex nature of the soil matrix, NIR analysis does not directly measure SOC, but rather, produces a spectrum based on the interaction of photons with molecules when striking a sample surface (Wight et al., 2016), creating overtones and combinations of fundamental bands of molecular vibrations (Bellon-Maurel and McBratney, 2011). These interactions consist of reflection, refraction or absorption and can be measured accordingly. To relate the measured spectra to SOC content, a spectral library and calibration models are needed, as well as reference analyses of SOC for calibration, such as DC or WB (Bellon-Maurel et al., 2010). In a 2004 review on the use of NIR for soil analysis, Roberts et al. (2004) identified the high potential of using NIR for soil carbon inventory and sequestration assessment to reduce the costs of analyses. However, the authors specified the need for more work on this topic to

refine the method and its calibration. Bispo et al. (2017) stated that, according to ISO soil quality standards (ISO 17184:2014), NIR may be used at larger scales (such as landscape, regional, and national) to quantify SOC in large sets of soil samples. Furthermore, the sampling strategy should be defined based on the necessary accuracy of SOC quantification.

Errors in SOC analysis may arise at all stages of sample handling, processing and analysis, accumulating as a method error. The actual values of these errors are specific to each individual laboratory, analyst, analyte and instrument. Therefore, to support routine chemical analysis and ensure the detection of small changes in analyte over time, analytical methods require sufficient accuracy, precision and ability to measure small quantities of analyte. Some critical statistical parameters or figures of merit (FOM) have been formulated to assess and compare the performance of analytical methods such as accuracy, precision, limit of detection (LOD), and limit of quantification (LOQ) (Bouabidi et al., 2010; Currie, 1999; De Vos et al., 2007; Eksperiandova et al., 2010; Harris, 2007; Sangmanee et al., 2017; Shrivastava and Gupta, 2011; Valderrama et al., 2007; Wenzl et al., 2016). Olivieri (2015) argues the additional importance of the mean prediction error or root mean square error (RMSE) and the relative error of prediction (REP).

As highlighted by Bellon-Maurel and McBratney (2011), the use of NIR spectroscopy as a future SOC reference method for would require that the method be compatible with metrology requirements, especially in terms of method performance and uncertainty. They report that the most commonly used performance parameter for NIR is the standard error of prediction (SEP) which is commonly calculated as the root mean square error of prediction (RMSEP) (the sum of squares of the difference between the predicted and actual values of the analyte). The SEP value generally increases as the measurement range of calibration increases.

Developments in multivariate analysis and computing power have recently led to a widening of applications for spectroscopic methods to detect a wide variety of components in complex mixtures. Dry NIR spectrometry is increasingly advocated as new means of SOC content predictions (England et al., 2018; Viscarra Rossel et al., 2017). An additional benefit NIR spectrometry is that it may be used in both proximal and remote sensing applications (Gomez et al., 2008).

The aim of this chapter is to determine whether NIR spectroscopy can be successfully used as a rapid SOC analysis method for the specific study area. To achieve this, DC was used as reference method and compared to WB and NIR to determine their limitations in terms of

method accuracy, precision, LOD and LOQ.

5.2 Materials and methods

5.2.1 Soil sampling and analysis

A total of 397 samples from 50 sampled soil profiles from various land uses (forestry, grasslands, croplands, natural forest, sugarcane) were used for this study. Sample preparation and analysis of bulk density and stone content were conducted as described in Chapter 3. The summary of soil classification, particle size distribution and pH characteristics is given in Chapter 2.

5.2.2 Organic carbon determination

Total SOC ($\%_{wt}$) was determined by DC gas chromatography elemental analysis as described in Chapter 3 and assumed to be total SOC due to the absence of inorganic carbon.

The < 2 mm samples were analysed for SOC using the WB (Walkley and Black, 1934) method at the Elsenburg Agricultural Laboratory, Western Cape Department of Agriculture.

The < 2 mm samples were also scanned to acquire the near-infrared (NIR) reflectance spectral characteristics using a Bruker MPA (Multi-Purpose Analyser) as described in Chapter 3. Following method optimization within OPUS based on partial least squares (PLS) analysis, spectra pre-processing using a combination of first derivative and vector normalization was applied for calibration, and validated using leave-one-out cross-validation. The calibration and validation graphs and relevant statistics generated in OPUS are presented in Figure 5-1. The small bias in the cross-validation model (Fig. 5-1b) can be ignored since it is insignificant (less than the stated precision of the DC method for reference measurements) and is much less than 30% of the total error (Maroto et al., 2002). It should be noted here that this NIR spectroscopy model is only intended for use within this study area and is not intended for application as-is in other locations.

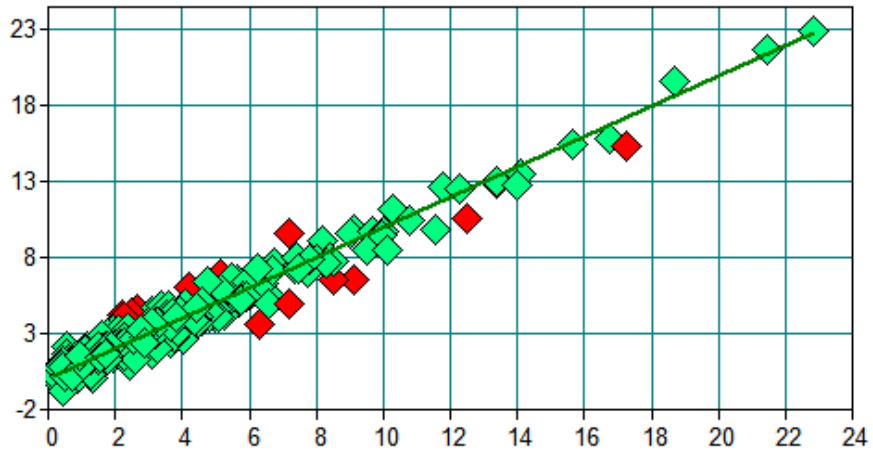

a

R^2 = 95.17

RMSEC = 0.691

RPD = 4.55

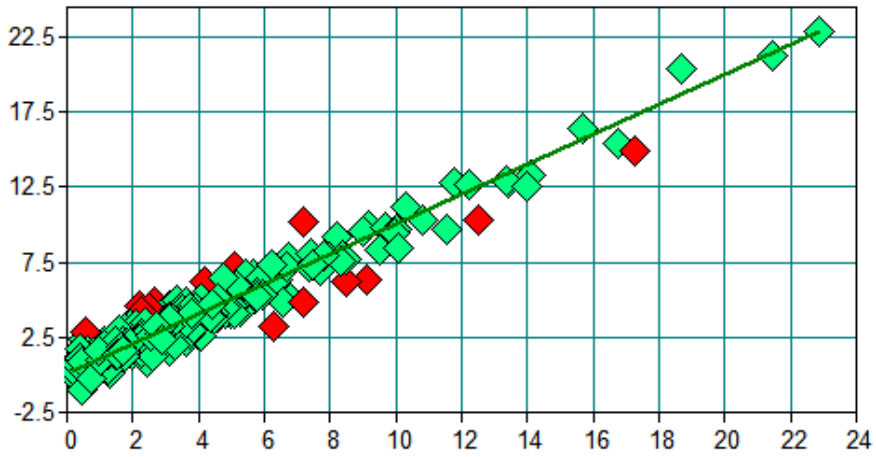

b

R^2 = 93.97

RMSECV = 0.758

Bias = -0.00779

RPD = 4.07

Figure 5-1. OPUS-generated graphs of (a) calibration and (b) cross validation (leave-one-out) of NIR reflectance spectra for SOC % analysed by dry combustion using single scans of 397 samples <2 mm. Calibration and validation statistics are shown next to each graph.

5.2.3 Figures of merit

Accuracy and precision:

Method accuracy was determined as the slope of linear regression curves of predicted (observed) versus reference SOC concentrations. Method precision was determined as the root mean square error of prediction (RMSE) of the predicted SOC concentration in relation to the reference concentrations as

$$RMSE = \sqrt{\sum \frac{(y_{obs} - y_{mean})^2}{n}} \quad (5\text{-}1)$$

Where y_{obs} is the measured SOC content, y_{mean} is the mean of 3 measurements and n is the number of measurements (3).

$$RMSEP = \sqrt{\sum \frac{(y_{pred} - y_{ref})^2}{n}} \quad (5\text{-}2)$$

For the comparison of methods, the RMSEP (RMSE of prediction) was calculated for paired sample analysis:

where y_{pred} is the predicted (measured) SOC concentrations, y_{ref} is the value measured by the reference (DC) method, and n presents the number of samples in the calibration set (Stumpf et al., 2017).

Limit of detection and limit of quantification:

The LOD was calculated based on the standard deviation of the response (predicted values) and the slope of the calibration curve (Chandran and Singh, 2007; International Conference on Harmonization, 2005; Ribani et al., 2007) as

$$\mathrm{LOD_{y0}} = \frac{3.3\delta_{\mathrm{y0}}}{\mathrm{b}} \quad (5\text{-}3)$$

where, δ_{y0} is the residual standard deviation (also known as the standard error of the estimate) of the y-intercept (δ_{y0}) of the regression lines of the calibration curve and *b* is the slope of the calibration curve and

$$\mathrm{LOD_{res}} = \frac{3.3\delta_{\mathrm{res}}}{\mathrm{b}} \quad (5\text{-}4)$$

where δ_{res} is the residual standard deviation of the regression line.

Similarly, the LOQ (Chandran and Singh, 2007; International Conference on Harmonization, 2005) was calculated as:

$$\mathrm{LOQ_{y0}} = \frac{10\delta_{\mathrm{y0}}}{\mathrm{b}} \quad (5\text{-}5)$$

and

$$\mathrm{LOQ_{res}} = \frac{10\delta_{\mathrm{res}}}{\mathrm{b}} \quad (5\text{-}6)$$

The relevant standard deviations (δ_{y0} and δ_{res}) were calculated in Microsoft Office Excel using the LINEST function.

5.2.4 Data sets for determining the figures of merit

Twelve samples with SOC DC μ ± δ = [0.75 ± 0.06, 0.90 ± 0.07, 1.06 ± 0.16, 1.15 ± 0.12, 1.85 ± 0.11, 2.51 ± 0.01, 3.05 ± 0.07, 4.96 ± 0.19, 5.72 ± 0.17, 9.01 ± 0.60, 11.79 ± 0.20, 17.13 ± 0.10] were used for the analysis of accuracy (trueness and precision) of individual methods. The above samples were subsampled and analyzed in triplicate using DC, WB and NIR.

Dry combustion:

The EuroVector EA3000 used for DC analysis was calibrated regularly using the standard samples SOIL1, SOIL2, SOIL3, SOIL4 supplied by EuroVector and containing respectively 0.732, 2.417, 3.5 and 4.401 % carbon. Subsamples of the standards (22 in total) were analysed as part of test batches as quality control (QC) samples included in batch determination during the analysis of our sample collection. Method accuracy, precision, LOD and LOQ for DC were determined using this dataset.

Walkley-Black and NIR:

The 12 calibration samples analyzed in triplicate were used to determine the accuracy and precision for the WB and NIR methods using DC as reference method.

For LOD and LOQ determination of the WB and NIR methods, six (6) of the 12 calibration samples were used with mean C analysed by DC ranging from 0.75 to 4.96 %. This was done to stay within the SOC concentration range used for the LOD and LOQ determination for DC (below 5% SOC).

5.3 Results and Discussion

5.3.1 Method accuracy

Accuracy and precision are the two main method characteristics used for comparison of analytical methods, where accuracy is the proximity to 1:1 correspondence between the results obtained by different methods, and precision is the RMSEP (Currie, 1999; Nalimov et al., 1963; Westgard, 1973). Recently, IUPAC (Thompson et al., 2002) suggested to use the term “accuracy” in a general qualitative manner, replacing the strict understanding of accuracy with the term “trueness” and making distinction between the mean and the mathematical expectation of the mean (τ). However, the term “trueness” was dropped and not replaced in the latest edition of the IUPAC Gold Book (IUPAC, 2014). Here the term accuracy will be used in its classical term referring to agreement between the methods in terms of proximity of the

results measured by the compared methods to the 1:1 line (line of agreement). Method accuracy or trueness refers to how close a measured value is to a standard or known value and should be established for the specified range of the analytical method. Such accuracy can be determined using reference material or standards in which the analyte concentrations are known (as used for DC in this study), or by comparing analysis results of one method with those of a second method for which the accuracy is known or defined (as used for WB and NIR in this study) (Chandran and Singh, 2007; International Conference on Harmonization, 2005).

Method precision refers to how close repeated measurements are to each other and precision analysis should aim to determine typical variability rather than minimum variability of measurement. Precision is usually expressed by statistical parameters that describe the spread of replicate measurements of suitable samples (Chandran and Singh, 2007; Eurachem, 2014). The recommended number of replicates for analysis to determine precision vary between authors, ranging from 3 (Chandran and Singh, 2007) up to 6 and 15 (Eurachem, 2014).

Either precision alone (as the error of zero) or the combination of precision and accuracy allow to derive an estimate of the LOD and LOQ, which are indeed important, but mostly underreported FOM, particularly in soil analysis. In terms of soil carbon determination, LOD and LOQ are rarely mentioned. Calculation of LOQ as 10 times the error of zero implies that the restriction on “quantification” is a relative error = 10% of the determined value (Nalimov et al., 1963). Such error tolerance level is sometimes seen as unnecessary, and higher levels of relative error may be considered acceptable, particularly in environmental sciences where high levels of natural variability often occurs in material composition. As for detecting SOC content for carbon accounting purposes, the analytical error has direct financial implications. In this case, the error tolerance has to be specified by the trading parties.

Dry combustion analysis:

The linear regression analysis of the EuroVector measurement of standard samples is presented in Figure 5-2. The slopes of the regression lines in Figure 5-2 are 1.00 for the prediction of mean SOC concentrations from several measurements and shows a slight inaccuracy (slope = 1.02) in terms of prediction of stated standard concentrations. On one hand the inaccuracy is negligibly small (Maroto et al., 2002) and may be ignored, on the other hand, it may be true and reflecting the deterioration of the standards which were 18 years old at the time of analysis.

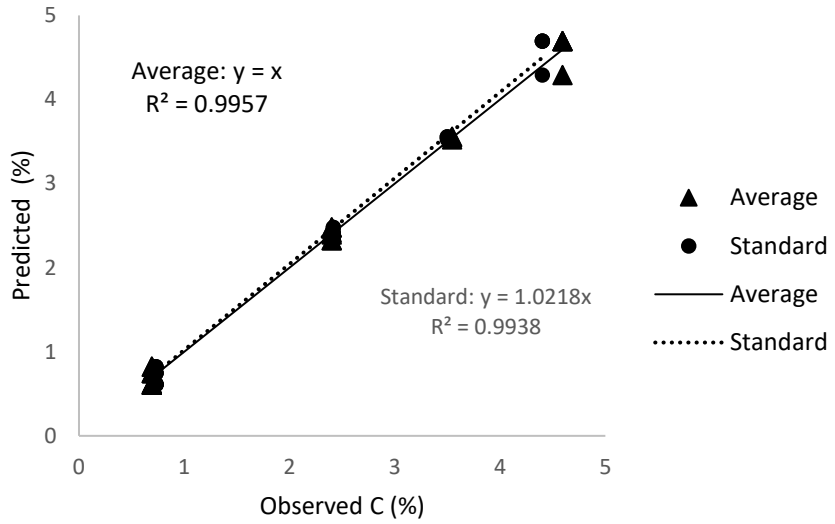

Figure 5-2. EuroVector EA3000 quality control with supplied standards (Standard) and relationship with reference concentrations calculated as a mean of replicated determination of standard sample concentrations (Mean).

The RMSE of true validation for declared standards was 0.13 % SOC. However, it was assumed that the mean of replicate determination concentrations may better represent the true concentration in the sample rather than the declared standard. Substituting the mean of replicate determination for the declared standard concentration, the RMSE calculated from the replications of standard sample analysis becomes 0.10 % SOC. This value represents an average precision of soil analysis within the given range and the variation in the composition of the analyte. This is an important result, since the stated operational range of the instrument is 0.01 to 100 % C. However, with an error of 0.1 % SOC, a 100 % relative error may still be expected for the 0.1 % SOC concentration, which in theory should be the LOQ. This error includes all the laboratory procedures and the variability in the composition within the volume of the standards.

The triplicate analysis of 12 subsamples (from calibration samples analyzed as reference values for WB and NIR) using DC has shown that the error from subsampling a well-prepared ball-milled soil sample does not dramatically increase the overall error of analysis (Figure 5-3). The error mainly lies below 0.2 % SOC and averages at 0.15 (RMSE = 0.17). Removing one outlier that may be attributed to poor sample homogenization with a δ = 0.60, the overall mean standard deviation falls to 0.11 (RMSE = 0.10) – almost exactly what was found with the analysis of standards. This shows that the variability in sample composition and subsampling procedure contribute to a rather small proportion of the method error. The relative standard deviation falls below 10 % for values exceeding 1 % SOC, but does not exceed 20 % throughout

the analysed range where:

$$\text{Relative } \delta = \frac{\delta}{\bar{y}} \cdot 100 \qquad (5\text{-}7)$$

where δ is the standard deviation and $\bar{y}$ is the mean of the triplicate analyses.

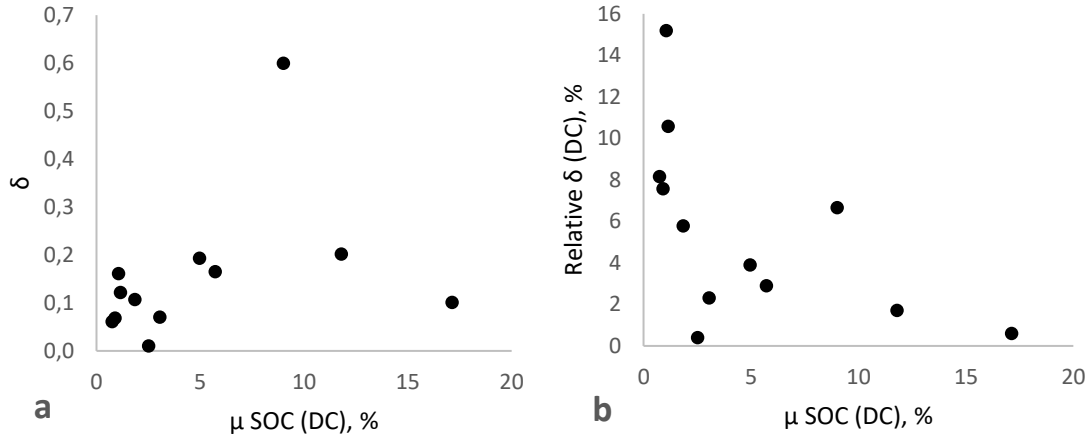

Figure 5-3. Standard deviation (δ) (a) and relative standard deviation (b) of measured SOC against mean SOC % for the soil samples analysed in triplicate using dry combustion with the EA-3000 analyser.

Walkley Black analysis:

The WB method was extensively evaluated since its initial development (Chatterjee et al., 2009). While De Vos et al. (2007) suggest 8 % as the upper boundary of reliable use for the WB method, it was decided to use the 9 % mean SOC content determined by DC as the upper limit for our statistical analysis. By applying this limit, ten (out of 12) calibration samples with SOC content up to 9 % were used.

The WB method displays a good reproducibility of results and prediction of the mean by repeated analysis of subsamples (Figure 5-4a) and an RMSE = 0.13 which is fairly similar to that of the DC method (RMSE = 0.10). The relative standard deviation is below 10 %, averaging at 5%. The sample with the highest mean SOC content of 9 % was an outlier in this analysis with a relative error of 29%. Based on the analysis of De Vos et al. (2007), this large error may be as a result of the upper boundary of reliable use for the WB method. Conversely, since the WB analyses were done using soil samples < 2mm, this error may also be due to poor sample homogenization.

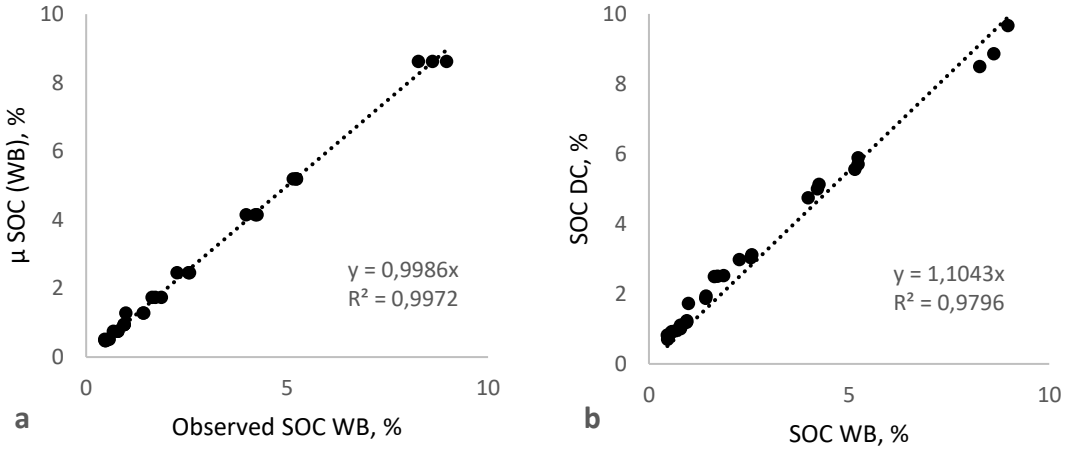

Figure 5-4. Prediction of the mean with triplicate SOC determinations by WB method (a) and the SOC content measured in triplicate by DC and WB methods (b).

A further concern with regards to WB analyses of SOC is the linear regression coefficient which is often approximated as a multiplication factor of 1.32 (Walkley and Black, 1934). This factor is required for comparison of the WB results with results obtained by the DC method (Abraham, 2013). However, this factor was shown to vary for different soils from 1.0 to 2.8 (Davis et al., 2018; De Vos et al., 2007; Mikhailova et al., 2003; Nelson and Sommers, 1996). The conversion factor for data in this study should be closer to 1.10 as determined by the slope of the regression line in Figure 5-4b (Abraham, 2013). The response is somewhat non-linear since the conversion factor increases to 1.18 if the data range is limited to less than 5 % SOC determined by DC.

Applying the multiplication factor of 1.10 to the results obtained by the WB method results in good correspondence between the WB and DC measurements with an RMSE of 0.37. However, the two-tailed t-test for paired samples with unequal variance shows that 50 % of the pairs had different means at α=0.05 (Table 5-1). A factor of 1.27 was subsequently selected through iterative substitution to minimize the number of statistically different means. Such a choice of conversion factor produced better comparison of the WB and DC means using the same t-test. In the latter case, only two out of ten samples had significantly different means when determined by these two analysis methods (Table 5-1).

For accuracy determination, it is usually recommended that a minimum of 9 to 15 determinations be conducted through 3 to 5 replicates each at a low, medium and high concentration within the expected analysis range (Chandran and Singh, 2007). Similarly, the recommended number of replicates for analysis to determine precision vary between authors, ranging from 3 (Chandran and Singh, 2007) up to 6 and 15 (Eurachem, 2014). However,

numerous studies comparing different SOC determination methods only perform single measurements with both the reference and test methods (Abraham, 2013; Chen et al., 2015; Dieckow et al., 2007; Fernandes et al., 2015; Harper and Tibbett, 2013; Kalembasa and Jenkinson, 1973; Mccarty et al., 2010; Périé and Ouimet, 2008; Sato et al., 2014; Wight et al., 2016), or multiple replicate measurements only with the test analysis method (Amare et al., 2013; X. Peng et al., 2014; Y. Peng et al., 2014; Sangmanee et al., 2017). Isolated studies were found that include duplicate reference method analyses (Beltrame et al., 2016; De Vos et al., 2007).

Table 5-1. Results of t-tests for differences between means (reported as P-value at α=0.05) determined by dry combustion (DC) and Walkley and Black method corrected by a factor of 1.10 (1.10WB) and 1.27 (1.27WB). (μ = mean; δ = standard deviation)

DC		1.10WB				1.27WB			
μ	δ	μ	δ	DC/WB	P-value	μ	δ	DC/WB	P-value
0.75	0.06	0.53	0.01	1.42	**0.022**	0.61	0.01	1.23	0.052
0.90	0.07	0.58	0.06	1.55	**0.003**	0.66	0.07	1.36	**0.019**
1.06	0.16	0.83	0.07	1.28	**0.036**	0.95	0.08	1.11	0.349
1.15	0.12	1.04	0.01	1.11	**0.001**	1.2	0.01	0.96	0.496
1.85	0.11	1.41	0.27	1.31	0.094	1.63	0.32	1.14	0.355
2.51	0.01	1.92	0.13	1.31	**0.016**	2.21	0.15	1.14	0.071
3.05	0.07	2.71	0.19	1.13	0.078	3.12	0.22	0.98	0.614
4.96	0.19	4.56	0.16	1.09	0.054	5.27	0.19	0.94	0.121
5.72	0.17	5.72	0.05	1.00	0.976	6.61	0.06	0.87	**0.006**
9.01	0.6	9.48	0.39	0.95	0.324	10.95	0.45	0.82	**0.013**

To assess the effect of triplicate measurements using the reference method (DC) versus single reference method measurements on the variance of method predictions (WB), results of single DC and WB determinations on 383 samples with DC SOC < 10 % were used (Figure 5-5). Since the standard deviation (and relative standard deviation) cannot be determined for single measurements, δ was substituted with RMSE, keeping in mind that for small model intervals, as the interval of observations around the mean approaches zero, the RMSE → δ. RMSE is calculated in the same manner as the standard deviation, except that the residuals

are calculated as the difference of "true" and predicted values rather than the difference between the measured values and the mean.

Regression analysis of this data set shows a linear relationship between WB and DC determinations that requires a correction factor of 1.1836 to predict SOC DC from SOC WB determination (Figure 5-5a). Upon applying this correction factor, a new set of SOC WB values (1.1836WB) was generated, resulting in an RMSE of 0.47 (from 0.37 determined by the analysis of triplicates using a correction factor of 1.10). Next, the absolute error per sample was calculated as the difference between the DC and WB measured SOC concentration. Outliers with an absolute error > 1.41 (3·RMSE of 0.47) were removed, which reduced the number of samples to 359 and the RMSE to 0.40. The above approach for the removal of outliers would be valid for constant (system) error. It is clear, though, that the absolute error increases with an increase in SOC concentrations within the interval from 0 to around 1.5 % SOC and is capped at 1.41 due to removal of outliers (Figure 5-5b).

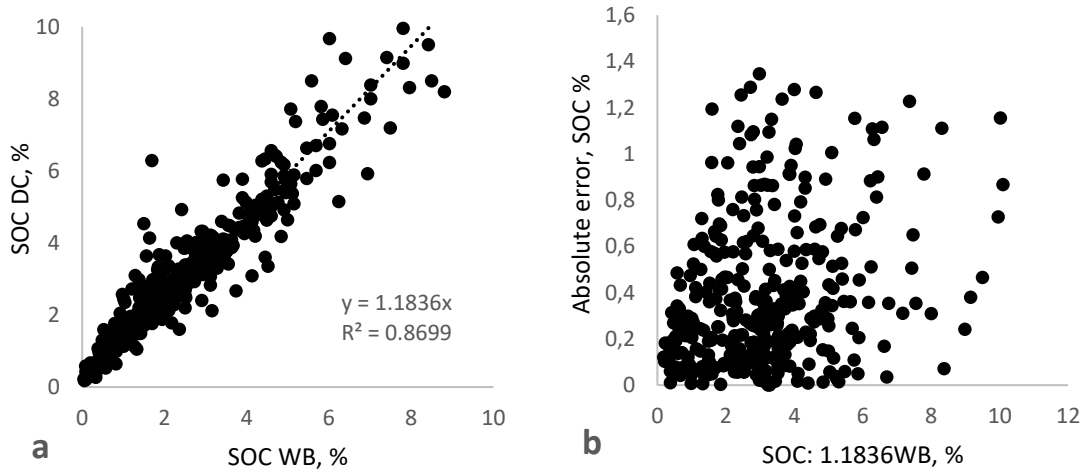

Figure 5-5. Regression between single SOC measurements by dry combustion vs. Walkley and Black method (a) and absolute error of the same measurements corrected by the factor 1.836 (b).

To understand the dependency of the RMSE on the observed value, the range of observations was split into intervals [a,b] of increasing width so that the range boundaries of the reference values would be set 25 % away from the mean (μ), i.e: a = μ - μ/4 and b = μ + μ/4 (Table 5-2). This was applied to the complete set of 383 samples, as well as the set of 359 samples with outliers removed as explained previously, using the 1.1836WB corrected values.

Table 5-2. The RMSE and relative RMSE values for the SOC concentration ranges. (a = lower limit of the range; b = upper limit of the range; μ = mean SOC % for the range; n = number of samples).

a	b	μ	Complete set (383 samples)			Outliers removed (359 samples)		
			n	RMSE	Rel.RMSE, %	n	RMSE	Rel.RMSE, %
0.135	0.225	0.18	3	0.11	61.1	3	0.11	61.1
0.225	0.375	0.30	4	0.15	50	4	0.15	50
0.375	0.625	0.50	17	0.23	46	17	0.23	46
0.625	1.042	0.83	30	0.23	27.6	30	0.23	27.6
1.042	1.736	1.39	37	0.46	33.1	37	0.46	33.1
1.736	2.893	2.31	87	0.58	25.1	84	0.51	22
2.893	4.822	3.86	134	0.7	18.1	125	0.52	13.5
4.822	8.037	6.43	71	1.08	16.8	59	0.6	9.3
Full model range:			383	0.47		359	0.40	

When comparing the number of samples (n) in the complete set compared to the set with outliers removed, the results in Table 5-2 show that using a single RMSE value for the whole range only allows the identification of outliers in the upper ranges (from a = 1.736). That is due to the dependence of the RMSE on the reference SOC % (Figure 5-6a). The magnitude of absolute error increases with increasing SOC content due to increased variation in analyte composition, which in turn increases the RMSE. It is also shows that such type of regression model calibration (matching single observations instead of observation means) results in high relative error (Figure 5-6b), which practically never falls below the 10 % threshold set for quantitative analysis. This would mean that the WB method of determining SOC remains semi-quantitative throughout the range.

The need for the experimental determination of a conversion factor for each study area as well as the range limitation of the WB method for determining high SOC concentrations makes it less attractive for carbon accounting purposes at locations with very or high soil carbon content. In fact, Abraham (2013) considers the WB method to be semi-quantitative in nature due to its incomplete recovery of SOC. De Vos et al. (2007) determined the lower and upper SOC quantification limits of the original WB method for forest soils as 0.42% and 8.00%

total organic carbon (TOC) respectively, with 76% carbon recovery using 542 mineral soil samples. In this case the correction factor for WB was calculated as 1.58. Nonetheless, the low cost of analysis and wide adoption of the method by commercial laboratories make it a viable option for intensive soil carbon surveys.

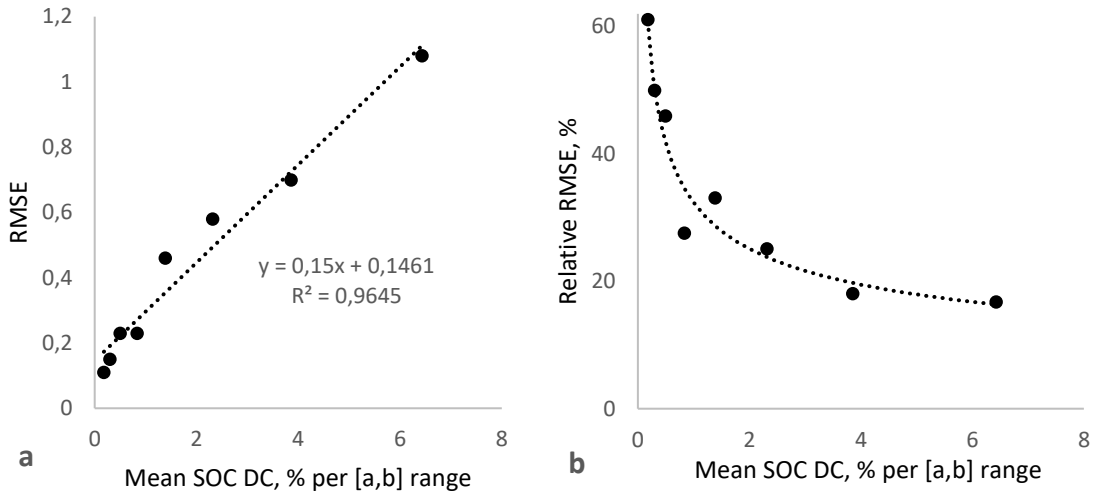

Figure 5-6. The RMSE (a) and relative RMSE (b) of SOC predicted from WB analysis using a single experimentally-determined correction factor of 1.1836, as a function of mean SOC DC % per [a,b] range.

NIR spectroscopy with PLS regression:

A striking feature of the calibration and cross-validation of the partial least squares (PLS) regression model relating reflectance spectra of these samples to single SOC DC measurements (Figure 5-1) is the rather high RMSE values (0.69 and 0.76 respectively). These figures are in line with the values reported by different authors and summarized by Bellon-Maurel and McBratney (2011) and Bellon-Maurel et al. (2010). Nonetheless, a closer look is required at this method's figures of merit.

The NIR method was evaluated further using the twelve triplicate samples with the DC values ranging from 0.75 to 17.13 % C as reference. Here, the NIR method shows reasonable accuracy producing close to 1:1 (regression slope = 1.04) results with R^2 = 0.988 (Figure 5-7a) and precision in terms of predicting the observed mean of DC analysis (Figure 5-7b). The comparison of multiple replications for the spectroscopic determination of SOC is not a common practice and often single or duplicate sample analysis are used (Beltrame et al., 2016).

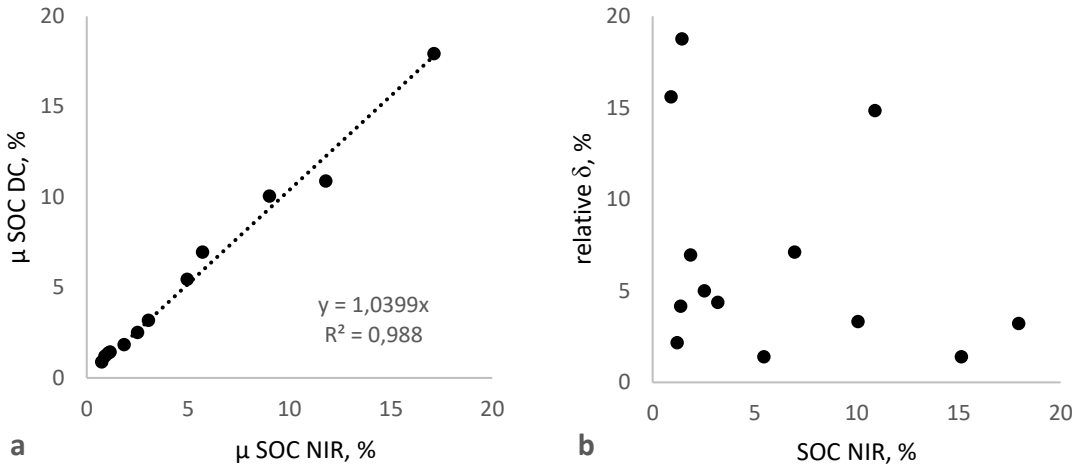

Figure 5-7. Mean SOC content (a) measured in triplicate by dry combustion (DC) and predicted in triplicate from the PLS regression model using NIR spectroscopy (Figure 5-1), and relative δ of the triplicate NIR predictions (b).

The RMSE of predicting the means of triplicate samples analysed by both the DC and NIR methods is substantially better (RMSE = 0.42) than that of the cross-validated PLS NIR model for paired samples without replication (RMSE = 0.76). Limiting the range to less than 5 % SOC DC, the RMSE falls to 0.11, which is comparable to the error of the DC analysis and requires further investigation of the error distribution within the initial (bigger) range of values.

Predicting the single-measurement SOC DC values with the SOC NIR PLS model for the set of 397 samples produced a good correlation (R^2 = 0.95) and 1:1 correspondence between the paired values (Figure 5-8a). However, the RMSE = 0.68 and the relative absolute error (RAE) for the lower part of the range exceeds 100 % (Figure 5-8b). This dramatically restricts the application of the method to samples with low SOC content. One of the solutions to enhancing the accuracy of NIR measurements is to successfully develop calibration models, hence different calibration models yield different results (Mouazen et al., 2010). Mouazen et al. (2010) evaluated NIR spectroscopy predictions of SOC in 168 samples using WB as reference method, reporting an R^2 = 0.84, RMSE = 0.68 and residual prediction deviation (RPD) = 2.54 when using a back propagation neural network analysis calibration method. These results were classified as “excellent”.

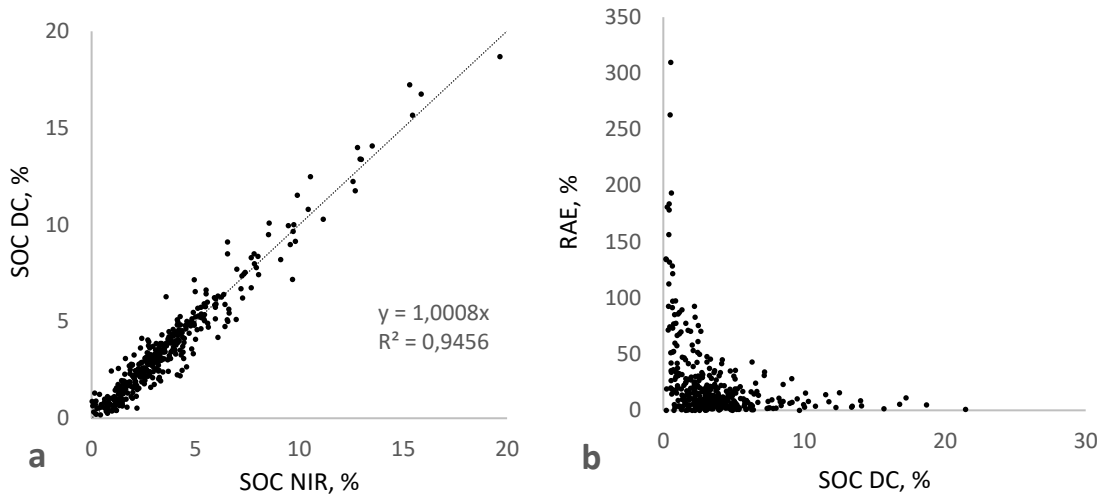

Figure 5-8. Regression of single-measured SOC DC values vs. predictions of the PLS regression from NIR spectra (a) and the relative absolute error (RAE) of predictions (b).

For further analysis, the range is once again split into intervals so that the range boundaries are set 25 % away from the mean (μ), i.e: a = μ - μ/4 and b = μ + μ/4 (Table 5-3). Similar to the WB analysis, the RMSE and MAE results indicate the dependence of the error on the magnitude of the absolute value which is reflected in Figure 5-9a. According to Bellon-Maurel and McBratney (2011), the RMSE value of NIR spectroscopy analysis generally increases as the measurement range of calibration increases.

Table 5-3. The RMSE, relative RMSE (RMSE), mean absolute error (MAE) and relative MAE (RMAE) for the [a,b) intervals of the calibration/cross-validation range of single SOC content measurements with DC and NIR PLS model. (a = lower limit of the range; b = upper limit of the range; μ = mean SOC % for the range; n = number of samples).

a	b	μ	n	RMSE	RRMSE, %	MAE	RMAE, %
0.135	0.225	0.18	4	0.19	105.5	0.14	78.9
0.225	0.375	0.30	5	0.44	146.6	0.42	139.2
0.375	0.625	0.50	15	0.70	140	0.52	103.7
0.625	1.042	0.83	30	0.47	56.4	0.40	47.6
1.042	1.736	1.39	37	0.50	36.0	0.36	26.2
1.736	2.893	2.31	89	0.67	28.9	0.48	20.6
2.893	4.822	3.86	107	0.56	14.5	0.42	10.9
4.822	8.037	6.43	19	0.62	9.6	0.47	7.3
8.037	13.396	10.72	84	0.93	8.7	0.69	6.5
13.396	22.326	17.86	7	1.03	5.8	0.86	4.8

Using the equation in Figure 5-9b it can be estimated that the relative RMSE will fall below 100 % for SOC content > 0.39 %, below 50 % for SOC content > 0.97 %, below 20 % for SOC content > 3.25 %, and below 10 % (quantitative range) for SOC content > 8.09 %. Therefore, contrary to the WB analysis, which in comparison practically never fell below the 10 % relative RMSE threshold, the evaluation of NIR analysis with single observations of the reference DC methods would mean that the NIR method of determining SOC becomes quantitative only for SOC content > 8.09 %.

Therefore, the above considerations impose serious limitations on the use of the locally-developed PLS regression models for NIR spectroscopy of soil samples with calibration/cross-validation based on single measurements within the model calibration set. Furthermore, the single SOC content measurements by DC method may be a rather poor data set for true model validation.

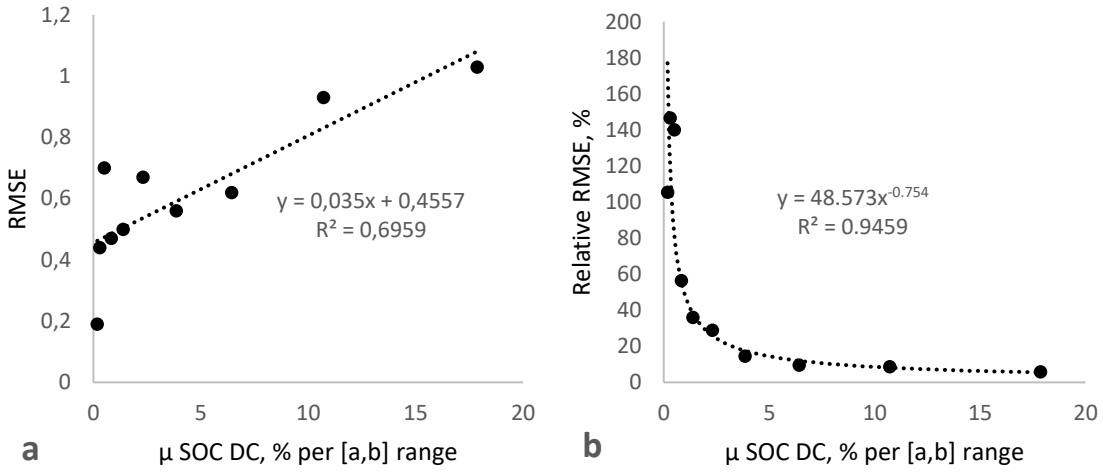

Figure 5-9. The RMSE (a) and relative RMSE (b) of SOC predicted with NIR analysis as a function of mean SOC DC % per [a,b] range.

From the above results it is clear that triplicate analyses using the reference (DC) and test (NIR) method yields higher accuracy and precision of analysis. This is confirmed by Beltrame et al. (2016) who stated that, according to ASTM E1655-05,13 standards, the accuracy of a component concentration or property value estimated using a multivariate infrared analysis is highly dependent on the accuracy and precision of the reference values used in the calibration. Judging from the WB results presented in this study, this is not only applicable to multivariate infrared analysis, but to any analysis method comparison. Beltrame et al. (2016, p. 1529) further stated that "the expected agreement between the infrared estimated values and those obtained from a single reference measurement can never exceed the repeatability of the reference method, since, even if the infrared estimated the true value, the

measurement of agreement is limited by the precision of the reference values".

5.3.2 Limit of detection and limit of quantification

The LOD is not the smallest measurable concentration of a particular method. Instead, it is the point at which it can be decided whether an element or compound is present in the sample or not (Payling, 2012). It is therefore the point where a measured signal can be distinguished from the background or blank measurement. Various equations are offered by different authors for the determination of LOD and LOQ. For example, both LOD and LOQ can be calculated from multiple blank measurements as:

$$LOD = x_{bi} + k * \delta_{bi} \quad (5\text{-}8)$$

where x_{bi} is the mean of the n blank measurements, δ_{bi} is the standard deviation of the n blank measurements, and k is a numerical factor chosen according to the desired confidence level (Currie, 1999; De Vos et al., 2007; Eksperiandova et al., 2010; Gustavo González and Ángeles Herrador, 2007; IUPAC, 1997; Sangmanee et al., 2017; Thomsen et al., 2003) which is usually set at a minimum of 3 (De Vos et al., 2007). This calculation usually involves analyzing at least 10 replicates of blank samples or, in the absence of suitable blanks, 10 independent sample blanks fortified or spiked to the lowest acceptable analyte concentration which serve as pseudo-blanks (Gustavo González and Ángeles Herrador, 2007; Wenzl et al., 2016).

The reason for the minimum value for k set as 3 is that, following the three sigma rule, the value exceeding three standard deviations is definitely (P=0.9973) a positive value and not an error of 0 (Pukelsheim, 1994). This allows the avoidance of both Type I and Type II errors with a very high degree of certainty.

In turn, the limit of quantification (LOQ) is generally stated to start at 10 standard deviations of the blank, which gives:

$$LOQ = 3.3 \cdot LOD \quad (5\text{-}9)$$

where LOQ is the lowest concentration of SOC that can be accurately determined with a particular method (De Vos et al., 2007; Sangmanee et al., 2017).

Alternatively, LOD and LOQ can be calculated based on the standard deviation of the response and the slope of the calibration curve (Chandran and Singh, 2007; International Conference on Harmonization, 2005) as was applied in this study using Equations 5-3 and 5-4

to calculate LOD and Equations 5-5 and 5-6 to calculate LOQ. In the latter two equations, the calculation of 10δ for LOQ (compared to 3.3δ for LOD) is because in chemical analysis the relative error or relative standard deviation of 10 % is often regarded as acceptable for quantitative analysis as explained above (Nalimov et al., 1963).

As stated by Wenzel et al. (2016) and Ribani et al. (2007), it is best to determine LOD and LOQ at concentration levels close to the expected values (based on expert knowledge or experience from previous experiments), especially when concentration estimates are derived from calibration measurements. Estimating LOD and LOQ were not initially intended as part of this study, hence the original study was not designed for this purpose. For example, replications of a blank (or pseudo-blank) were not measured using the DC, WB or NIR methods. However, as the importance of understanding the detection capabilities of analysis methods became evident, the available data was used as a scoping exercise to determine the relative differences in LOD and LOQ between the three methods. Furthermore, since method LOD and LOQ is very rarely determined in SOC studies, limited literature exists for comparison of obtained values.

The summary statistics for the determination of LOD and LOQ for the three analysis methods are presented in Table 5-4. From these results it is clear that the LOD and LOQ values calculated using δ_{y0} were substantially lower than those calculated using δ_{res}. The same trend was observed when the same methodology was applied in pharmaceutical studies (Ismail et al., 2014; Ribani et al., 2007; Vial and Jardy, 1999). Differences in these values vary since they depend on a range of parameters such as the number of analyte levels, their position, the number of replicates per level and data heteroscedacity (Vial and Jardy, 1999). Vial and Jardy (1999) evaluated three methods of LOD and LOQ determination (including the method used in this study), yielding five different LOD and LOQ values for the same gas chromatography analyses. They stated that extreme estimates could vary by as much as a factor of 6 for LOD and a factor 10 for LOQ. As a result, they stressed the importance of rigorous stipulation of the approach chosen to estimate LOD and LOQ in method validation reports to avoid serious discrepancies. Of the three methods evaluated, the authors found that calculating LOD and LOQ using δ_{y0} and δ_{res} obtained from weighted least squares regression data reduced the effect of data heteroscedacity and recommended this method especially for determination of LOD.

Table 5-4. Regression line parameters for SOC analysis and estimated LOD and LOQ based on linear regression for the three methods: DC - dry combustion, WB – Walkley-Black, NIR – near-infrared spectroscopy. (y-int = y-intercept)

						LOD (SOC %)		LOQ (SOC %)	
Method	R^2	Slope	y-int	δ_{y0}	δ_{res}	δ_{y0}	δ_{res}	δ_{y0}	δ_{res}
DC	0.995	1.053	-0.94	0.043	0.113	0.14	0.36	0.41	1.08
WB	0.984	0.882	-0.287	0.077	0.164	0.29	0.61	0.87	1.86
NIR	0.991	1.093	-0.083	0.070	0.151	0.21	0.45	0.64	1.38

Dry combustion:

The instrumental limit of detection (LOD) of the EuroEA3000 series used for the DC determination of total SOC is not quantified by the manufacturer, but is rather advertised as less than one microgram for each element (Eurovector, 2010). Eksperiandova et al. (2011) summarized the relevant technical specifications for the EuroVector EA-3000 as presented in Table 5-5. As a result, it is expected that in this study, the concentration ranges used for regression analysis of the DC method are substantially higher than the potentially detectible and measurable concentrations using this method. From Table 5-4, the LOD and LOQ for DC using δ_{res} were calculated as 0.32 % and 1.06 % SOC respectively which are the lowest results of the three methods. This result was expected since DC enables the direct determination of C and the regression analysis to determine δ_{y0} and δ_{res} was done using reference standards supplied by EuroVector with known true values. For the WB and NIR methods, the means of the triplicate DC analyses of six calibration samples were used as reference.

Table 5-5. Technical specifications of the EuroVector EA-3000 CHNS-analyser (Eksperiandova et al., 2011).

Element	Concentration range	Declared accuracy	Sample mass
C	0.01–100 %	± 0.3 %	1-2 mg

Walkley-Black:

The WB method yielded the highest LOD and LOQ values of the three methods with LODδ_{res} = 0.61 and LOQδ_{res} = 1.86 (Table 5-4). This implies that in this study, of the three methods, the WB method had the lowest capability to quantitatively determine low values of

SOC. It is possible that, should a study be devised specifically to determine the LOD and LOQ values by determining replicates of samples with lower SOC levels, these results for the WB method may be improved. The importance in this instance is the relative difference between the three analysis methods which indicates that the appeal of the WB method in terms of its low cost of analysis may need to be weighed up against its overall accuracy and ability to quantify SOC at low levels.

Sangmanee et al. (2017) determined the LOD and LOQ of a modified WB method for C determination using pure kaolinite as background to quantify small C concentrations (< 0.05 %) in deep kaolinitic regolith. Seven sets of kaolinite with three replications were used for total organic carbon (TOC) determination of the blank and the LOD was calculated using Eq. 5-6 with k = 3 and LOQ was calculated using Equation 5-7. Values for LOD and LOQ were determined as 0.015 and 0.050% TOC respectively.

NIR spectroscopy with PLS regression:

The LOD and LOQ results for the NIR method compare favourably to those of the WB method with LODδ_{res} = 0.45 and LOQδ_{res} = 1.38 (Table 5-4). These results were obtained despite the high heteroscedacity of the NIR method as observed from the increase in RMSEP with an increase in analyte range in Table 5-3. Therefore, it is expected that these values could be markedly improved by purposely analysing replicates of samples with SOC content lower than the 0.75 % to 5 % range used here. Furthermore, alternative calculation methods for LOD and LOQ can be applied to remove the heteroscedacity of the dataset.

Here it is relevant to note that different variations for the calculation of LOD and LOQ from the ones discussed so far have been used in multivariate calibration to assess NIR spectroscopy analysis for various substrates (Allegrini and Olivieri, 2014; Olivieri, 2015; Valderrama et al., 2007). According to several authors, these methods are considered to require additional effort to obtain a reasonable convention between univariate and multivariate LOD definitions (Allegrini and Olivieri, 2014; He et al., 2018).

Two studies reporting LOD and LOQ determination for NIR analysis of SOC specifically were conducted using multivariate LOD calculations on the NIR spectra scanned in reflectance mode (Beltrame et al., 2016; De Souza et al., 2016). For example, De Souza et al. (2016) reported the calculation of LOD and LOQ as

$$LOD = 3.3\delta_x b_k \quad (5\text{-}10)$$

$$LOQ = 10\delta_x b_k \quad (5\text{-}11)$$

where δ_x is an estimation of the noise level in the data and b_k is the regression coefficient for the k^{th} variable based on a regression model.

Beltrame et al. (2016) evaluated NIR spectroscopy as SOC determination method by comparing the DC and modified WB methods as reference on 161 samples. NIR spectra were obtained for samples < 2 mm at the percentage of reflectance mode, following which multivariate calibration models were developed based on PLS regression with external validation. LOD and LOQ were calculated for first order multivariate calibration using Equations 5-8 and 5-9 as 0.4377 $g.kg^{-1}$ and 1.3262 $g.kg^{-1}$ C respectively using the modified WB method as reference, and 0.3710 $g.kg^{-1}$ and 1.1244 $g.kg^{-1}$ C respectively using the DC method as reference.

It is clear that considerable discrepancies in LOD and LOQ exist between methods. In addition, such discrepancies may also exist between laboratories as a function of individual practice performance and experimental design. As a result, harmonization of approaches to estimate LOD and LOQ are necessary (Wenzl et al., 2016).

In this study, the multivariate model calibration was optimized and performed automatically using the Quant2 method in the OPUS software. Therefore, the resultant PLS calibration model is considered as the method and tested the univariate determination of LOD and LOQ accordingly for further application in this study.

5.4 Conclusions

It was shown that the use of paired tests without replication dramatically decreases the precision of SOC predictions of all methods, possibly due to high variability of SOC content in reference values analysed by DC. In the case of the WB method the use of the paired samples without replication also substantially affected the model accuracy (the slope of linear regression changes from 1.1045 to 1.1835). In the case of NIR spectroscopy, the accuracy was improved with the introduction of a large number of paired samples showing the 1.0008 slope of linear regression (R^2 = 0.95). However, the use of paired samples with single DC determination rather than mean values substantially decreases the model precision – the RMSE increased from 0.42 to 0.68. It was therefore concluded that for method comparison of

soil analysis, reference sample analysis be replicated for all methods (reference and test methods) to determine the “true” value of analyte as the mean value analysed using the reference method.

Considering the fact that carbon accounting also requires error reporting, it was further concluded that the common practice of using paired samples with single determination (without replication) of SOC DC for NIR model calibration and (cross)validation should be abandoned in favour of finding the mean values for the calibration/validation sets using at least three replicates. The common practice of single determinations, which is mostly justified by financial constraints, substantially decreases the model precision and reduces the range of quantitative SOC determination.

While reasonable figures of merit were obtained for all the methods, the analysis of non-replicated paired samples has shown that the relative RMSE for the SOC NIR method only falls below 10 % for values above ~8 % SOC, while for the corrected SOC WB method the relative RMSE practically never falls below 10 %, rendering the method as semi-quantitative across the range.

6 Improving input parameters for soil organic carbon assessment – effect on errors from point measurements to final map

6.1 Introduction

Interest in the assessment and monitoring of SOC stocks and stock changes has markedly increased in recent years in relation to the agricultural and environmental importance of maintaining and increasing SOC (Chenu et al., 2018). Numerous global initiatives have targets related to the maintenance, increase and assessment of SOC stocks (England et al., 2018). For example, the United Nations Sustainable Development Goal (SDG) Indicator 15.3.1 on the "Proportion of land that is degraded over total land area", includes the assessment of SOC stock along with above ground carbon as one of its metrics in the assessment of land degradation. This same indicator (SDG 15.3.1) and its metrics will be used to monitor progress towards the land degradation neutrality targets of the United Nations Convention to Combat Desertification (UNCCD) (Orr et al., 2017). The "4 per 1000" initiative, which was launched during the 21st session of the United Nations Framework Convention on Climate Change, specifically targets the maintenance and increase of global SOC stocks at a rate of 0.4 % (i.e. 4 per 1000) per year and places particular focus on agricultural land (Soussana et al., 2017).

These international developments have greatly stimulated SOC studies aimed at assessing and improving the accuracy and cost-effectiveness of SOC stock determinations which is a critical step in carbon quantification and accounting (Bellon-Maurel and McBratney, 2011; Bispo et al., 2017; Cremers et al., 2001; De Gruijter et al., 2016; England et al., 2018). However, the assessment and reporting of errors in soil organic carbon (SOC) assessments is rarely quantified or reported. Assessing these errors is important in order to develop ways to reduce the overall uncertainty of SOC estimates, especially in relation to assessing carbon stock changes (Goidts et al., 2009).

Errors in the determination of SOC stocks may arise at various stages of sample handling, processing and analysis (measurement errors), as well as during the prediction of stocks using different models (Batjes and Wesemael, 2015; Brodský et al., 2013; Brown and Heuvelink, 2005). However, quantifying these errors and associated uncertainties may be challenging due to the complex interactions between different variables included in SOC stock determinations (Goidts et al., 2009). The assessment of SOC stock requires the determination of soil bulk

density, SOC concentration [$\%_{wt}$], coarse fragments (>2 mm) and soil depth (Batjes and Wesemael, 2015; England et al., 2018). Therefore, measurement errors may occur during each of these determinations (Batjes and Wesemael, 2015; Goidts et al., 2009). In addition, varying levels of interactions may occur between variables, such as the interaction between SOC concentration and bulk density (Goidts et al., 2009). Furthermore, the sources of uncertainty in SOC stocks may vary according to the scale and landscape unit of assessment and SOC stock assessment designs need to be developed or adapted accordingly (Goidts et al., 2009).

The aim of this study was to assess the changes in SOC stock prediction errors as a function of increased complexity and detail of the model input parameters by mapping the propagated error (measurement and prediction errors) of SOC stock determinations in a quaternary study catchment.

6.2 Materials and Methods

6.2.1 Soil sampling and analysis

Surface (0-5 cm) samples from 47 of the 69 sampled profiles described in Chapter 3were used. Only samples falling within the boundary of the quaternary catchment were used and samples from wetlands were excluded. Samples were prepared and analysed for bulk density (ρ_b) and fraction of stones by weight (S_{wt}) as described in Chapter 3. Each < 2 mm sample was scanned once using NIR spectroscopy as described in Chapter 3 and the SOC content [$\%_{wt}$] was determined using the NIR partial least squares (PLS) model described in Chapter 5.

The 966 surface (0-5 cm) samples taken at 322 sampling sites (three samples per site) in quaternary catchment U40A as described in Chapter 2 were used. All 966 samples were prepared and analysed the same way as above for bulk density analysis. In this case, however, triplicate samples were not combined following bulk density analysis as described in Chapter 3. Instead, each triplicate sample was pounded and sieved to 2 mm, analysed using NIR spectroscopy as described in Chapter 3, and the SOC content [$\%_{wt}$] determined using the NIR PLS model described in Chapter 5. Samples for which the predicted SOC % fell outside the range of the NIR PLS calibration curve were removed as outliers, leaving 949 samples at 322 sites. As a result, a total of 996 (47 + 951) surface (0-5 cm) samples from 369 (47 + 322) locations were used in this study.

Exponential SOC distribution functions and relevant exponential coefficients (*k*-values) as

developed for individual soil profiles under different land uses in Chapters 3 and 4 were applied in this study. *K*-values from a total of 45 profiles under forestry (20), grassland (11) and cropland (14) were used and grouped in various ways for the production of four (4) SOC stock maps based on land use and soil type. The piecewise distribution functions developed from eight profiles in croplands under reduced tillage in Chapter 4 with associated *k* and *b*-values (linear decline gradient) were also used.

6.2.2 Calculation of SOC volumetric content and stock

As described in Chapter 3, the volumetric carbon content Cv [kg·m^{-3}] within the upper 5cm depth interval z=[z0,z0.05] was calculated as:

$$C_v^0 = 10 \cdot SOC \cdot \rho_b \cdot \left(1 - S_{wt} \frac{\rho_b}{\rho_s}\right) \quad (6\text{-}1)$$

where:

C_v^0 is the volumetric carbon content at 0-5 cm [kg·m^{-3}],

SOC is the weight percentage [%$_{wt}$] of soil organic carbon in the 2 mm soil fraction,

ρ_b and ρ_s (2.65) are the bulk and particle density [Mg·m^{-3}] respectively,

S_{wt} is the fraction of stones by weight, and

10 is the conversion factor for SOC from [%$_{wt}$] to kg·Mg^{-1}.

The SOC stock (C_s) [kg·m^{-2}] for continuous exponential decline functions was calculated as described in Chapter 3 as the integral of the exponential decline function to a depth of 1 m [z_0,z_1] as:

$$C_s = \int_0^1 C_v^0 e^{-kz} = \frac{C_v^0}{k}\left(1 - e^{-kz_1}\right) \quad (6\text{-}2)$$

where:

k is the coefficient of the exponential function, and

z is the soil depth [m].

The SOC stock (C_s) [kg·m^{-2}] for piecewise decline function characterizing the cultivated

fields with reduced tillage was calculated using two integrals as described in Chapter 4. The value of C_s at 0-30 cm [z_0,$z_{0.3}$] was calculated as the integral of the linear decline function as:

$$\int_{z_0}^{z_{0.3}} C_v^0 \cdot (1 - bz)dz = C_v^0 \cdot \left(\left(z_1 - \frac{b(z_1)^2}{2}\right) - 1\right) \quad (6\text{-}3)$$

where:

b is the trendline gradient.

The value of C_s at 30-100 cm [$z_{0.3}$,z_1] was calculated as the integral of the exponential decline function to a depth of 30 cm as:

$$\int_{z_{0.3}}^{z_1} C_v^{30} \cdot 1.3e^{-kz}\, dz = 1.3 \cdot \frac{C_v^{30}}{k} \cdot \left(e^{-kz_{0.3}} - e^{-kz_1}\right) \quad (6\text{-}4)$$

where:

C_v^{30} is the volumetric SOC content at 30 cm depth, and

1.3 is the y-intercept of the exponential function.

According to information received from a local farmers' association, most farmers in the catchment use some form of reduced tillage for maize production. However, ground-truthing this information was not possible, which on its own creates an additional level of uncertainty. This uncertainty was not assessed.

6.2.3 Calculation of measurement error

The total (propagated) measurement error (RMSE) for the determination of C_v^0 may be approximately calculated by a method commonly used in engineering, physics and chemistry (Harvey, 2000) as:

$$\text{RMSE}(C_v^0) = \sqrt{{C_v^0}^2 \left(\left(\frac{\delta \text{SOC}}{\overline{\text{SOC}}}\right)^2 + \left(\frac{RMSE(SOC)}{\overline{\text{SOC}}}\right)^2 + \left(\frac{\delta \rho_b}{\overline{\rho_b}}\right)^2 + \left(\frac{\delta S_{wt}}{\overline{S_{wt}}}\right)^2\right)} \quad (6\text{-}5)$$

where:

$\overline{\text{SOC}}$ is the mean of the three soil organic carbon measurements per sampling point using NIR spectroscopy,

δSOC is the standard deviation of the three soil organic carbon measurements per sampling point using NIR spectroscopy,

$RMSE(\text{SOC})$ is the RMSE of the NIR method to determine SOC (obtained from Chapter 5),

$\overline{\rho_b}$ is the mean of the three bulk density measurements sampling point,

$\delta\rho_b$ is the standard deviation of the three bulk density measurements,

$\overline{S_{wt}}$ is the mean of the three gravimetric stone content measurements, and

δS_{wt} is the standard deviation of the three gravimetric stone content measurements. The error for the determination of SOC stock (C_s) using Eq. 6-2 was calculated as:

$$\text{RMSE}(C_s) = \sqrt{{C_s}^2\left(\left(\frac{RMSEC_v^0}{\overline{C_v^0}}\right)^2 + 2\cdot\left(\frac{\delta k}{\bar{k}}\right)^2\right)} \quad (6\text{-}6)$$

where:

$RMSE(C_v^0)$ is calculated in Eq. 6.5,

$\overline{C_v^0}$ is the mean of the C_v^0 values,

$\bar{k}$ is the mean of the k-values, and

δk is the standard deviation of the k-values.

The cumulative error for the determination of SOC stock (C_s) using Eqs. 6-3 and 6-4 was calculated as:

$$\text{RMSE}(C_s) = \sqrt{{C_s}^2\left(2\cdot\left(\frac{RMSEC_v^0}{\overline{C_v^0}}\right)^2 + 3\cdot\left(\frac{\delta k}{\bar{k}}\right)^2 + \left(\frac{\delta b}{\bar{b}}\right)^2\right)} \quad (6\text{-}7)$$

where:

$\bar{b}$ is the mean of the *b*-values, and

δb is the standard deviation of the *b*-values.

6.2.4 Digital soil organic carbon and error mapping

All calculations and spatial interpolations were performed in R. During the spatial interpolation of C_v^0, C_s and the propagated errors associated with C_s determination, the relevant parameters were first calculated for each sample using Eqs. 6-1 to 6-7 and then interpolated. All maps were interpolated at 10 m resolution.

Interpolations of C_v^0 and C_s were done using random forest regression. The sample set was split into a 70 % training and 30 % validation set and a component-wise linear feature selection was used on all covariates. The number of covariates randomly tested at each split was optimised through 25 bootstrap resamples and the number of trees was held constant at 2000 to obtain accurate covariate importance measures. The model was validated using the 30% external samples and the out-of-bag (OOB) error.

Interpolation of the errors associated with C_s determination was performed through variogram analysis and universal kriging using only the C_v^0 as a covariate. A variogram function for each C_s prediction was fit through residual maximum likelihood analysis and then kriged over the C_v^0 layer.

Three maps of C_s and their associated errors were developed. For each subsequent set of maps, the level of detail in the input parameters were increased to evaluate the effect on map accuracy and cumulative error. The input parameters and equations used for their determination are summarized in Table 6-2.

Soil type and land use rasters, as well as the covariate layers used were developed at 10 m resolution by T. Flynn for a yet unpublished digital soil mapping project in the study area which does not form part of this study. These rasters were developed using proprietary soil point data provided by Mondi Forests (Pty) Ltd and a 30 m digital elevation model (DEM) resampled from the ALOS-2 satellite as well as spectral 30 m grids from the Landsat 7 ETM+ satellite. All covariates were resampled to 10 m. A resolution of 10 m was used because it achieved a higher accuracy than the original 30 m data. The 44 covariates were used in the feature selection are presented in Table 6-2.

Table 6-1. Summary of input parameters and equations used for the development of three maps of C_s and its associated propagated errors. (LU – Land use; FO = Forestry; GL = Grasslands; CL = Croplands; n = number of samples; Eq. = Equation)

Map	LU	Calculation of C_s (Total n = 369)			Calculation of RMSE(C_s) (Total n = 322)		
		Name	Eq.	Input parameters	Name	Eq.	Input parameters
1	All	Map C1	6-2	Single *k*-value: calculated as the mean *k* for all profiles	Map E1a	6-6	Single $RMSE(\mathrm{SOC})$ value for the NIR method for all values of SOC [%$_{wt}$]
					Map E1b	6-6	Different $RMSE(\mathrm{SOC})$ values for the NIR method for different range intervals [a,b] of SOC [%$_{wt}$]
2	FO	Map C2	6-2	Single *k*-value: calculated as the mean *k* for forestry profiles	Map E2	6-6	As for Map E1b
	GL		6-2	Single *k*-value: calculated as the mean *k* for grassland profiles		6-6	As for Map E1b
	CL		6-2	Single *k*-value: calculated as the mean *k* for cropland profiles		6-6	As for Map E1b
3	FO	Map C3	6-2	Single *k*-value per group of soil types: calculated as the mean *k* per group of soil types under forestry	Map E3	6-6	As for Map E1b
	GL		6-2	Single *k*-value per group of soil types: calculated as the mean *k* per group of soil types under grasslands		6-6	As for Map E1b
	CL		6-3	Single *b*-value for the 0-30 cm interval: calculated as the mean *b* for reduced tillage profiles (obtained from Chapter 4)		6-7	As for Map E1b
			6-4	Single *k*-value for 30-100 cm interval: calculated as the mean *k* for reduced tillage profiles (obtained from Chapter 4)		6-7	As for Map E1b

Table 6-2. List of 44 covariates at 10 m resolution used in the feature selection.

Covariate	Covariate	Covariate
Analytical hillshading[1]	Land types	SAGA wetness index
Aspect[1]	Land use	Saturation index
Blue	LS factor	SAVI[2]
Brightness index	Mid slope position	Sky view
Catchment area	MRRTF[2]	Slope
Catchment slope	MRVBF[2]	Slope height
Colouration index	NDVI[2]	SWIR[2]
Convergence index	Negative openness	Terrain factor
Convexity	NIR[2]	Terrain position index
DEM	Normalised height	Terrain ruggedness index
Flow direction	Plan curvature	Terrain units
Geomorphons	Positive openness	Valley depth
Gradient	Profile curvature	Vector ruggedness measure
Gradient difference	Red	Visible sky
Green	Redness index (Hematite)	

[1] These covariates were placed into the component wise-linear feature selection

[2] MRRTF = multiresolution ridge top flatness, MRVBF = multiresolution valley bottom flatness, NDVI = normalized difference vegetation index, NIR = near-infrared, SAVI = soil adjusted vegetation index, SWIR = short-wave infrared

6.3 Results and Discussion

6.3.1 Grouping of exponential and linear coefficients of vertical SOC distribution

The level of detail in Maps C1 to C3 was increased by increasing the specificity of *k*-values as a function of land use and soil type. The natural variation in profile SOC distribution could be captured by grouping *k*-values to either land use or soil type (Khalil et al., 2013; Ros Mesa, 2015; Wiese et al., 2016). These values can then be related to spatial information of the particular feature. In Chapter 3 the *k*-values were ultimately grouped according to soil types and mapped accordingly (Wiese et al., 2016).

In Chapter 4 it was shown that the accuracy of exponential SOC distribution functions

were improved by grouping *k*-values per land use for grasslands and croplands. In cultivated soils, however, the SOC concentration in the tillage layer is strongly affected by the relevant tillage practices (Liu et al., 2016; Meersmans et al., 2009; Stockfisch et al., 1999; VandenBygaart and Kay, 2004). As a result, the vertical SOC distribution models for croplands in Chapter 4 were further improved by developing piecewise SOC distribution functions for maize production under reduced tillage and conventional tillage.

As indicated in Table 6-2, a single *k*-value was used for the entire catchment in Map C1 and for Map C2 the *k*-values were grouped per land use. Figure 6-1a shows the land use map produced by T. Flynn that was used to relate mean *k*-values to forests, grasslands and croplands and Table 6-3 shows the lookup table with the respective *k*-values used per land use.

For Map C3 the *k*-values for forestry and grasslands were further subdivided and grouped by soil types actually sampled in these land uses. K-means clustering applied to the *k*-values of 11 grassland profiles identified two distinct groups of soil types. The first group was a combination of Kp/Ia/Pn/Ma (Kranskop/Inanda/Pinedene/Magwa) and the second a combination of No/Gs/Ka (Nomanci/Glenrosa/Katspruit). Based on the k-means clustering results it was also possible to separate Ka soils into a third class. Considering that No and Gs soils are generally shallower soils with a lithocutanic B horizon, this may have been a good option. However, due to the overall low number of profiles, of which only two were Ka soils, it was opted to use only two groups. A T-test analysis at α=0.05 confirmed that the mean *k*-values for the two groups were significantly different with P = 0.0066 (Table 6-3).

Results of k-means clustering for *k*-values of 20 forestry profiles were less distinct, but good enough to enable the selection of two groups. It was clear that the *k*-values of Ma soils grouped well together, while Ia and Kp soils grouped together. The No grouped more towards the Ia/Kp group, with some profiles interspersed with the Ma soils. The selection of three groups was tested (based on the shallowness of the No soils) as Ma, No and Ia/Kp using t-test analysis, but there was no significant different between the means of the No and Ia/Kp groups. As a result, two groups of *k*-values were selected as Ma and Ia/Kp/No. T-test analysis confirmed the highly significant difference of the mean *k*-values between the groups with P = 0.0013 (Table 6-3).

Figure 6-1b shows the map of nine soil types produced by T. Flynn that was used to relate the *k*-values and *b*-values to soil types. However, profile data was only available for seven soil

types in grasslands and four soil types in forests. As a result, soil types in Figure 6-1b without measured *k*-values were termed “other” in Table 6-3 and assigned the mean *k*-value for the particular land use that was used in Map C2.

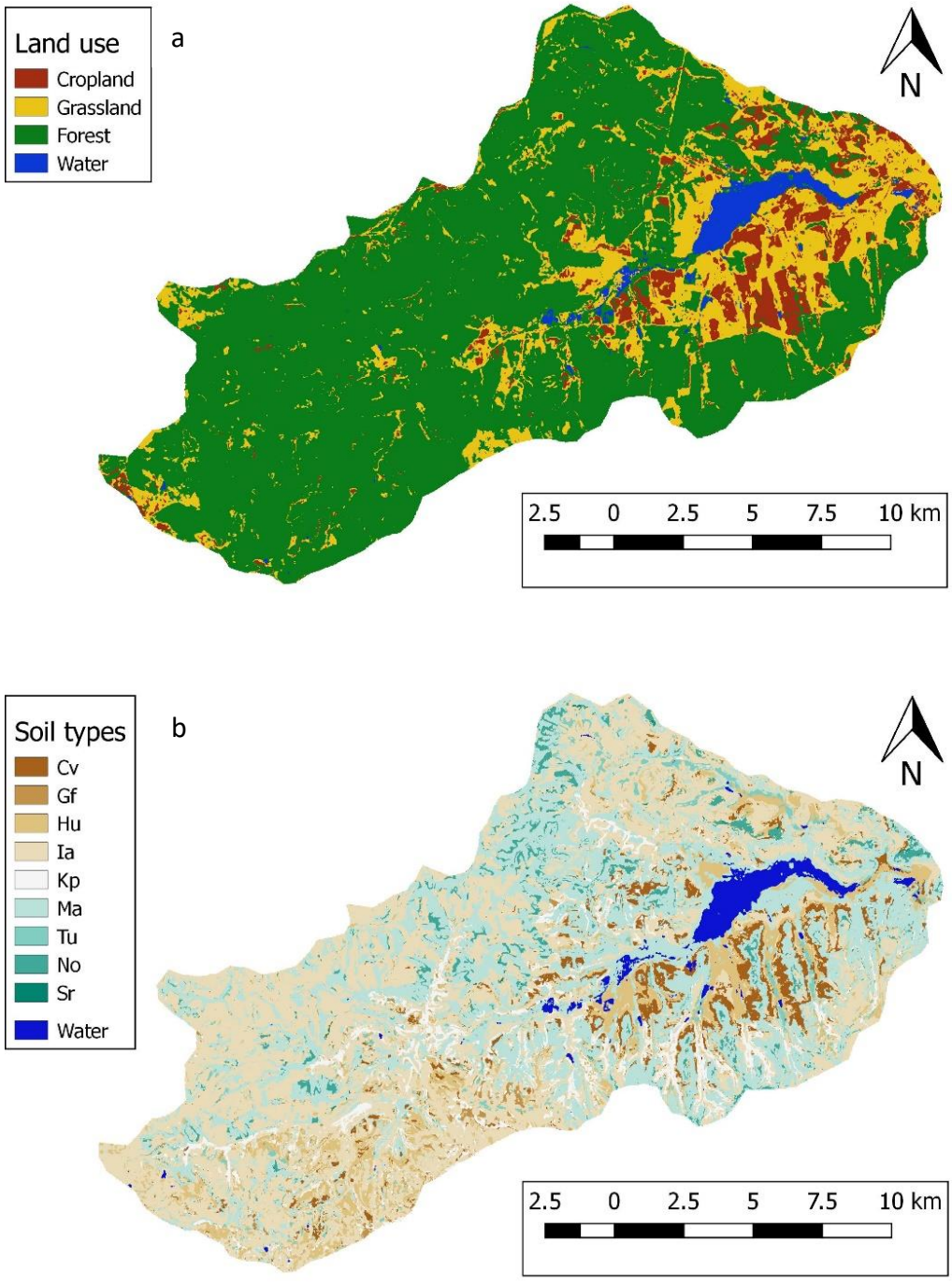

Figure 6-1. Distribution of croplands, grasslands and forestry (a) and soil types (b) in the study catchment (Developed by T. Flynn).

Table 6-3. Lookup table used for the development of SOC stock maps showing the mean ($\bar{k}$ and $\bar{b}$) and standard deviations (δk and δb) for the input parameters used in the calculation of SOC stocks. The t-test results show the significant differences between the soil type groupings for Grasslands and Forest at α=0.05.

Land use	Soil type	$\bar{k}$	δk	$\bar{b}$	δb	t-test
Maps 1 and 2						
All land use		2.13	0.79			
Map 3						
Grassland		2.81	0.77			
Forest		2.13	0.7			
Cropland		1.59	0.48			
Map 4						
Grassland	Kp/Ia/Pn/Ma	2.3	0.61			0.0066
	No/Gs/Ka	3.41	0.43			
	Other	2.81	0.77			
Forest	Ia/Kp/No	2.56	0.44			0.0013
	Ma	1.61	0.6			
	Other	2.13	0.7			
Cropland	All	1.96	0.48	0.81	0.31	

As indicated in Chapter 2, the main form of agriculture in the study area is maize production. During the field excursion it was evident that the majority of maize producers apply some form of reduced tillage. However, the specific tillage systems used is not known for all croplands in the study area. For the development of Map C3 the assumption was therefore made that all croplands in the catchment are cultivated using reduced tillage. In Chapter 4 it was shown that the SOC distribution in soils under reduced tillage follow a piecewise distribution with a linear decline in the top 30 cm and an exponential decline from 30-100 cm. For Map C3 the croplands were therefore assigned single values for the linear and exponential decline coefficients (*b* and *k*) (Table 6-3) which were obtained from Chapter 4.

6.3.2 Calculation of error propagation

The error calculation for the determination of SOC stocks (C_s) incorporated the measurement error of the ($RMSE(C_v^0)$) and the error for the determination of SOC stock that

used the vertical distribution coefficients. In Chapter 5 it was shown that, when SOC [$\%_{wt}$] is analysed using the NIR partial least squares model with single-measurement SOC values obtained from dry combustion (DC) as reference method, the results are highly heteroscedastic. This was demonstrated by splitting the range of SOC values analysed by DC into a range of intervals [a,b] of increasing range and calculating the RMSE of the NIR analysis for each range. Due to the heteroscedasticity of the data, the RMSE increases with an increase in SOC content as illustrated in Table 5-3.

As shown in Table 5-3, the mean RMSE for the full dataset is 0.68. However, when splitting the dataset into intervals, it shows that for several smaller intervals the RMSE is well below the mean. Therefore, Table 6-4 was used as a lookup table for the calculation of RMSE(C_s) in the development of error Map 2 to determine whether increasing the level of detail of RMSE would reduce the overall error of the SOC stock determination.

Table 6-4. Lookup table for the RMSE of the [a,b] intervals of the calibration/cross-validation range of single SOC content measurements with DC and NIR PLS model. (a = lower limit of the range; b = upper limit of the range; μ = mean SOC % for the range; n = number of samples).

a	b	μ	n	RMSE
All				0.68
0.135	0.225	0.18	4	0.19
0.225	0.375	0.30	5	0.44
0.375	0.625	0.50	15	0.70
0.625	1.042	0.83	30	0.47
1.042	1.736	1.39	37	0.50
1.736	2.893	2.31	89	0.67
2.893	4.822	3.86	107	0.56
4.822	8.037	6.43	19	0.62
8.037	13.396	10.72	84	0.93
13.396	22.326	17.86	7	1.03

Other methods to determine the combined error more accurately, particularly in the presence of interactions between parameters (i.e. between SOC content and bulk density)

(Elamir and Seheult, 2004; Goodman, 1960) may be used (Goidts et al., 2009). This would have been useful if the techniques of measuring the variables in Eq. 6-5 were to be further improved. Since such a task is beyond the scope of this work, it was decided to simply assess the error of C_v^0 measurements from three sample replications rather than through error propagation from determination of individual parameters.

Error propagation method was used to assess the precision of the SOC stocks, which could not have been done otherwise and clearly separates the contribution of the C_v^0 measurements and the vertical distribution model towards overall spatial precision.

6.3.3 Interpolation of surface volumetric SOC content (C_v^0)

The SOC content in the 996 samples determined by NIR spectroscopy ranged from a minimum of 1.91 % to a maximum of 22.78 % (μ = 9.01 % C). In Chapter 5 the limit of detection and limit of quantification for the NIR method were estimated as 0.45 % and 1.38 % carbon respectively. Therefore, all the estimates in this study fall sufficiently above the limits of the analysis method.

The values of C_v^0 calculated using Eq. 6-1 ranged from 18.79 kg·m^{-3} to 191.92 kg·m^{-3} with a mean of 65.78 kg·m^{-3}. The C_v^0 values per land use were compared using a T-test to test for significant differences between the means. The results in Table 6-5 show that the mean for croplands (n = 88) was highly significantly different from the means of forestry (n = 698) and grasslands (n = 210), but there was no significant difference between the means for forestry and grasslands. Table 6-5 also shows the means and standard deviations of C_v^0 for each of the land uses.

Table 6-5. Mean and standard deviation of the volumetric SOC content [kg·m^{-3}] in the surface samples under different land uses indicating significant differences between the means based on a Student's t-test for α=0.05. (FO = Forestry [n = 698]; GL = Grassland [n = 210]; CL = Cropland [n = 88])

	FO 67.6 ± 23	GL 68.4 ± 22.6
GL 68.4 ± 22.6	0.6204	
CL 45.3 ± 18.6	**< 0,0001**	**< 0,0001**

The interpolated map of C_v^0 values across the study area is shown in Figure 6-2, including the locations of the 369 samples used for the interpolation. According to the OOB calculated during validation of 30% external samples, the model explained 59% of the variance.

Statistically the map has an R^2 of 72, RMSE of 13.41 and Bias of 1.63. The covariates used in the interpolation are shown in Table 6-6 in order of importance.

Table 6-6. Covariates used in the interpolation of the surface volumetric SOC values (C_v^0) in order of importance.

Rank	Covariate	Rank	Covariate
1	DEM	9	Gradient
2	Valley depth	10	SWIR
3	Terrain view	11	Blue
4	Vector ruggedness index	12	LS factor
5	Negative openness	13	Positive openness
6	Convergence index	14	Geomorphon
7	Coloration index	15	Terrain ruggedness index
8	Gradient difference	16	MRVBF

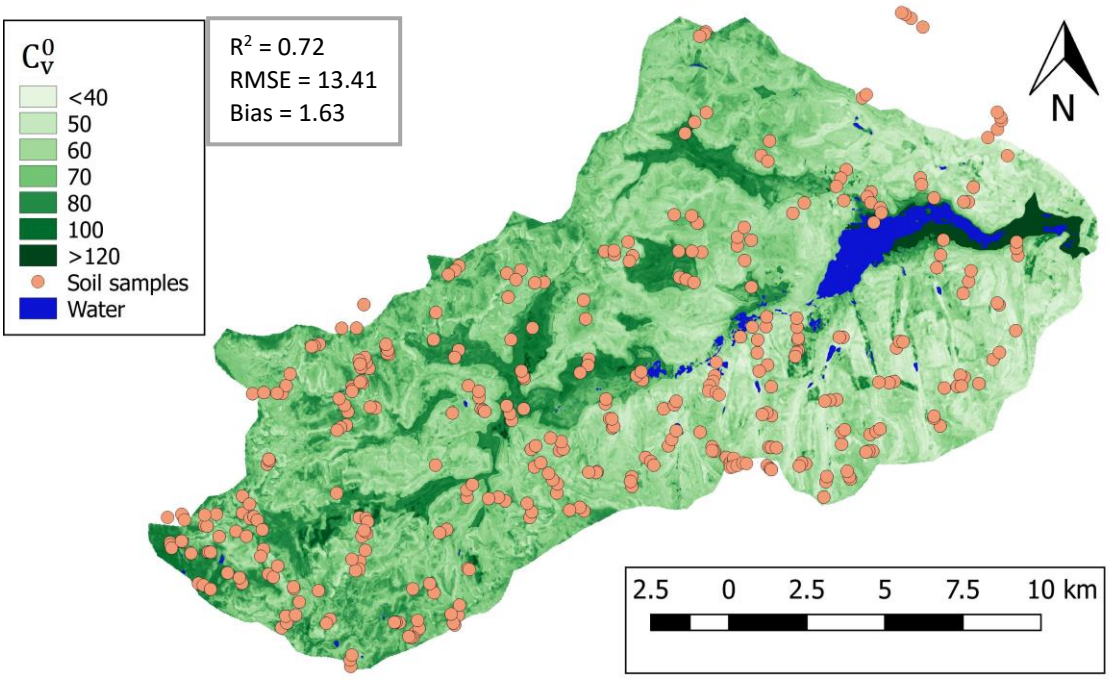

Figure 6-2. Interpolation result of the surface volumetric SOC values (C_v^0) (kg·m^{-3}) within the upper 5cm depth interval at 369 surface locations using random forest regression in R.

6.3.4 Soil organic carbon stocks and associated errors

Calculation of the SOC stocks done for the first meter of soil without taking into consideration actual soil depth <1 m. This decision was made based on both pragmatic and theoretical considerations. All the cultivated areas in the catchment are located on deep soils, while the spatial distribution of shallow soils in the forestry and grassland areas is difficult to predict. Attempts to do so with the analysis of the detailed (1:10 000) soil maps (used in Chapter 3) available for Mondi Forest plantations within the catchment so far yielded very poor results with R^2 below 0.5. Soil depth is also mostly characterized by very coarse measurements recorded in the data set as 30 cm increments (30, 60, 90, >120 cm). The use of these values would introduce additional uncertainty if the depth to bedrock indeed prohibited root penetration into and carbon accumulation in the fractured rock.

The theoretical considerations for keeping the model depth to 1m were based on the understanding that roots would be the main source of SOC in deeper soil layers (Hütsch et al., 2002). The occurrence of roots in fractured shale, which dominates the landscape of the study catchment will not be restricted by the Effective Soil Depth (ERD) indicated in the Mondi data set, since root penetration of both grasslands (Nippert and Holdo, 2015) and forest plantation genera (pine, eucalyptus and wattle) will exceed the 1m depth even in shallow soils (Harper and Tibbett, 2013; Laclau et al., 2013; Schenk, 2008; Schenk and Jackson, 2005). While the presence of fractured rock does restrict manual excavation, it has much less effect on the penetration of tree roots (Ficarelli et al., 2003; Hubbert et al., 2001; Schwinning, 2010; Zwieniecki and Newton, 1995). Here it is assumed that the exponential decline model will adequately describe the SOM behaviour as the transition occurs from fine-earth sediment into the fractured rock within the 1 m depth.

The interpolated map of C_v^0 (Figure 6-2) was used as an additional covariate in the development of maps for C_s (Maps C1 to C3) and the only covariate for the interpolation of RMSE(C_s) (Maps E1a to E3). The covariates used in the interpolation of Maps C1 to C3 are shown in Table 6-7 in order of importance, and their map interpolation statistics are given in Table 6-8. Map C1 and its associated error maps (E1a and E1b) are shown in Figure 6-3; Maps C2 and C3 and their associated error maps (E2 and E3) are shown in Figure 6-4 and Figure 6-5 respectively.

Table 6-7. Covariates used in the interpolation of the SOC stock (C_s) in order of importance for Maps C1 to C3.

Rank	Map C1	Map C2	Map C3
1	Cv0	Cv0	Cv0
2	DEM	DEM	LS factor
3	Negative Openness	Negative openness	DEM
4	Valley Depth	LS factor	Negative openness
5	VRM	Profile curvature	Valley depth
6	Profile curvature	MRVBF	RI
7	LS factor	VRM	VRM
8	RI	Valley depth	Aspect
9	MRVBF	MRRFT	NIR
10	MRRTF	RI	CI
11	Aspect	CI	Profile curvature
12	CI	Aspect	MRVBF
13	NIR	NIR	MRRTF

Table 6-8. Summary of map interpolation statistics for Maps C1 to C3.

Map	R^2	RMSE [kg·m^{-2}]	Bias
C1	0.86	5.75	1.28
C2	0.77	6.03	1.23
C3	0.64	7.79	0.76

From Table 6-8 there are two important results to consider. Firstly, the results show that an increase in the detail of input parameters used to model SOC stocks in the first 1 m of soil leads to a clear decrease (41 %) in the bias (from 1.28 in Map C1 to 0.76 in Map C3). This indicates that improved modelling of the SOC stocks results in increased accuracy of the resulting SOC stock maps and is supported by the simultaneous decrease in the propagated error of SOC stock determination (RMSE(C_s)).

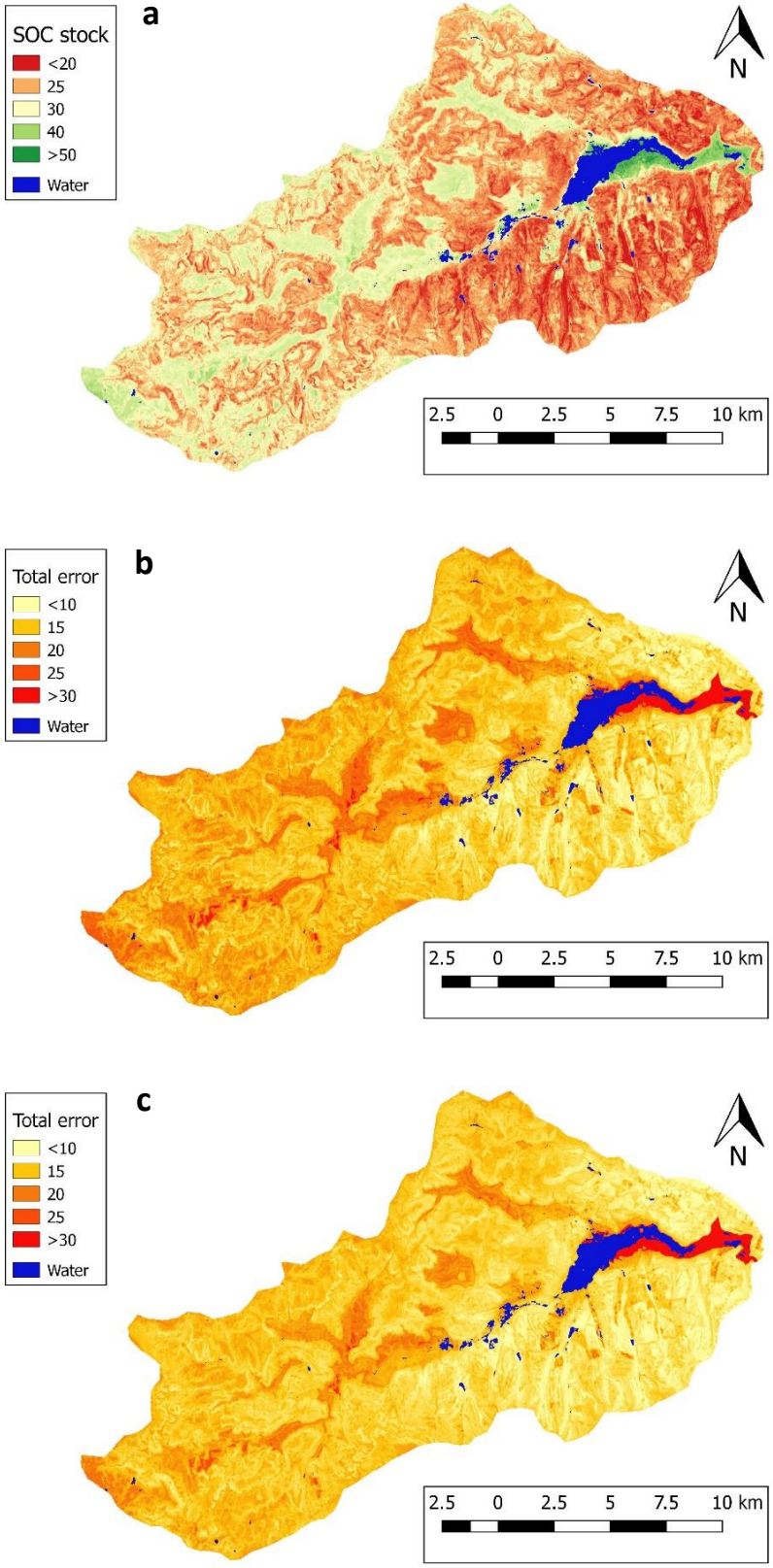

Figure 6-3. Map of SOC stock (C_s) [kg·m^{-2}] in the upper 1 m of soil determined using a single k-value for the entire catchment (Map 1) (a) and the associated propagated measurement and prediction errors (RMSE(C_s)) [kg·m^{-2}] calculated using a single value of $RMSE(SOC)$ for the entire catchment (Map E1a) (b), and using different values of $RMSE(SOC)$ based on different range intervals of SOC [%wt] (Map E1b) (c).

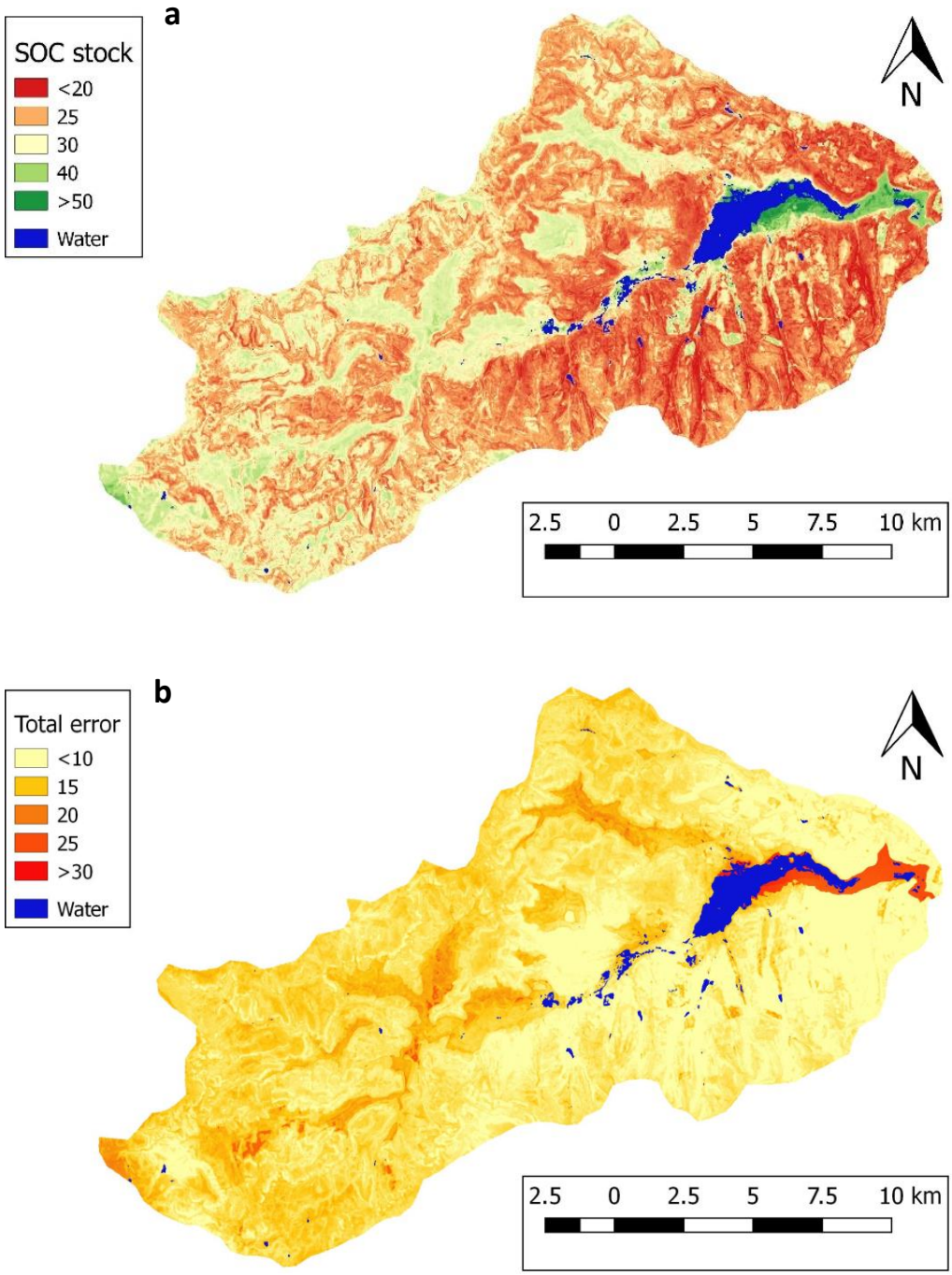

Figure 6-4. Map of SOC stock (C_s) [kg·m^{-2}] in the upper 1 m of soil determined using a single k-value per land use (Map 2) (a) and the associated propagated measurement and prediction errors (RMSE(C_s)) [kg·m^{-2}] calculated using different values of $RMSE(SOC)$ based on different range intervals of SOC [%$_{wt}$] (Map E2) (b).

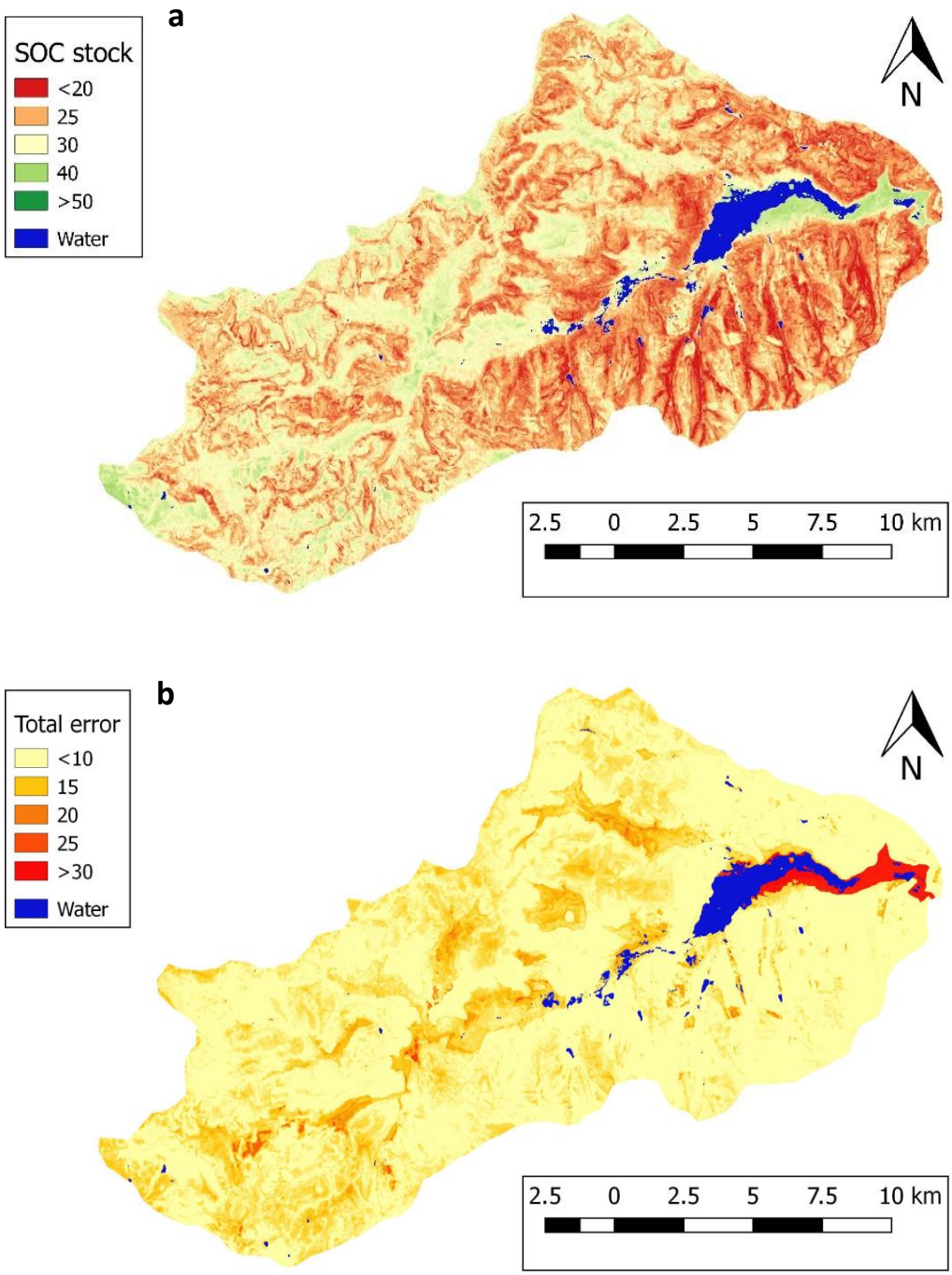

Figure 6-5. Map of SOC stock (C_s) [kg·m^{-2}] in the upper 1 m of soil determined using k-values differentiated per soil type (in forests and grasslands) and a piecewise distribution function in croplands (Map 3) (a) and the associated propagated measurement and prediction errors (RMSE(C_s)) [kg·m^{-2}] calculated using different values of $RMSE(SOC)$ based on different range intervals of SOC [%$_{wt}$] (Map E3) (b).

On the other hand, the same increase in input parameters results in a decrease in the map R^2 (from 0.86 in Map C1 to 0.64 in Map C3) and an increase in the RMSE (from 5.75 in Map C1 to 7.79 in Map C3) which in turn indicates a decrease in map precision. To investigate this further, the results from the error estimates in Maps E1a to E3 were analysed relative to the SOC stock maps (Maps C1 to C3) to determine the relative RMSE [%] as summarized in Table 6-9 and presented form Maps E1a and E3 in Figure 6-6.

Table 6-9. Relative RMSE [%] calculated from Maps E1a to E3 for the prediction of SOC stocks in the catchment, shown as the minimum, maximum, mean and standard deviation (δ) for each map.

Error Map	Relative RMSE [%]			
	Minimum	Maximum	μ	δ
1a	28.0	102.1	56.6	6.2
1b	29.7	86.8	52.8	4.5
2	15.6	76.5	45.6	5.2
3	4.9	104.9	38.2	9.6

The progression of relative RMSE from Map E1a to E3 shows the narrowing of mean relative error across the quaternary catchment along with the increase of input detail. Both RMSE and relative RMSE are high around the Mvoti vlei – the protected wetland surrounded by grasslands, which was not sampled. This area borders on private farms with maize fields, fallow lands and pastures. The spatial pattern of these land uses also leads to high uncertainty due to patchiness and complexity of the land cover. Although very high carbon stocks are predicted for this area, the error of these predictions is close to 100 % (Figure 6-6). No matter how accurately the models are adjusted to land use and soil conditions, this error associated with spatial variability is persistent and carries across from Map C1 to C3. This error is primarily associated with low density of surface sampling and C_v^0 determination resulting in large interpolation errors. A significantly higher sampling density would be required for farm-scale carbon accounting to reduce the uncertainty compared to the sampling density used for the whole sub-catchment used in this study.

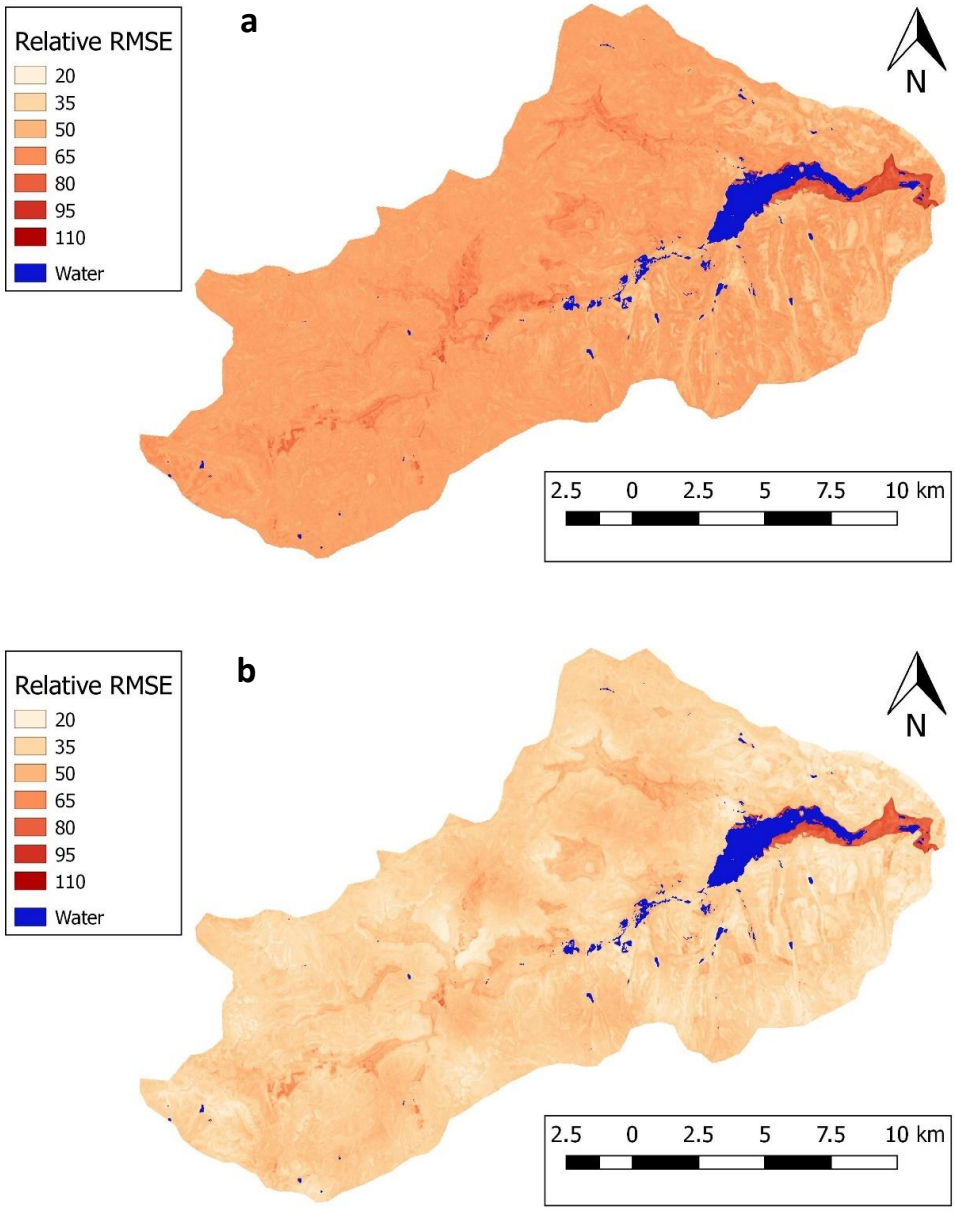

Figure 6-6. Relative RMSE [%] for Maps E1a (a) and E3 (b).

6.4 Conclusions

The overall accuracy (R^2 = 86; bias = 1.28) and precision (RMSE = 5.75) of the map generated using a single *k*-value for the entire catchment were considered acceptable for a general assessment of carbon stocks in the first 1 m of soil and visualisation of their distribution at the scale of the study quaternary catchment covering 317 km^2. This level of accuracy and precision was achieved using 322 triplicate sampling locations and 47 single sampling locations randomly distributed across the catchment, together with a single generic SOC vertical distribution function for the entire catchment. The associated error for this

generic prediction of SOC stocks was improved when applying a sliding scale of the RMSE(SOC) based on different range intervals of SOC [$\%_{wt}$] content.

For the studied catchment dominated by forest plantations and native grasslands, increasing the level of input detail in terms of the SOC vertical distribution functions applied from a single generic function for the entire catchment to to functions differentiated by land use and soil grouping improved the map precision. In addition, a strong improvement in the accuracy of SOC stocks was observed with the decrease in bias. Still, the relative error mostly exceeds 20 % which may be seen as unacceptably high for carbon accounting and trade purposes, and the SOC stock accuracy decreases in terms of R^2 and RMSE.

The increase in precision (decreasing relative RMSE) and partial increase in accuracy (decreasing bias) show potential for the increase in overall accuracy of SOC predictions by increasing the R^2 and RMSE. These results are especially positive in terms of the progressive increase in complexity associated with transition from applying single to differentiated SOC vertical distribution functions and shows the need for a substantial increase in sampling density to maintain or increase the accuracy while increasing precision. This would include an increase both in surface samples for the determination of C_v^0, as well as an increase in the sampling of profiles to include more soil types and improve the vertical SOC distribution models used as input for SOC stock prediction.

7 General Conclusions

For soils characterized by a mean exponential decline in SOC content with depth, normalization of the volumetric SOC (Cv) vertical distribution curve by the volumetric SOC content at the surface (0-5 cm) (C_v^0) allowed isolation of the rate of SOC decline for several groups of soils in the study catchment. The rate of SOC decline was expressed as the *k* coefficient specific to each group. The confidence level for *k* coefficients was numerically characterized by standard deviation, and in combination with the measured C_v^0 value may be used for mapping and monitoring carbon stocks over large areas where land use and soil type information is available. Since the C_v^0 values were measured, the uncertainty in SOC stock predictions was largely associated with the C_v^0 measurement error, the standard deviation of *k* values, the density of C_v^0 observations and their interpolation. It was shown that the two independent variables of the volumetric carbon content at the soil surface (C_v^0) and the coefficient *k* were sufficient for predicting and mapping soil carbon stocks in the areas covered by soil survey.

The vertical distributions of SOC stocks under grasslands and croplands with three different types of tillage systems were successfully modelled to a depth of 1 m. For on-farm SOC accounting, a small number (<10) of individual soil profile observations per land use (in this case 8) to a depth of one meter was sufficient to develop a robust model of mean vertical normalized SOC (Cv_s) distribution for stable land use systems practiced for more than 10 years. The vertical distribution of SOC stocks normalized by C_v^0 may be described with a continuous exponential function in the native grasslands of the study area, as well as in the adjacent fields cultivated using a no-till mixed cattle/maize production system.

In the case of reduced and conventional (full) tillage systems, piecewise functions separately describing the vertical distribution of SOC stocks normalized by the C_v^0 for the plough layer and deeper layers were better suited for predicting SOC stocks compared to a single exponential function. In the case of reduced tillage, a linear decline function may be used for predicting the SOC stocks in the plough layer (0-30 cm). For conventional tillage the mean vertical SOC stock distribution throughout the plough layer may be approximated to a constant value equal to the value at the soil surface (0-5 cm).

It was shown that for all the studied land use systems, irrespective of specific soil type, the vertical distribution of soil organic carbon stocks in the first meter of soil may be successfully predicted with varying degrees of accuracy from only sampling the 0-5 cm

increment to determine bulk density, volume of stones (>2 mm fraction) and SOC content in the <2 mm fraction.

The SOC analysis by dry combustion showed good accuracy and precision for estimating the mean from triplicate SOC determination in 12 samples with SOC % ranging from 0.75 to 17.13. The relative standard deviation (δ) remained below 10 % throughout the range. The RMSE for eleven triplicate determinations after outlier removal was 0.10 % C. Although the stated instrument precision is 0.01 % C, it cannot be used as an estimation of the method precision as a whole without considering the variation in the analyte composition, errors of weighing the subsample, etc., which impose their own restrictions on the overall method characteristics. The higher than expected level of error should be taken into account for use of natural soil samples as reference material for comparison of different analytical methods. It was therefore concluded that, for comparison of different analytical methods, multiple replicates (at least three) of natural soil reference samples should be analysed using the reference method to determine the "true" value of analyte as the mean value.

Both wet oxidation using the Walkley and Black (1934) method and the SOC determination with the PLS regression model based on NIR spectroscopy have shown substantially worse results compared to the dry combustion method. The error of predicting the mean SOC concentration determined by the Walkley and Black method showed good reproducibility of results and was comparable to that of the dry combustion method. The accuracy was variable with the slope of linear regression (conversion factor) varying between 1.10 and 1.27 depending on the regression optimization method and was below the commonly used generic conversion factor of 1.32. Predicting the dry combustion SOC from Walkley Black SOC determinations using paired single observations yielded rather poor results with a regression slope (conversion factor) of 1.1835. The regression between single observations (without replication) of dry combustion SOC versus corrected Walkley Black SOC values showed an R^2 = 0.8699 and an RMSE = 0.47. For the analysis of non-replicated paired samples using the corrected Walkley Black SOC method, the relative RMSE practically never fell below 10 %, rendering the method as semi-quantitative across the analyte range. Therefore, it was concluded that the variable accuracy (correction factor) of the Walkley Black method poses a serious challenge for its use in carbon accounting.

The analysis of means from triplicate SOC determination has shown reasonable accuracy and precision of SOC detection with NIR spectroscopy across the wide range of values, though inferior to dry combustion method. A small deviation from the 1:1 regression line (1.04) with

R^2 = 0.99 and RMSE = 0.42 % SOC. The model also showed the relative RMSE below 20 % (and in 78 % of observations – below 10 %) of measured values, which may be seen as acceptable for some applications. The NIR method accuracy deteriorated when comparing analyses of single measurements with DC and NIR, with R^2 = 0.95, 1:1 correspondence between the paired values, and an RMSE = 0.68. The relative RMSE for the SOC NIR method analysis of non-replicated paired samples only fell below 10 % for values above ~8 % SOC. It was therefore concluded that for method comparison, analysis of the reference samples using the NIR method should be replicated at least three times.

Considering the fact that carbon accounting also requires error reporting, it was further concluded that the common practice of using paired samples with single determination (without replication) of dry combustion SOC for NIR model calibration and (cross) validation should be abandoned in favour of finding the mean values for the calibration/validation sets using at least three replicates. The common practice of single determinations, which is mostly justified by financial constraints, substantially decreases the model precision and reduces the range of quantitative SOC determination.

The level of input detail in terms of the vertical distribution functions used to predict SOC stocks in the catchment affected the accuracy and precision of the resultant SOC stock maps, as well as the associated propagated errors. Using a single *k* value for all land uses to predict the SOC stock resulted in the highest accuracy based on map R^2 values, but lower accuracy based on map bias compared to using functions differentiated by land use and soil grouping. On the other hand, SOC stock map precision (RMSE) was improved with an increase in detail by using differentiated SOC distribution functions. However, the relative error mostly exceeded 20 %, even when using differentiated SOC distribution functions, which may be unacceptably high for carbon accounting, trade and taxation purposes.

It was concluded that the observed increase in SOC stock map precision (decreasing relative RMSE) and partial increase in accuracy (decreasing bias) obtained by using differentiated SOC distribution functions show potential for the increase in overall accuracy of SOC predictions by increasing the R^2 and RMSE of resultant maps. The observed results suggest the need for a substantial increase in sampling density to maintain or increase the map accuracy while simultaneously increasing precision. Increased sampling density would be necessary in the sampling of profiles to include more soil types and improve the vertical SOC distribution models used as input for SOC stock prediction, as well as an increase in surface samples per land use or soul grouping for the determination of C_v^0.

8 References

Abraham, J., 2013. Organic carbon estimations in soils: Analytical protocols and their implications. Rubber Sci. 26, 45–54.

Adhikari, K., Hartemink, A.E., Minasny, B., Bou Kheir, R., Greve, M.B., Greve, M.H., 2014. Digital mapping of soil organic carbon contents and stocks in Denmark. PLoS One 9. doi:10.1371/journal.pone.0105519

Akumu, C.E., McLaughlin, J.W., 2013. Regional variation in peatland carbon stock assessments, northern Ontario, Canada. Geoderma 209–210, 161–167. doi:10.1016/j.geoderma.2013.06.021

Aldana Jague, E., Sommer, M., Saby, N.P.A., Cornelis, J.T., Van Wesemael, B., Van Oost, K., 2016. High resolution characterization of the soil organic carbon depth profile in a soil landscape affected by erosion. Soil Tillage Res. 156, 185–193. doi:10.1016/j.still.2015.05.014

Allegrini, F., Olivieri, A.C., 2014. IUPAC-Consistent Approach to the Limit of Detection in Partial Least-Squares Calibration. Anal. Chem. 86, 7858–7866. doi:10.1021/ac501786u

Allen, D.E., Pringle, M.J., Page, K.L., Dalal, R.C., 2010. A review of sampling designs for the measurement of soil organic carbon in Australian grazing lands 227–246.

Amare, T., Hergarten, C., Hurni, H., Wolfgramm, B., Yitaferu, B., Selassie, Y.G., 2013. Prediction of Soil Organic Carbon for Ethiopian Highlands Using Soil Spectroscopy. ISRN Soil Sci. 2013, 1–11. doi:10.1155/2013/720589

Askari, M.S., O'Rourke, S.M., Holden, N.M., 2018. A comparison of point and imaging visible-near infrared spectroscopy for determining soil organic carbon. J. Near Infrared Spectrosc. doi:10.1177/0967033518766668

Australia Department of Climate Change and Energy Efficiency, 2012. The Carbon Farming Initiative Handbook (Version 1.0), Department of Climate Change and Energy Efficiency. Canberra, A.C.T.

Awiti, A.O., Walsh, M.G., Shepherd, K.D., Kinyamario, J., 2008. Soil condition classification using infrared spectroscopy: A proposition for assessment of soil condition along a tropical forest-cropland chronosequence. Geoderma 143, 73–84.

doi:10.1016/j.geoderma.2007.08.021

Bai, J., Zhang, G., Zhao, Q., Lu, Q., Jia, J., Cui, B., Liu, X., 2016. Depth-distribution patterns and control of soil organic carbon in coastal salt marshes with different plant covers. Sci. Rep. 6. doi:10.1038/srep34835

Baldock, J., 2008. Soils in a Carbon Accounting System. 6th Aust. Control. Traffic Farming Conf. 2008 19–26.

Batjes, N.H., 2014. Total carbon and nitrogen in the soils of the world. Eur. J. Soil Sci. 65, 10–21. doi:10.1111/ejss.12114_2

Batjes, N.H., 1996. Total carbon and nitrogen in the soils of the world. Eur. J. Soil Sci. 47, 151–163. doi:10.1111/ejss.12114_2

Batjes, N.H., Wesemael, B. Van, 2015. Measuring and Monitoring Soil Carbon, in: Banwart, S.A., Noellemeyer, E., Milne, E. (Ed.), Soil Carbon: Science, Management and Policy for Multiple Benefits. CAB International, pp. 188–201.

Beaudette, D.E., Roudier, P., O'Geen, A.T., 2013. Algorithms for quantitative pedology: A toolkit for soil scientists. Comput. Geosci. 52, 258–268. doi:10.1016/j.cageo.2012.10.020

Bellon-Maurel, V., Fernandez-ahumada, E., Palagos, B., Roger, J.-M., McBratney, A., 2010. Critical review of chemometric indicators commonly used for assessing the quality of the prediction of soil attributes by NIR spectroscopy. TrAC Trends Anal. Chem. 29, 1073–1081. doi:10.1016/j.trac.2010.05.006

Bellon-Maurel, V., McBratney, A., 2011. Near-infrared (NIR) and mid-infrared (MIR) spectroscopic techniques for assessing the amount of carbon stock in soils – Critical review and research perspectives. Soil Biol. Biochem. 43, 1398–1410. doi:10.1016/j.soilbio.2011.02.019

Beltrame, K.K., Souza, A.M., Coelho, M.R., Winkler, T.C.B., Souza, W.E., Valderrama, P., 2016. Soil Organic Carbon Determination Using NIRS: Evaluation of Dichromate Oxidation and Dry Combustion Analysis as Reference Methods in Multivariate Calibration. Artic. J. Braz. Chem. Soc 27, 1527–1532. doi:10.5935/0103-5053.20160031

Bernoux, M., Arrouays, D., Cerri, C.C., Bourennane, H., 1998. Modeling Vertical Distribution of Carbon in Oxisols of the Western Brazilian Amazon (Rondonia). Soil Sci. 163,

941–951. doi:10.1097/00010694-199812000-00004

Bispo, A., Andersen, L., Angers, D.A., Bernoux, M., Brossard, M., Cécillon, L., Comans, R.N.J., Harmsen, J., Jonassen, K., Lamé, F., Lhuillery, C., Maly, S., Martin, E., Mcelnea, A.E., Sakai, H., Watabe, Y., Eglin, T.K., 2017. Accounting for Carbon Stocks in Soils and Measuring GHGs Emission Fluxes from Soils: Do We Have the Necessary Standards? Front. Environ. Sci. 5, 1–12. doi:10.3389/fenvs.2017.00041

Bisutti, I., Hilke, I., Raessler, M., 2004. Determination of total organic carbon – an overview of current methods. TrAC Trends Anal. Chem. 23, 716–726. doi:10.1016/j.trac.2004.09.003

Bouabidi, A., Rozet, E., Fillet, M., Ziemons, E., Chapuzet, E., Mertens, B., Klinkenberg, R., Ceccato, A., Talbi, M., Streel, B., Bouklouze, A., Boulanger, B., Hubert, P., 2010. Critical analysis of several analytical method validation strategies in the framework of the fit for purpose concept. J. Chromatogr. A 1217, 3180–3192. doi:10.1016/j.chroma.2009.08.051

Brahim, N., Ibrahim, H., Hatira, A., 2014. Tunisian Soil Organic Carbon Stock - Spatial and Vertical Variation. Procedia Eng. 69, 1549–1555. doi:10.1016/j.proeng.2014.03.154

Brenna, S., Acutis, M., Tabaglio, V., Grandi, M., 2014. Conservation Agriculture as a driver for Carbon Credit market, in: European Conference on “Green Carbon: Making Sustainable Agriculture Real.” Brussels, 1-3 April 2014, pp. 1–9.

Brodský, L., Vašát, R., Klement, A., Zádorová, T., Jakšík, O., 2013. Uncertainty propagation in VNIR reflectance spectroscopy soil organic carbon mapping. Geoderma 199, 54–63. doi:10.1016/j.geoderma.2012.11.006

Brown, J.D., Heuvelink, G.B.M., 2005. Assessing Uncertainty Propagation through Physically Based Models of Soil Water Flow and Solute Transport, in: Encyclopedia of Hydrological Sciences. John Wiley & Sons, Ltd, Chichester, UK, pp. 1–15. doi:10.1002/0470848944.hsa081

Bushong, J.T., Norman, R.J., Slaton, N.A., 2015. Near-Infrared Reflectance Spectroscopy as a Method for Determining Organic Carbon Concentrations in Soil. Commun. Soil Sci. Plant Anal. 46, 1791–1801. doi:10.1080/00103624.2015.1048250

Camp, K.G.T., 1999. A bioresource classification for KwaZulu-Natal, South Africa. University of Natal, Pietermaritzburg.

Chai, H., Yu, G., He, N., Wen, D., Li, J., Fang, J., 2015. Vertical distribution of soil carbon, nitrogen, and phosphorus in typical Chinese terrestrial ecosystems. Chinese Geogr. Sci. 25, 549–560. doi:10.1007/s11769-015-0756-z

Chandran, S., Singh, R.S.P., 2007. Comparison of various international guidelines for analytical method validation. Pharmazie 62, 4–14. doi:10.1691/ph2007.1.5064

Chatterjee, A., Lal, R., Wielopolski, L., Martin, M.Z., Ebinger, M.H., 2009. Evaluation of different soil carbon determination methods. CRC. Crit. Rev. Plant Sci. 28, 164–178. doi:10.1080/07352680902776556

Chen, L., Flynn, D.F.B., Jing, X., Kühn, P., Scholten, T., He, J.-S., 2015. A Comparison of Two Methods for Quantifying Soil Organic Carbon of Alpine Grasslands on the Tibetan Plateau. PLoS One 10, e0126372. doi:10.1371/journal.pone.0126372

Chenu, C., Angers, D.A., Barré, P., Derrien, D., Arrouays, D., Balesdent, J., 2018. Increasing organic stocks in agricultural soils: Knowledge gaps and potential innovations. Soil Tillage Res. 0–1. doi:10.1016/j.still.2018.04.011

Ciric, V., Manojlovi, M., Belic (1), M., Neši, L., Švarc-Gaji, J., Sitaula, B.K., 2014. Comparison, limitations and uncertainty of wet chemistry techniques, loss on ignition and dry combustion in soil organic carbon analysis. Geophys. Res. Abstr. 16, 16597.

Clairotte, M., Grinand, C., Kouakoua, E., Thébault, A., Saby, N.P.A., Bernoux, M., Barthès, B.G., 2016. National calibration of soil organic carbon concentration using diffuse infrared reflectance spectroscopy. Geoderma 276, 41–52. doi:10.1016/j.geoderma.2016.04.021

Conyers, M.K., Poile, G.J., Oates, A.A., Waters, D., Chan, K.Y., 2011. Comparison of three carbon determination methods on naturally occurring substrates and the implication for the quantification of “soil carbon.” Soil Res. 49, 27–33. doi:10.1071/SR10103

Corbeels, M., Cardinael, R., Naudin, K., Guibert, H., Torquebiau, E., 2018. The 4 per 1000 goal and soil carbon storage under agroforestry and conservation agriculture systems in sub-Saharan Africa. Soil Tillage Res. 0–1. doi:10.1016/j.still.2018.02.015

Corbeels, M., Marchão, R.L., Neto, M.S., Ferreira, E.G., Madari, B.E., Scopel, E., Brito, O.R., 2016. Evidence of limited carbon sequestration in soils under no-tillage systems in the Cerrado of Brazil. Sci. Rep. 6, 1–8. doi:10.1038/srep21450

Cremers, D. a, Ebinger, M.H., Breshears, D.D., Unkefer, P.J., Kammerdiener, S. a, Ferris, M.J., Catlett, K.M., Brown, J.R., 2001. Measuring total soil carbon with laser-induced breakdown spectroscopy (LIBS). J. Environ. Qual. 30, 2202–6. doi:10.2134/jeq2001.2202

Currie, L.A., 1999. Detection and quantification limits: origins and historical overview1Adapted from the Proceedings of the 1996 Joint Statistical Meetings (American Statistical Association, 1997). Original title: “Foundations and future of detection and quantification limi. Anal. Chim. Acta 391, 127–134. doi:10.1016/S0003-2670(99)00105-1

Davis, M.R., Alves, B.J.R., Karlen, D.L., Kline, K.L., Galdos, M., Abulebdeh, D., 2018. Review of soil organic carbon measurement protocols: A US and Brazil comparison and recommendation. Sustain. 10, 4–8. doi:10.3390/su10010053

De Brogniez, D., Ballabio, C., Stevens, A., Jones, R.J.A., Montanarella, L., van Wesemael, B., 2015. A map of the topsoil organic carbon content of Europe generated by a generalized additive model. Eur. J. Soil Sci. 66, 121–134. doi:10.1111/ejss.12193

De Gruijter, J.J., McBratney, A.B., Minasny, B., Wheeler, I., Malone, B.P., Stockmann, U., 2016. Farm-scale soil carbon auditing. Geoderma 265, 120–130. doi:10.1016/j.geoderma.2015.11.010

De Souza, A.M., Filgueiras, P.R., Coelho, M.R., Fontana, A., Winkler, T.C.B., Valderrama, P., Poppi, R.J., 2016. Validation of the near infrared spectroscopy method for determining soil organic carbon by employing a proficiency assay for fertility laboratories. J. Near Infrared Spectrosc. 24, 293–303. doi:10.1255/jnirs.1219

De Vos, B., Lettens, S., Muys, B., Deckers, J.A., 2007. Walkley-Black analysis of forest soil organic carbon: Recovery, limitations and uncertainty. Soil Use Manag. 23, 221–229. doi:10.1111/j.1475-2743.2007.00084.x

Deng, F., Knadel, M., Peng, Y., Heckrath, G., Greve, M.H., 2012. Soil profile organic carbon prediction with visible-near infrared reflectance spectroscopy based on a national database 1986, 409–413.

Deng, F., Minasny, B., Knadel, M., Mcbratney, A., Heckrath, G., Greve, M.H., 2013. Using Vis-NIR Spectroscopy for Monitoring Temporal Changes in Soil Organic Carbon. Soil Sci. 178, 389–399. doi:10.1097/SS.0000000000000002

Department of Water and Sanitation, 2018. General notice. Gov. Gaz. 632, 16 Fe, 202–274.

Dieckow, J., Mielniczuk, J., Knicker, H., Bayer, C., Dick, D.P., Kögel-Knabner, I., 2007. Comparison of Carbon and Nitrogen Determination Methods for Samples of a Paleudult Subjected To No-Till Cropping Systems Comparação De Métodos De Determinação De Carbono E Nitrogênio Em Amostras De Argissolo Sob Plantio Direto. Sci. Agric. (Piracicaba 64, 532–540. doi:Doi 10.1590/S0103-90162007000500011

Dietzel, R., Liebman, M., Archontoulis, S., 2017. A deeper look at the relationship between root carbon pools and the vertical distribution of the soil carbon pool. SOIL Discuss. 1–20. doi:10.5194/soil-2017-5

Dolan, M.S., Clapp, C.E., Allmaras, R.R., Baker, J.M., Molina, J.A.E., 2006. Soil organic carbon and nitrogen in a Minnesota soil as related to tillage, residue and nitrogen management. Soil Tillage Res. 89, 221–231. doi:10.1016/j.still.2005.07.015

Dorji, T., Odeh, I., Field, D., 2014a. Vertical Distribution of Soil Organic Carbon Density in Relation to Land Use/Cover, Altitude and Slope Aspect in the Eastern Himalayas. Land 3, 1232–1250. doi:10.3390/land3041232

Dorji, T., Odeh, I.O. a., Field, D.J., Baillie, I.C., 2014b. Digital soil mapping of soil organic carbon stocks under different land use and land cover types in montane ecosystems, Eastern Himalayas. For. Ecol. Manage. 318. doi:10.1016/j.foreco.2014.01.003

Eksperiandova, L.P., Belikov, K.N., Khimchenko, S. V., Blank, T. a., 2010. Once again about determination and detection limits. J. Anal. Chem. 65, 223–228. doi:10.1134/S1061934810030020

Eksperiandova, L.P., Fedorov, O.I., Stepanenko, N.A., 2011. Estimation of metrological characteristics of the element analyzer EuroVector EA-3000 and its potential in the single-reactor CHNS mode. Microchem. J. 99, 235–238. doi:10.1016/j.microc.2011.05.005

Elamir, E.A.H., Seheult, A.H., 2004. Exact variance structure of sample L-moments. J. Stat. Plan. Inference 124, 337–359. doi:10.1016/S0378-3758(03)00213-1

England, J.R., Viscarra Rossel, R.A., Armando, R., Rossel, V., 2018. Proximal sensing for soil carbon accounting 101–122. doi:10.5194/soil-4-101-2018

Esmeraldo, M.Q., 2016. Effects of tillage practices on some key soil parameters: A case study in the Kwazulu-Natal Midlands, South Africa. Stellenbosch University.

Eurachem, 2014. Eurachem Guide: The Fitness for Purpose of Analytical Methods – A Laboratory Guide to Method Validation and Related Topics., Eurachem. doi:978-91-87461-59-0

Eurovector, 2010. EuroEA3000. Compact, fully automatic Elemental Analyser for the most exacting CHNS-O determinations. Eurovector Istruments Softw.

Fernandes, R.B.A., Carvalho Junior, I.A. de, Ribeiro Junior, E.S., Mendonça, E. de S., 2015. Comparison of different methods for the determination of total organic carbon and humic substances in Brazilian soils. Rev. Ceres 62, 496–501. doi:10.1590/0034-737X201562050011

Ficarelli, P., Chuma, E., Ramaru, J., Murwira, K., Hagmann, J., 2003. Strengthening local organizations for conservation agriculture - some experiences from South Africa and Zimbabwe. Proc. 2nd World Congr. Conserv. Agric. 11–15.

Gershenson, A., Barsimantov, J., EcoShift Consulting, 2011. Accounting for Carbon in Soils. Climate Action Reserve White Paper. doi:10.13140/RG.2.1.3188.9044

Gobrecht, A., Roger, J., Bellon-Maurel, V., 2014. Major Issues of Diffuse Reflectance NIR Spectroscopy in the Specific Context of Soil Carbon Content Estimation, in: Sparks, D.L. (Ed.), Advances in Agronomy. Elsevier Inc., pp. 145–175. doi:10.1016/B978-0-12-420225-2.00004-2

Goglio, P., Smith, W.N., Grant, B.B., Desjardins, R.L., McConkey, B.G., Campbell, C.A., Nemecek, T., 2015. Accounting for soil carbon changes in agricultural life cycle assessment (LCA): A review. J. Clean. Prod. 104, 23–39. doi:10.1016/j.jclepro.2015.05.040

Goidts, E., van Wesemael, B., Crucifix, M., 2009. Magnitude and sources of uncertainties in soil organic carbon (SOC) stock assessments at various scales. Eur. J. Soil Sci. 60, 723–739. doi:10.1111/j.1365-2389.2009.01157.x

Gomez, C., Viscarra Rossel, R.A., McBratney, A.B., 2008. Soil organic carbon prediction by hyperspectral remote sensing and field vis-NIR spectroscopy: An Australian case study. Geoderma 146, 403–411. doi:10.1016/j.geoderma.2008.06.011

Goodman, L.A., 1960. On the Exact Variance of Products. J. Am. Stat. Assoc. 55, 708. doi:10.2307/2281592

Guerrero, C., Stenberg, B., Wetterlind, J., Viscarra Rossel, R. a., Maestre, F.T., Mouazen, a. M., Zornoza, R., Ruiz-Sinoga, J.D., Kuang, B., 2014. Assessment of soil organic carbon at local scale with spiked NIR calibrations: effects of selection and extra-weighting on the spiking subset. Eur. J. Soil Sci. 65, 248–263. doi:10.1111/ejss.12129

Guevara, M., Federico Olmedo, G., Stell, E., Yigini, Y., Aguilar Duarte, Y., Arellano Hernández, C., Arévalo, G.E., Eduardo Arroyo-Cruz, C., Bolivar, A., Bunning, S., Bustamante Cañas, N., Omar Cruz-Gaistardo, C., Davila, F., Dell Acqua, M., Encina, A., Tacona, H.F., Fontes, F., Herrera, J.A.H., Roberto Ibelles Navarro, A., Loayza, V., Manueles, A.M., Mendoza Jara, F., Olivera, C., Osorio Hermosilla, R., Pereira, G., Prieto, P., Ramos, I.A., Carlos Rey Brina, J., Rivera, R., Rodríguez-Rodríguez, J., Roopnarine, R., Ibarra, A.R., Amaury Rosales Riveiro, K., Andrés Schulz, G., Spence, A., Vasques, G.M., Vargas, R.R., Vargas, R., 2018. No silver bullet for digital soil mapping: Country-specific soil organic carbon estimates across Latin America. Soil 4, 173–193. doi:10.5194/soil-4-173-2018

Gustavo González, A., Ángeles Herrador, M., 2007. A practical guide to analytical method validation, including measurement uncertainty and accuracy profiles. TrAC - Trends Anal. Chem. 26, 227–238. doi:10.1016/j.trac.2007.01.009

Haddaway, N.R., Hedlund, K., Jackson, L.E., Kätterer, T., Lugato, E., Thomsen, I.K., Jørgensen, H.B., Isberg, P.-E., 2017. How does tillage intensity affect soil organic carbon? A systematic review. Environ. Evid. 6, 30. doi:10.1186/s13750-017-0108-9

Harper, R.J., Tibbett, M., 2013. The hidden organic carbon in deep mineral soils. Plant Soil 368, 641–648. doi:10.1007/s11104-013-1600-9

Harris, D.C., 2007. Quantitative chemical analysis of ocular melanosomes in stained and non-stained tissues, 7th ed. W. H. Freeman and Company, New York, NY.

Harvey, D., 2000. Modern analytical chemistry. McGraw-Hill.

He, Y., Liu, X., Lv, Y., Liu, F., Peng, J., Shen, T., Zhao, Y., Tang, Y., Luo, S., 2018. Quantitative Analysis of Nutrient Elements in Soil Using Single and Double-Pulse Laser-Induced Breakdown Spectroscopy. Sensors 18, 1526. doi:10.3390/s18051526

Heath, L.S., Smith, J.E., 2000. Soil Carbon Accounting and Assumptions for Forestry and Forest-Related Land Use Change. USDA For. Serv. Gen. Tech. Rep. RMRS-GTR-5, 89–101.

Heim, a., Wehrli, L., Eugster, W., Schmidt, M.W.I., 2009. Effects of sampling design on the probability to detect soil carbon stock changes at the Swiss CarboEurope site Lägeren. Geoderma 149, 347–354. doi:10.1016/j.geoderma.2008.12.018

Henry, M., Valentini, R., Bernoux, M., 2009. Soil carbon stocks in ecoregions of Africa. Biogeosciences Discuss. 6, 797–823. doi:10.5194/bgd-6-797-2009

Heuvelink, G.B.M., 2018. Pedometrics, Progress in Soil Science. Springer International Publishing, Cham. doi:10.1007/978-3-319-63439-5

Hilinski, T., 2001. Implementation of exponential depth distribution of organic carbon in the CENTURY model. Dep. Soil Crop Sci. 1997–2001.

Hobley, E.U.E.U., Wilson, B., 2016. The depth distribution of organic carbon in the soils of eastern Australia. Ecosphere 7, 0–21. doi:10.1002/ecs2.1214

Hubbert, K.R., Graham, R.C., Anderson, M.A., 2001. Soil and Weathered Bedrock. Soil Sci. Soc. Am. J. 65, 1255. doi:10.2136/sssaj2001.6541255x

Hütsch, B.W., Augustin, J., Merbach, W., 2002. Plant rhizodeposition - An important source for carbon turnover in soils. J. Plant Nutr. Soil Sci. 165, 397–407. doi:10.1002/1522-2624(200208)165:4<397::AID-JPLN397>3.0.CO;2-C

International Conference on Harmonization, 2005. ICH Harmonised Triplicate Guideline. Validation of Analytical Procedures: Text and Methodology Q2(R1). Int. Conf. Harmon. 17. doi:http://www.ich.org/fileadmin/Public_Web_Site/ICH_Products/Guidelines/Quality/Q2_R1/Step4/Q2_R1__Guideline.pdf

Ismail, R., Lee, H.Y., Mahyudin, N.A., Abu Bakar, F., 2014. Linearity study on detection and quantification limits for the determination of avermectins using linear regression. J. Food Drug Anal. 22, 407–412. doi:10.1016/j.jfda.2014.01.026

IUPAC, 2014. Compendium of Chemical Terminology - Gold Book.

IUPAC, 1997. Compendium of Chemical Terminology, 2nd ed. (the “Gold Book”)., Compendium of Chemical Terminology (the “Gold Book”). doi:10.1351/goldbook.I03352

Jackson, R.B., Lajtha, K., Crow, S.E., Hugelius, G., Kramer, M.G., Piñeiro, G., 2017. The Ecology of Soil Carbon: Pools, Vulnerabilities, and Biotic and Abiotic Controls. Annu. Rev. Ecol.

Evol. Syst. 48, annurev-ecolsys-112414-054234. doi:10.1146/annurev-ecolsys-112414-054234

Jobbagy, E.G., Jackson, R.B., Jobbágy, E.G., Jackson, R.B., 2000. The Vertical Distribution of Soil Organic Carbon and Its Relation to Climate and Vegetation. Ecol. Appl. 10, 423–436. doi:10.1890/1051-0761(2000)010%5B0423:TVDOSO%5D2.0.CO;2

Kalembasa, S.J., Jenkinson, D.S., 1973. A comparative study of titrimetric and gravimetric methods for the determination of organic carbon in soil. J. Sci. Food Agric. 24, 1085–1090. doi:10.1002/jsfa.2740240910

Kamara, A., Rhodes, E.R., Sawyerr, P. a., 2007. Dry Combustion Carbon, Walkley–Black Carbon, and Loss on Ignition for Aggregate Size Fractions on a Toposequence. Commun. Soil Sci. Plant Anal. 38, 2005–2012. doi:10.1080/00103620701548639

Kempen, B., Brus, D.J., Stoorvogel, J.J., 2011. Three-dimensional mapping of soil organic matter content using soil type–specific depth functions. Geoderma 162, 107–123. doi:10.1016/j.geoderma.2011.01.010

Kempen, B., Dalsgaard, S., Kaaya, A.K., Chamuya, N., Ruipérez-González, M., Pekkarinen, A., Walsh, M.G., 2019. Mapping topsoil organic carbon concentrations and stocks for Tanzania. Geoderma 337, 164–180. doi:10.1016/j.geoderma.2018.09.011

Kempen, B., Heuvelink, G.B.M., Brus, D.J., Stoorvogel, J.J., 2010. Pedometric mapping of soil organic matter using a soil map with quantified uncertainty. Eur. J. Soil Sci. 61, 333–347. doi:10.1111/j.1365-2389.2010.01232.x

Khalil, M.I., Kiely, G., O'Brien, P., Müller, C., 2013. Organic carbon stocks in agricultural soils in Ireland using combined empirical and GIS approaches. Geoderma 193–194, 222–235. doi:10.1016/j.geoderma.2012.10.005

Kulmatiski, A., Vogt, D.J., Siccama, T.G., Beard, K.H., 2003. Detecting nutrient pool changes in rocky forest soils. Soil Sci. Soc. Am. J 67, 1282–1286. doi:10.2136/sssaj2003.1282

Laclau, J.-P., da Silva, E.A., Rodrigues Lambais, G., Bernoux, M., le Maire, G., Stape, J.L., Bouillet, J.-P., Gonçalves, J.L. de M., Jourdan, C., Nouvellon, Y., 2013. Dynamics of soil exploration by fine roots down to a depth of 10 m throughout the entire rotation in Eucalyptus grandis plantations. Front. Plant Sci. 4, 243. doi:10.3389/fpls.2013.00243

Lacoste, M., Minasny, B., McBratney, A., Michot, D., Viaud, V., Walter, C., 2014. High resolution 3D mapping of soil organic carbon in a heterogeneous agricultural landscape. Geoderma 213. doi:10.1016/j.geoderma.2013.07.002

Lal, R., Stewart, B.A., 2011. World Soil Resources and Food Security (Advances in Soil Science), 1st ed, Soil Science Society of America Journal. CRC Press.

Le Quéré, C., Andrew, R.M., Canadell, J.G., Sitch, S., Ivar Korsbakken, J., Peters, G.P., Manning, A.C., Boden, T.A., Tans, P.P., Houghton, R.A., Keeling, R.F., Alin, S., Andrews, O.D., Anthoni, P., Barbero, L., Bopp, L., Chevallier, F., Chini, L.P., Ciais, P., Currie, K., Delire, C., Doney, S.C., Friedlingstein, P., Gkritzalis, T., Harris, I., Hauck, J., Haverd, V., Hoppema, M., Klein Goldewijk, K., Jain, A.K., Kato, E., Körtzinger, A., Landschützer, P., Lefèvre, N., Lenton, A., Lienert, S., Lombardozzi, D., Melton, J.R., Metzl, N., Millero, F., Monteiro, P.M.S., Munro, D.R., Nabel, J.E.M.S., Nakaoka, S.I., O'Brien, K., Olsen, A., Omar, A.M., Ono, T., Pierrot, D., Poulter, B., Rödenbeck, C., Salisbury, J., Schuster, U., Schwinger, J., Séférian, R., Skjelvan, I., Stocker, B.D., Sutton, A.J., Takahashi, T., Tian, H., Tilbrook, B., Van Der Laan-Luijkx, I.T., Van Der Werf, G.R., Viovy, N., Walker, A.P., Wiltshire, A.J., Zaehle, S., 2016. Global Carbon Budget 2016. Earth Syst. Sci. Data 8, 605–649. doi:10.5194/essd-8-605-2016

Lettens, S., De Vos, B., Quataert, P., van Wesemael, B., Muys, B., van Orshoven, J., 2007. Variable carbon recovery of Walkley-Black analysis and implications for national soil organic carbon accounting. Eur. J. Soil Sci. 58, 1244–1253. doi:10.1111/j.1365-2389.2007.00916.x

Liu, F., Rossiter, D.G., Song, X., Zhang, G., Yang, R., Zhao, Y., Li, D., Ju, B., 2016. A similarity-based method for three-dimensional prediction of soil organic matter concentration. Geoderma 263, 254–263. doi:10.1016/j.geoderma.2015.05.013

Mäkipää, R., Häkkinen, M., Muukkonen, P., Peltoniemi, M., 2008. The costs of monitoring changes in forest soil carbon stocks. Boreal Environ. Res. 13, 120–130.

Malone, B.P., Styc, Q., Minasny, B., McBratney, A.B., 2017. Digital soil mapping of soil carbon at the farm scale: A spatial downscaling approach in consideration of measured and uncertain data. Geoderma 290, 91–99. doi:10.1016/j.geoderma.2016.12.008

Maroto, A., Boqué, R., Riu, J., Rius, F.X., 2002. Should non-significant bias be included in the uncertainty budget? Accredit. Qual. Assur. 7, 90–94. doi:10.1007/s00769-001-0434-y

Mccarty, G.W., Iii, J.B.R., Russell, Y., Doraiswamy, P.C., Doumbia, M., 2010. Evaluation of

methods for measuring soil organic carbon in West African soils. African J. Agric. Res. 5, 2169–2177. doi:10.5897/AJAR10.616

Meersmans, J., Van Wesemael, B., De Ridder, F., Dotti, M.F., De Baets, S., Van Molle, M., 2009. Changes in organic carbon distribution with depth in agricultural soils in northern Belgium, 1960-2006. Glob. Chang. Biol. 15, 2739–2750. doi:10.1111/j.1365-2486.2009.01855.x

Mikhailova, E.A., Noble, R.R.P., Post, C.J., 2003. Comparison of soil organic carbon recovery by Walkley-Black and dry combustion methods in the Russian Chernozem. Commun. Soil Sci. Plant Anal. 34, 1853–1860. doi:10.1081/CSS-120023220

Minasny, B., Malone, B.P., McBratney, A.B., Angers, D.A., Arrouays, D., Chambers, A., Chaplot, V., Chen, Z.S., Cheng, K., Das, B.S., Field, D.J., Gimona, A., Hedley, C.B., Hong, S.Y., Mandal, B., Marchant, B.P., Martin, M., McConkey, B.G., Mulder, V.L., O'Rourke, S., Richer-de-Forges, A.C., Odeh, I., Padarian, J.J., Paustian, K., Pan, G., Poggio, L., Savin, I., Stolbovoy, V., Stockmann, U., Sulaeman, Y., Tsui, C.C., Vågen, T.G., van Wesemael, B., Winowiecki, L., Vï¿½gen, T.G., van Wesemael, B., Winowiecki, L., 2017. Soil carbon 4 per mille. Geoderma 292, 59–86. doi:10.1016/j.geoderma.2017.01.002

Minasny, B., McBratney, A.B., 2016. Digital soil mapping: A brief history and some lessons. Geoderma 264, 301–311. doi:10.1016/j.geoderma.2015.07.017

Minasny, B., McBratney, A.B., Malone, B.P., Wheeler, I., A, B.M.B.M., A, A.B.M.B., A, B.M.B.M., B, Y.S., 2013. Digital Mapping of Soil Carbon, in: Adv. Agron. pp. 1–47. doi:10.1016/B978-0-12-405942-9.00001-3

Minasny, B., McBratney, A.B., Mendonça-Santos, M.L., Odeh, I.O.A.A., Guyon, B., 2006. Prediction and digital mapping of soil carbon storage in the Lower Namoi Valley. Soil Res. 44, 233. doi:10.1071/SR05136

Mishra, U., Lal, R., Slater, B., Calhoun, F., Liu, D., Van Meirvenne, M., 2009. Predicting Soil Organic Carbon Stock Using Profile Depth Distribution Functions and Ordinary Kriging. Soil Sci. Soc. Am. J. 73, 614. doi:10.2136/sssaj2007.0410

Mouazen, A.M., Kuang, B., De Baerdemaeker, J., Ramon, H., 2010. Comparison among principal component, partial least squares and back propagation neural network analyses for accuracy of measurement of selected soil properties with visible and near infrared

spectroscopy. Geoderma 158, 23–31. doi:10.1016/j.geoderma.2010.03.001

Nalimov, V. V., Basu, P., Williams, M., 1963. The application of mathematical statistics to chemical analysis. Pergamon Press.

Nave, L.E., Domke, G.M., Hofmeister, K.L., Mishra, U., Perry, C.H., Walters, B.F., Swanston, C.W., 2018. Reforestation can sequester two petagrams of carbon in US topsoils in a century. Proc. Natl. Acad. Sci. 115, 201719685. doi:10.1073/pnas.1719685115

Nelson, D.W., Sommers, L.E., 1996. Total Carbon, Organic Carbon, and Organic Matter, in: Sparks, D.L., Page, A.L., Helmke, P.A., Loeppert, R.H., Nelson, D.W., Sommers, L.E. (Eds.), Methods of Soil Analysis. Part 3-Chemical Methods. SSSA Book Series No. 5. SSSA and ASA, Madison, WI, pp. 961–1010. doi:10.2136/sssabookser5.3.c34

Nelson, D.W., Sommers, L.E., 1974. A rapid and accurate procedure for estimation of organic carbon in soils. Soil Atmos. Sci. 84, 456–462.

Nippert, J.B., Holdo, R.M., 2015. Challenging the maximum rooting depth paradigm in grasslands and savannas. Funct. Ecol. 29, 739–745. doi:10.1111/1365-2435.12390

Olivieri, A.C., 2015. Practical guidelines for reporting results in single- and multi-component analytical calibration: A tutorial. Anal. Chim. Acta 868, 10–22. doi:10.1016/j.aca.2015.01.017

Olson, K.R., Al-Kaisi, M.M., 2015. The importance of soil sampling depth for accurate account of soil organic carbon sequestration, storage, retention and loss. Catena 125, 33–37. doi:10.1016/j.catena.2014.10.004

Olson, K.R., Ebelhar, S.A., Lang, J.M., 2013. Effects of 24 years of conservation tillage systems on soil organic carbon and soil productivity. Appl. Environ. Soil Sci. 2013. doi:10.1155/2013/617504

Omonode, R.A., Vyn, T.J., 2006. Vertical distribution of soil organic carbon and nitrogen under warm-season native grasses relative to croplands in west-central Indiana, USA. Agric. Ecosyst. Environ. 117, 159–170. doi:10.1016/j.agee.2006.03.031

Orr, B.J., Cowie, A.L., Castillo, V.M., Sanchez, P., Chasek, N.D., Crossman, Erlewein, A., Louwagie, G., Maron, M., Metternicht, G.I., Minelli, S., Tengberg, A.E., Walter, S., Welton, S., 2017. Scientific Conceptual Framework for Land Degradation Neutrality. A Report of the

Science-Policy Interface, United Nations Convention to Combat Desertification - UNCCD.

Ottoy, S., Elsen, A., Van De Vreken, P., Gobin, A., Merckx, R., Hermy, M., Van Orshoven, J., 2016. An exponential change decline function to estimate soil organic carbon stocks and their changes from topsoil measurements. Eur. J. Soil Sci. 67, 816–826. doi:10.1111/ejss.12394

Paustian, K., Andrén, O., Janzen, H.H., Lal, R., Smith, P., Tian, G., Tiessen, H., Van Noordwijk, M., Woomer, P.L., 1997. Agricultural soils as a sink to mitigate CO2 emissions. Soil Use Manag. 13, 230–244. doi:10.1111/j.1475-2743.1997.tb00594.x

Paustian, K., Lehmann, J., Ogle, S., Reay, D., Robertson, G.P., Smith, P., 2016. Climate-smart soils. Nature 532, 49–57. doi:10.1038/nature17174

Payling, R., 2012. Detection Limit [WWW Document]. Wikipedia. URL http://en.wikipedia.org/wiki/Detection_limit (accessed 9.21.18).

Peng, X., Shi, T., Song, A., Chen, Y., Gao, W., 2014. Estimating soil organic carbon using VIS/NIR spectroscopy with SVMR and SPA methods. Remote Sens. 6, 2699–2717. doi:10.3390/rs6042699

Peng, Y., Knadel, M., Gislum, R., Schelde, K., Thomsen, A., Greve, M.H., 2014. Quantification of SOC and clay content using visible near-infrared reflectance-mid-infrared reflectance spectroscopy with jack-knifing partial least squares regression. Soil Sci. 179, 325–332. doi:10.1097/SS.0000000000000074

Périé, C., Ouimet, R., 2008. Organic carbon, organic matter and bulk density relationships in boreal forest soils. Can. J. Soil Sci. 88, 315–325. doi:10.4141/CJSS06008

Poeplau, C., Don, A., 2013. Sensitivity of soil organic carbon stocks and fractions to different land-use changes across Europe. Geoderma 192, 189–201. doi:10.1016/j.geoderma.2012.08.003

Porter, C.H., Jones, J.W., Adiku, S., Gijsman, a. J., Gargiulo, O., Naab, J.B., 2009. Modeling organic carbon and carbon-mediated soil processes in DSSAT v4.5. Oper. Res. 10, 247–278. doi:10.1007/s12351-009-0059-1

Pukelsheim, F., 1994. The Three Sigma Rule. Am. Stat. 48, 88–91. doi:10.1080/00031305.1994.10476030

Reeves, J.B., 2010. Near- versus mid-infrared diffuse reflectance spectroscopy for soil analysis emphasizing carbon and laboratory versus on-site analysis: Where are we and what needs to be done? Geoderma 158, 3–14. doi:10.1016/j.geoderma.2009.04.005

Ribani, M., Collins, C.H., Bottoli, C.B.G., 2007. Validation of chromatographic methods: Evaluation of detection and quantification limits in the determination of impurities in omeprazole. J. Chromatogr. A 1156, 201–205. doi:10.1016/j.chroma.2006.12.080

Roberts, C.A., Workman Jr., J., Reeves III, J.B., Malley, D.F., Martin, P.D., Ben-Dor, E., 2004. Application in Analysis of Soils, in: Near-Infrared Spectroscopy in Agriculture, in: Agronomy Series, Vol 44. American Society of Agronomy, Crop Science Society of America, Soil Science Society of America, pp. 729–784. doi:10.2134/agronmonogr44.c26

Ros Mesa, I., 2015. Stochastic modelling of soil carbon stocks under different land uses: a case study in South Africa. Stellenbosch University.

Roudier, P., Hedley, C., Ross, C., 2012. Farm-scale mapping of soil organic carbon using visible-near infra-red spectroscopy, Landcare Research. Palmerston, NZ.

Sanderman, J., Baldock, J.A., 2010. Accounting for soil carbon sequestration in national inventories: a soil scientist's perspective. Environ. Res. Lett. 5, 034003. doi:10.1088/1748-9326/5/3/034003

Sangmanee, P., Dell, B., Harper, R.J., Henry, D.J., 2017. Quantification of deep soil carbon by a wet digestion technique. Soil Res. 55, 78–85. doi:10.1071/SR15297

Santi, C., Certini, G., D'Acqui, L.P., 2006. Direct determination of organic carbon by dry combustion in soils with carbonates. Commun. Soil Sci. Plant Anal. 37, 155–162. doi:10.1080/00103620500403531

Sato, J.H., Figueiredo, C.C. de, Marchão, R.L., Madari, B.E., Benedito, L.E.C., Busato, J.G., Souza, D.M. de, 2014. Methods of soil organic carbon determination in Brazilian savannah soils. Sci. Agric. 71, 302–308. doi:10.1590/0103-9016-2013-0306

Schaltegger, S., Csutora, M., 2012. Carbon accounting for sustainability and management. Status quo and challenges. J. Clean. Prod. 36, 1–16. doi:10.1016/j.jclepro.2012.06.024

Schenk, H.J., 2008. Soil depth, plant rooting strategies and species' niches. New Phytol. 178, 223–225. doi:10.1111/j.1469-8137.2008.02427.x

Schenk, H.J., Jackson, R.B., 2005. Mapping the global distribution of deep roots in relation to climate and soil characteristics. Geoderma 126, 129–140. doi:10.1016/j.geoderma.2004.11.018

Schwinning, S., 2010. The ecohydrology of roots in rocks. Ecohydrology 3, 238–245. doi:10.1002/eco.134

Shrivastava, A., Gupta, V., 2011. Methods for the determination of limit of detection and limit of quantitation of the analytical methods. Chronicles Young Sci. 2, 21. doi:10.4103/2229-5186.79345

Sindayihebura, A., Ottoy, S., Dondeyne, S., Van Meirvenne, M., Van Orshoven, J., 2017. Comparing digital soil mapping techniques for organic carbon and clay content: Case study in Burundi's central plateaus. Catena 156, 161–175. doi:10.1016/j.catena.2017.04.003

Skjemstad, J.O., Spouncer, L.R. & Beech, A., 2000. National Carbon Accounting System Technical Report no . 12 Pre-clearing Soil Carbon Levels in Australia. Office.

Sleutel, S., de Neve, S., Hofman, G., 2003. Estimates of carbon stock changes in Belgian cropland. Soil Use Manag. 19, 166–171. doi:10.1079/SUM2003187

Sleutel, S., De Neve, S., Singier, B., Hofman, G., 2007. Quantification of organic carbon in soils: A comparison of methodologies and assessment of the carbon content of organic matter. Commun. Soil Sci. Plant Anal. 38, 2647–2657. doi:10.1080/00103620701662877

Smith, P., 2008. Soil Organic Carbon Dynamics and Land-Use Change, in: Land Use and Soil Resources. Springer Netherlands, Dordrecht, pp. 9–22. doi:10.1007/978-1-4020-6778-5_2

Soil Classification Working Group, 1991. Soil Classification: A Taxonomic System for South Africa. Memoirs of the Agricultural Natural Resources of South Africa No. 15. Department of Agricultural Development, Pretoria.

Soil Survey Staff, 2014. Keys to Soil Taxonomy, United States Department of Agriculture, Natural Resources Conservation Service.

Somarathna, P.D.S.N., Malone, B.P., Minasny, B., 2016. Mapping soil organic carbon content over New South Wales, Australia using local regression kriging. Geoderma Reg. 7, 38–48. doi:10.1016/j.geodrs.2015.12.002

Soussana, J.F., Lutfalla, S., Ehrhardt, F., Rosenstock, T., Lamanna, C., Havlík, P., Richards, M., Wollenberg, E., Chotte, J.L., Torquebiau, E., Ciais, P., Smith, P., Lal, R., 2017. Matching policy and science: Rationale for the "4 per 1000 - soils for food security and climate" initiative. Soil Tillage Res. 0–1. doi:10.1016/j.still.2017.12.002

Stechemesser, K., Guenther, E., 2012. Carbon accounting: a systematic literature review. J. Clean. Prod. 36, 17–38. doi:10.1016/j.jclepro.2012.02.021

Stockfisch, N., Forstreuter, T., Ehlers, W., 1999. Ploughing effects on soil organic matter after twenty years of conservation tillage in Lower Saxony, Germany. Soil Tillage Res. 52, 91–101. doi:10.1016/S0167-1987(99)00063-X

Stolbovoy, V., Montanarella, L., Jones, A., Gallego, J., 2007. Soil sampling protocol to certify the changes of organic carbon stock in mineral soil of the European Union. Version 2. EUR 21576 EN/2. Office for Official Publications of the European Communities, Luxembourg. ISBN: 978-92-79-05379-5.

Stumpf, F., Schmidt, K., Goebes, P., Behrens, T., Schönbrodt-Stitt, S., Wadoux, A., Xiang, W., Scholten, T., 2017. Uncertainty-guided sampling to improve digital soil maps. Catena 153, 30–38. doi:10.1016/j.catena.2017.01.033

Suddick, E.C., Ngugi, M.K., Paustian, K., Six, J., 2013. Monitoring soil carbon will prepare growers for a carbon trading system. Calif. Agric. 67, 162–171. doi:10.3733/ca.v067n03p162

Swanepoel, C.M., van der Laan, M., Weepener, H.L., du Preez, C.C., Annandale, J.G., 2016. Review and meta-analysis of organic matter in cultivated soils in southern Africa. Nutr. Cycl. Agroecosystems 104, 107–123. doi:10.1007/s10705-016-9763-4

Tan, Z., Lal, R., Owens, L., Izaurralde, R., 2007. Distribution of light and heavy fractions of soil organic carbon as related to land use and tillage practice. Soil Tillage Res. 92, 53–59. doi:10.1016/j.still.2006.01.003

Thompson, J.A., Prescott, T., Moore, A.C., Bell, J.S., Kautz, D., Hempel, F., Waltman, S.W., Perry, C.H., 2010. Regional Approach to Soil Property Mapping using Legacy Data and Spatial Disaggregation Techniques. 19th World Congr. Soil Sci. Soil Solut. a Chang. World. 4 pages.

Thompson, M., Ellison, S.L.R., Wood, R., 2002. Harmonized guidelines for single-laboratory validation of methods of analysis (IUPAC Technical Report). Pure Appl. Chem. 74, 835–855.

doi:10.1351/pac200274050835

Thomsen, V., Schatzlein, D., Mercuro, D., 2003. Limits of Detection in Spectroscopy. Pure Appl. Chem. 18, 112–114. doi:Article

Tsui, C., Guo, H., Che, Z.-S., 2013. Estimation of Soil Carbon Stock in Taiwan Arable Soils by Using Legacy Database and Digital Soil Mapping, in: Soil Processes and Current Trends in Quality Assessment. InTech. doi:10.5772/53211

Turner, D.P., 2000. Soils of Kwazulu-Natal and Mpumalanga: Recognition of Natural Soil Bodies. University of Pretoria.

Vågen, T.-G., Winowiecki, L.A., 2013. Mapping of soil organic carbon stocks for spatially explicit assessments of climate change mitigation potential. Environ. Res. Lett. 8, 015011. doi:10.1088/1748-9326/8/1/015011

Valderrama, P., Braga, J., Poppi, R.J., 2007. Variable Selection, Outlier Detection, and Figures of Merit Estimation in a Partial Least-Squares Regression Multivariate Calibration Model. A Case Study for the Determination of Quality Parameters in the Alcohol Industry by Near-Infrared Spectroscopy. J. Agric. Food Chem 55, 8331–8338.

VandenBygaart, A.J., Kay, B.D., 2004. Persistence of Soil Organic Carbon after Plowing a Long-Term No-Till Field in Southern Ontario, Canada. Soil Sci. Soc. Am. J. 68, 1394. doi:10.2136/sssaj2004.1394

Veronesi, F., Corstanje, R., Mayr, T., 2014. Landscape scale estimation of soil carbon stock using 3D modelling. Sci. Total Environ. 487, 578–586. doi:10.1016/j.scitotenv.2014.02.061

Vial, J., Jardy, A., 1999. Experimental Comparison of the Different Approaches To Estimate LOD and LOQ of an HPLC Method. Anal. Chem. 71, 2672–2677. doi:10.1021/ac981179n

Viscarra Rossel, R.A., Brus, D.J., 2018. The cost-efficiency and reliability of two methods for soil organic C accounting. L. Degrad. Dev. 29, 506–520. doi:10.1002/ldr.2887

Viscarra Rossel, R.A., Brus, D.J., Lobsey, C., Shi, Z., McLachlan, G., 2016. Baseline estimates of soil organic carbon by proximal sensing: Comparing design-based, model-assisted and model-based inference. Geoderma 265, 152–163. doi:10.1016/j.geoderma.2015.11.016

Viscarra Rossel, R.A., Lobsey, C.R., Sharman, C., Flick, P., McLachlan, G., 2017. Novel

Proximal Sensing for Monitoring Soil Organic C Stocks and Condition. Environ. Sci. Technol. 51, 5630–5641. doi:10.1021/acs.est.7b00889

Viscarra Rossel, R.A., Webster, R., Bui, E.N., Baldock, J.A., 2014. Baseline map of organic carbon in Australian soil to support national carbon accounting and monitoring under climate change. Glob. Chang. Biol. 20, 2953–2970. doi:10.1111/gcb.12569

Vitharana, U.W.A., Mishra, U., Mapa, R.B., 2019. National soil organic carbon estimates can improve global estimates. Geoderma 337, 55–64. doi:10.1016/j.geoderma.2018.09.005

Walkley, A., Black, I.A., 1934. An examination of the Degtjareff method for determining soil organic matter, and a proposed modification of the chromic acid titration method. Soil Sci. 37, 29–38. doi:10.1097/00010694-193401000-00003

Waltman, S.W., Olson, C., West, L., Moore, A., Thompson, J., 2010. Preparing a soil organic carbon inventory for the United States using soil surveys and site measurements: why carbon stocks at depth are important. Proc. 19th World Congr. Soil Sci. Soil Solut. a Chang. world, Brisbane, Aust. 1-6 August 2010. Symp. 1.2.2 Soil Geogr. Ecol. 32–35.

Wang, S., Huang, M., Shao, X., Mickler, R. a., Li, K., Ji, J., 2004. Vertical Distribution of Soil Organic Carbon in China. Environ. Manage. 33, 200–209. doi:10.1007/s00267-003-9130-5

Wang, X., Wang, J., Zhang, J., 2012a. Comparisons of Three Methods for Organic and Inorganic Carbon in Calcareous Soils of Northwestern China. PLoS One 7, e44334. doi:10.1371/journal.pone.0044334

Wang, Z., Liu, G.-B., Xu, M.-X., Zhang, J., Wang, Y., Tang, L., 2012b. Temporal and spatial variations in soil organic carbon sequestration following revegetation in the hilly Loess Plateau, China. CATENA 99, 26–33. doi:10.1016/j.catena.2012.07.003

Wenzl, T., Haedrich, J., Schaechtele, A., Robouch, P., Stroka, J., 2016. Guidance Document on the Estimation of LOD and LOQ for Measurements in the Field of Contaminants in Feed and Food. EUR 28099 EN, European Union Reference Laboratory. Publications Office of the European Union, Luxembourg, ISBN 978-92-79-61768-3; doi:10.2787/8931. doi:10.2787/8931

Westgard, J.O., 1973. Use and Interpretation of Common Statistical Tests in Method-Comparison Studies. Clin. Chem. 19, 49–57.

White, R.E., Davidson, B., 2015. The cost effectiveness of a policy to store carbon in

Australian agricultural soils to abate greenhouse gas emissions. IOP Conf. Ser. Earth Environ. Sci. 25, 012004. doi:10.1088/1755-1315/25/1/012004

Wiese, L., Ros, I., Rozanov, A., Boshoff, A., de Clercq, W., Seifert, T., 2016. An approach to soil carbon accounting and mapping using vertical distribution functions for known soil types. Geoderma 263, 264–273. doi:10.1016/j.geoderma.2015.07.012

Wight, J.P., Allen, F.L., Ashworth, A.J., Tyler, D.D., Labbé, N., Rials, T.G., 2016. Comparison of Near Infrared Reflectance Spectroscopy with Combustion and Chemical Methods for Soil Carbon Measurements in Agricultural Soils. Commun. Soil Sci. Plant Anal. 47, 731–742. doi:10.1080/00103624.2016.1146750

Wight, J.P., Allen, F.L., Zanetti, M.Z., Rials, T.G., 2005. Comparison of Combustion, Chemical, and Near-Infrared Spectroscopic Methods to Determine Soil Organic Carbon, in: Southern Conservation Tillage Systems Conference. Clemson University, pp. 179–184.

Winter, S., Morris, C.D., 2001. Mistbelt grassland fragmentation in the Umvoti conservancy, KwaZulu-Natal, South Africa. South African J. Bot. 67, 303–311. doi:10.1016/S0254-6299(15)31133-9

Yang, R.-M., Zhang, G.-L., Yang, F., Zhi, J.-J., Yang, F., Liu, F., Zhao, Y.-G., Li, D.-C., 2016. Precise estimation of soil organic carbon stocks in the northeast Tibetan Plateau. Sci. Rep. 6, 21842. doi:10.1038/srep21842

Yang, X., Drury, C., Reynolds, W., Tan, C., 2008. Impacts of long-term and recently imposed tillage practices on the vertical distribution of soil organic carbon. Soil Tillage Res. 100, 120–124. doi:10.1016/j.still.2008.05.003

Yang, X., Ren, W., Sun, B., Zhang, S., 2012. Effects of contrasting soil management regimes on total and labile soil organic carbon fractions in a loess soil in China. Geoderma 177–178, 49–56. doi:10.1016/j.geoderma.2012.01.033

Zhao, Y., Shi, X., Yu, D., Wang, H., Sun, W., 2005. Uncertainty assessment of spatial patterns of soil organic carbon density using sequential indicator simulation, a case study of Hebei province, China. Chemosphere 59, 1527–1535. doi:10.1016/j.chemosphere.2005.01.002

Zwieniecki, M.A., Newton, M., 1995. Roots growing in rock fissures: Their morphological

adaptation. Plant Soil 172, 181–187. doi:10.1007/BF00011320